January 2012

The Study Of Vinyl Ester Copolymers Derived From Bio-Sourced Fatty Acids

Hai Wang

THE STUDY OF VINYL ESTER COPOLYMERS DERIVED FROM BIO-SOURCED FATTY ACIDS

by

Hai Wang
Bachelor of Science, Dalian University of Technology, 2008

A Dissertation

Submitted to the Graduate Faculty

of the

University of North Dakota

In partial fulfillment of the requirements

for the degree of Doctor of Philosophy

Grand Forks, North Dakota
December
2012

This dissertation, submitted by Hai Wang in partial fulfillment of the requirements for the Degree of Doctor of Philosophy from the University of North Dakota, has been read by the Faculty Advisory Committee under whom the work has been done, and is hereby approved.

Dr. Edward Kolodka

Dr. Brian M. Tande

Dr. Yun Ji

Dr. Frank Bowman

Dr. Irina P. Smoliakova

This dissertation is being submitted by the appointed advisory committee as having met all of the requirements of the Graduate School at the University of North Dakota and is hereby approved.

Dr. Wayne Swisher
Dean of the Graduate School

Nov-19-2012

Title The Study of Vinyl Ester Copolymers Derived from Bio-Sourced Fatty Acids

Department Chemical Engineering

Degree Doctor of Philosophy

In presenting this dissertation in partial fulfillment of the requirements for a graduate degree from the University of North Dakota, I agree that the library of this University shall make it freely available for inspection. I further agree that permission for extensive copying for scholarly purposes may be granted by the professor who supervised my dissertation work or, in hrs absence, by the Chairperson of the department or the dean of the Graduate School. It is understood that any copying or publication or other use of this dissertation or part thereof for financial gain shall not be allowed without my written permission. It is also understood that due recognition shall be given to me and to the University of North Dakota in any scholarly use which may be made of any material in my Dissertation.

Hai Wang
December 2012

TABLE OF CONTENTS

LIST OF FIGURES

LIST OF TABLES

ACKNOWLEDGEMENTS

The completion of this dissertation is one of the most important experiences of my life. I appreciate those people who give me a lot of help in the four years of my graduate study. First of all, I give my sincere gratitude to my advisor Dr. Edward Kolodka, who is an excellent mentor on my academic research. At the same time, I appreciate sincerely my co-advisor Dr. Brian M. Tande, who was also very helpful on my research. Both my advisor and co-advisor have given me great guidance and support during my graduate study, which have been greatly beneficial in my life. Also, it is of great honor to have Dr. Yun Ji, Dr. Frank Bowman, and Dr. Irina P. Smoliakova in my committee, and who have helped me a lot during my studying at UND.

Meanwhile, I appreciate the technical support from Mr. Joe Miller. There are several other people, including Xuefei Zhang, Srinivas Reddy Kamireddy, Kirtipal Barse, Andrew Onken, Jinbao Li, and Jiexia Wu who were helpful in various ways. I also give my acknowledgements to USDA, which supported my research.

Finally, I would like to thank my mother Rong Wang and my father Guangliang Wang for their encouragement and love.

ABSTRACT

Biobased polymers have attracted significant attention since the 1990s. Research has focused on the conversion of biomass, such as crop oils, into useful polymeric materials. The Departments of Chemical Engineering and Chemistry at the University of North Dakota have developed a process to convert crop oils into jetfuel and a suite of other chemicals including fatty acids with a variety of molecular weights. This dissertation focuses on the preparation and property measurements of thermoplastics using monomers, especially linear vinyl esters (LVEs), which originate from cracked oil-based fatty acids. Commercial LVEs were used in this dissertation study in order to explore some key properties of the resultant copolymers using current polymer synthesis and characterization technology.

Copolymers of LVEs with a variety of monomers, including styrene, methyl methacrylate, acrylic acid, and ethylene, have been successfully synthesized using bulk or solution copolymerizations. The LVE compositions were varied by adjusted the feed ratio. The average molecular weights (MWs) decreased with increasing LVE composition.

Thermomechanical property measurements showed that the glass transition temperatures of the resultant copolymers decreased with increasing LVE compositions. This indicates the side chains of LVEs resulted in easier segmental movements. When the MWs and LVE compositions of the copolymers were similar, the glass transition temperatures decreased for copolymers that had longer side chains. This shows LVEs with longer chains had a greater reduction on the energy required for segmental diffusion. At the same time, the storage moduli (E') of the resultant copolymers

decreased with increasing LVE compositions. Therefore, the rigidity of the copolymers could be reduced by incorporation of LVEs. Copolymers with longer side chains but similar MWs and LVE compositions exhibited lower storage moduli (E'), which indicates LVEs with longer chains had a greater impact on the storage moduli (E') than lower molecular weight LVEs.

The rheological property measurements showed that the shear storage moduli (G'), shear loss moduli (G''), and complex viscosity of resultant copolymers were mostly determined by the MWs. The effects of side chains on the shear flow behaviors of LVE based copolymer melts were not significant.

CHAPTER I

INTRODUCTION

Background

Biobased energy and materials have attracted considerable attention in recent decades because of escalating petroleum prices and climate change attributed to CO_2. Biomass and agricultural products are the most widely studied renewable materials, including agricultural and animal wastes, cereals, and crop oils. Researchers working in this field have made a lot of contributions to the exploration of feasible processes, including fermentation, gasification, pyrolysis, and distillation, from which useful biofuels and chemicals, such as alcohol and syngas, can be derived. The Departments of Chemical Engineering and Chemistry at the University of North Dakota have developed a successful process to convert crop oils, such as canola and soybean oils, into transportation fuels, including jetfuel and cold weather diesel. At the same time, a suite of useful chemicals including benzene and fatty acids, separated and purified from byproducts of cracked crop oils, can be used in preparation of polymers.

Polymers, especially synthetic polymers, were first reported in early 20th century and have become one of the most important materials. Plastics, rubbers, and fibers are the three main types of polymers, almost all of which are derived from petroleum sourced chemicals. However, the development of biobased polymeric materials has the potential to bring great change to the contemporary polymer market. Polymers with structures similar to commercial polymers, or with entirely new structures, are being developed based on chemicals from biomass using traditional polymer synthesis technologies and processes.

Currently, crop oils are one of the most widely used forms of biomass for polymer synthesis. From the original triglyceride structure many thermosets and a few thermoplastics with complex molecular structures have been synthesized. The main liability of crop oil-derived monomers is their slow reaction kinetics due to their high molecular weights. The polymers produced have also generally been thermosets with limited applications. Also, new infrastructure must be developed for newly developed polymers. Therefore, the content of crop oil sources in the resultant polymers is limited to a rather low level. However, crop oil-based thermoplastics with structures identical to existing commercial polymers can solve these problems. These thermoplastics have higher biobased content, more versatile thermomechanical properties, and better processability, all of which lead to great value of studies.

Outlines of the Dissertation Study

The primary purpose of this study was to prepare polymeric materials from fatty acids produced from cracked crop oils. Linear vinyl esters were the target monomers which are ultimately planned to be derived from fatty acids sourced from crop oils. Therefore, commercial linear vinyl esters, including vinyl acetate, vinyl propionate, vinyl hexanoate, and vinyl decanoate, were selected to copolymerize with other commercial monomers, which included styrene, methyl methacrylate, acrylic acid, and ethylene. Commercially available LVEs were used in this work in order to study the effects of LVE molecular weight and content on the copolymer properties to determine optimal properties for future studies with crop oil-derived LVEs. All copolymerizations were carried out by free radical polymerization in bulk or solution at constant temperatures. The thermomechanical and rheological properties of the resultant copolymers were measured. Biobased thermoplastics, similar or identical to,

existing commercial copolymers were prepared and analyzed, making this study very unique.

The copolymerization kinetic parameters, such as reactivity ratios of comonomers, average molecular weights, molecular weight distributions, and the compositions of the resultant polymers, were studied using Fourier transform infrared spectroscopy, proton nuclear magnetic resonance, and gel permeation chromatography.

The thermomechanical properties of the synthesized polymers were measured by differential scanning calorimeter and dynamic mechanical analysis to determine glass transition temperatures, crystallinity, storage modulus, loss modulus and tan δ. The effects of linear vinyl ester composition and molecular weight on the thermomechanical properties were analyzed.

The rheological properties of the resultant copolymers were analyzed by parallel-plate rheometry. The shear storage modulus and shear loss modulus were measured in order to learn the effects of linear vinyl ester composition, the average molecular weight, and side chain length on the rheological behaviors. The information obtained from the study can be used as reference for further preparation of other copolymers derived from biomass.

CHAPTER II

LITERATURE REVIEW AND POLYMER CHARACTERIZATION

Crop Oil-Based Polymers

Crop oils, such as soybean oil, have triglyceride structures with varying numbers of double bonds on the long chain of fatty acids as shown in Figure 2.1. Crop oils can be hydrolyzed to produce long chain fatty acids, monoglycerides, diglycerides, and glycerols, all of which are chemicals with functional groups. There are a number of strategies that have been employed to produce polymers from crop oils by using these functional groups. Research has been done on synthesis of crop oil-based polymers, almost all of which were based on the original structures or the partially hydrolyzed analogues (Güner et al., 2006, Sharma et al., 2006).

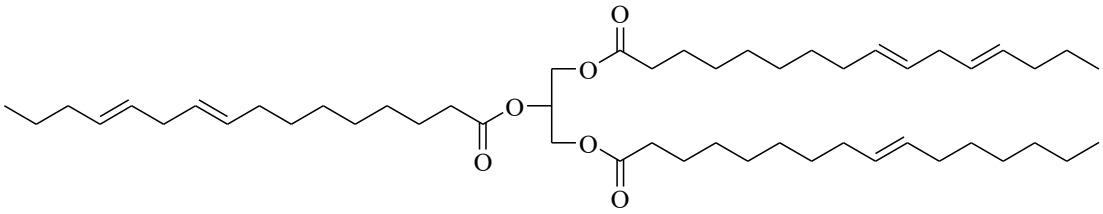

Figure 2.1. The chemical structure of soybean oil.

The common strategies used were to modify the double bonds of the crop oils in order to produce crop oil-based polymers or desired macrointermediates for further reactions. A simple way to achieve this is the peroxidation treatment of the double bonds using transition metal complexes to obtain epoxy bonds and acid groups on the back bone of crop oils for subsequent reactions (Mallégol et al., 2000). Another

method usually used in the treatment of the double bonds in crop oils is epoxidation using peroxide combined with acetic acid (Uyama et al., 2003). Crop oils with epoxy bonds can be applied in reactions with monofunctional alcohols, amines, and acids. Acrylic acid, for example, can be used in this reaction, forming ester bonds on crop oil chains. The unreacted double bonds of acrylic acids can be used in further polymerizations (Ahmad et al., 2002). Network structures can be prepared from epoxied crop oils if bifucntional or trifunctional compounds are used, such as maleic anhydride (Khot et al., 2001). Further reactions of epoxy bonds with peroxide can form hydroxyl groups, which were employed in future reactions. For example, modified crop oils with hydroxyl groups were reacted with diisocyanate to form polyurethane (Eren et al., 2004A). Other combinations of chemicals, such as N-bromosuccinimide/acetone/H_2O, were also used to modify double bonds (Eren et al., 2004B). Styrene and divinylbenzene were both selected to be crosslinking agents to connect crop oil molecules together in polymer networks (Li et al., 2001, 2003). Maleic anhydride was a frequently used chemical in the maleinization of triglyceride oils. By reacting with maleic anhydride and glycerol sequentially, carboxyl and hydroxyl functionality was added to the triglyceride. These intermediates were used to prepare polyurethanes with interpenetrating or semi interpenetrating network structures (Yenwo et al., 1977A, 1977B). Different from the previous methods, metathesis reactions provided a method of preparation of crop oil-based polymers by direct reaction between carbon double bonds in the presence of Grubbs' ruthenium catalysts (Erhan et al., 1997). In addition, olefin metathesis reaction between ethylene and crop oils formed double bonds at the end of the fatty acid chains, which were used in further reactions (Tian et al., 2002, Warwel et al., 2001, 2004).

In general, the double bonds of crop oils were first functionalized and

subsequently polymerized. However, the complex triglyceride structures of crop oils limit the flow of polymer molecules. At the same time, the reactivity ratios of triglycerides and small monomers are very different, which result in limited conversion during copolymerizations. Therefore, the content of crop oil in copolymers are limited to a great extent.

Crop oils were also partially hydrolyzed to form monoglycerides or diglycerides, or fully hydrolyzed to form long chain fatty acids and glycerols using a variety of methods, including alcoholysis and interesterification. These intermediates were usually used in preparation of polyurethanes and polyesters (Güner et al., 2006).

Monoglycerides derived from crop oils, were reacted with methyl methacrylate (MMA) and acrylic acid (AA) (Tuman et al., 1996) to form a new triglyceride with double bonds at the end of fatty acid chains. The terminal double bonds were subsequently reacted with other vinyl monomers such as styrene (Gultekin et al., 2000). Another popular method of making use of monoglycerides was the preparation of macroinitiator by the reaction of free hydroxyl with 4,4'-azobis(4-cyanopentanoic chloride) (ACPC). This monoglyceride based macroinitiator was then used in reactions with vinyl monomers to form crop oil based polymers (Erkal et al., 1993). Diglycerides with two hydroxyl groups were more convenient in making polymers. In this case, anhydrides including phthalic anhydride, maleic anhydride, and succinic anhydride, were used in the synthesis of alkyd resins by esterification reactions (Aydin et al., 2004). Another common application of crop oil-based diglycerides is the synthesis of polyurethanes. Different types of diisocyanates, including hexamethylenediisocyanate, toluenediisocyanate, and isophoronediisocyanate, were applied in polycondensation reactios in order to produce various polyurethanes (Güner et al., 2002, 2004, Ozkaynak, 2005). In order

to increase the strength of polymers from partially hydrolyzed crop oils, interpenetrating and semi- interpenetrating networks were obtained by the reactions of residual double bonds of crop oil-based polyurethane with crosslinkers, which include methyl methacrylate (MMA), styrene (St), divinyl benzene (DVB), and butyl acrylate (BA) (Sperling et al., 1980, Nayak et al., 2000). As mentioned before, long chain fatty acids were obtained from fully hydrolyzed triglycerides. Long chain fatty acids containing double bonds were used as intermediates in polymer synthesis, which underwent the Diels-Alder reaction to prepare difucntional molecules for preparation of polyesters and polyamides (Oldring et al., 2000). The chemical pathways in Figure 2.2 and Figure 2.3 below summarize the preparations of crop oil-based polymers from the literatures.

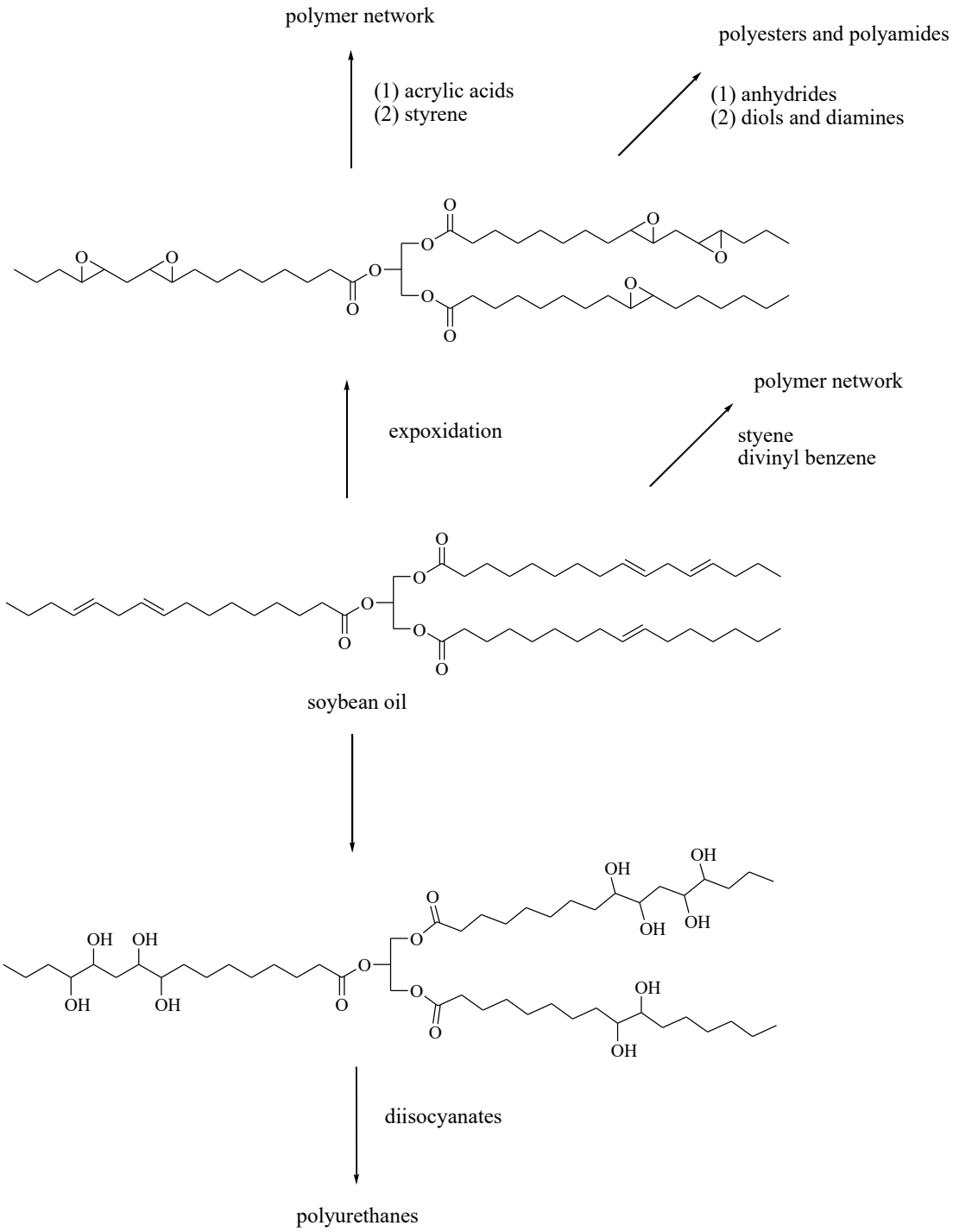

Figure 2.2. Polymers derived from the original soybean oil (Güner et al., 2006).

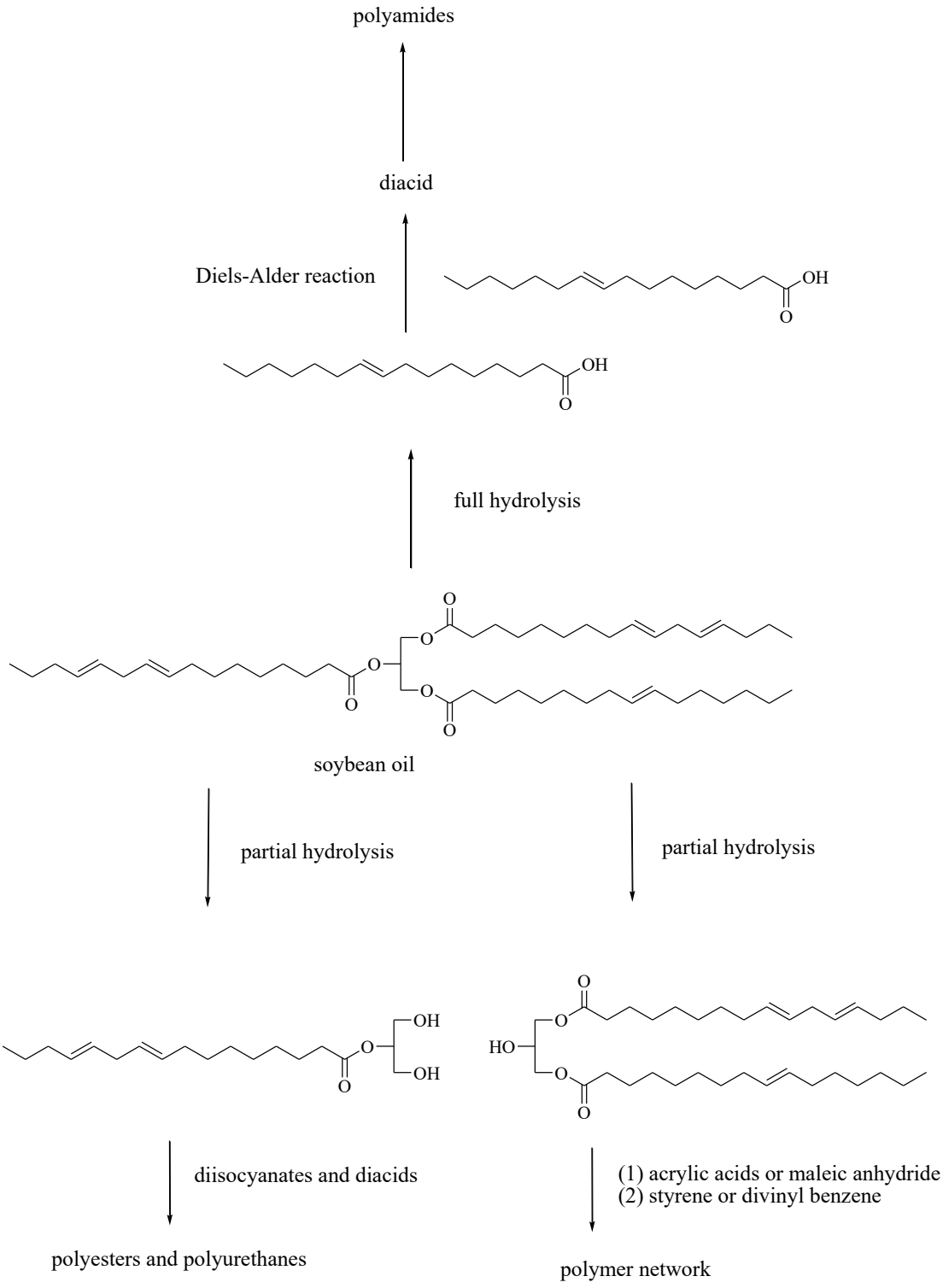

Figure 2.3. Polymers derived from hydrolyzed soybean oil (Güner et al., 2006).

Current biobased polyurethanes are primarily new polymer types generally with increased cost, decreased properties, and low bio content. Meanwhile, thermosets cannot be processed any longer after precursors are injected into the mold and heated to solidification, which limits recycling. Compared to thermosets, thermoplastics have great advantages in synthesis and processing. They can be produced by bulk, solution, emulsion, and suspension polymerization. At the same time, their good processibility allows for molding, extruding and other processing methods, which results in versatile applications and diverse products. Therefore, in order to overcome these limitations, crop oil-based thermoplastics, which have very similar structures with current commercial thermoplastic products, are considered to be an interesting field of research. Commercially available monomers, including styrene (St), methyl methacrylate (MMA), acrylic acid (AA), and ethylene (Et) were selected to be comonomers in copolymerizations with linear vinyl esters (LVEs) to achieve copolymers with desirable characteristics.

Polymers of Linear Vinyl Esters (LVEs)

Polymers of LVEs are derived from monomers, such as vinyl acetate (VA) and vinyl propionate (VP), which have different numbers of carbon atoms in the linear fatty acid chains as shown in Figure 2.4. Their homopolymers and copolymers can be used as water-based paints, adhesives, coatings, and plasticizers (Mark et al., 1989A). Currently, only VA is widely used in the production of polymeric materials. Meanwhile, VP is usually used in the preparation of homopolymers and copolymers used as surface-coatings, but in small quantities (Mark et al., 1989B). However, other LVEs with higher molecular weights such as vinyl hexanoate (VH) and vinyl decanoate (VD) are rarely used because of their low productivity and the high cost of

these monomers, and the very low glass transition temperatures of their homopolymers (Mark et al., 1989C).

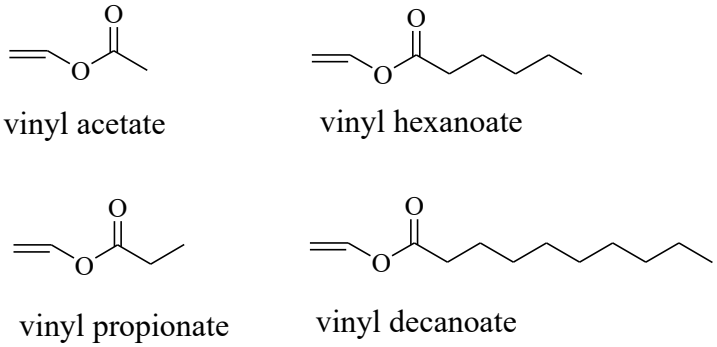

Figure 2.4. The chemical structures of LVEs.

The Department of Chemical Engineering and Chemistry at the University of North Dakota have developed a technology to produce biofuels, as shown in Figure 2.5, from which aromatics, such as toluene and xylene, and a suite of fatty acids, including acetic acid, propionic acid, hexanoic acid and decanoic acid, have been collected and purified (Gandhi et al, 2012, Braegelmann et al., 2011). The conversion of short chain fatty acids into corresponding LVEs is a traditional process. Both VA and VP can be produced by the vinylization of acetic acid or propionic acid in the presence of ethylene and oxygen catalyzed by palladium based catalysts (Mark et al., 1989D, Han et al., 2005). LVEs with higher molecular weights can be synthesized by reacting excess VA with the corresponding fatty acids in the presence of a mercury (Daniel et al., 1963), or iridium catalyst (Vilela et al., 2010). Therefore, LVEs with different molecular weights can be derived from crop oil sources.

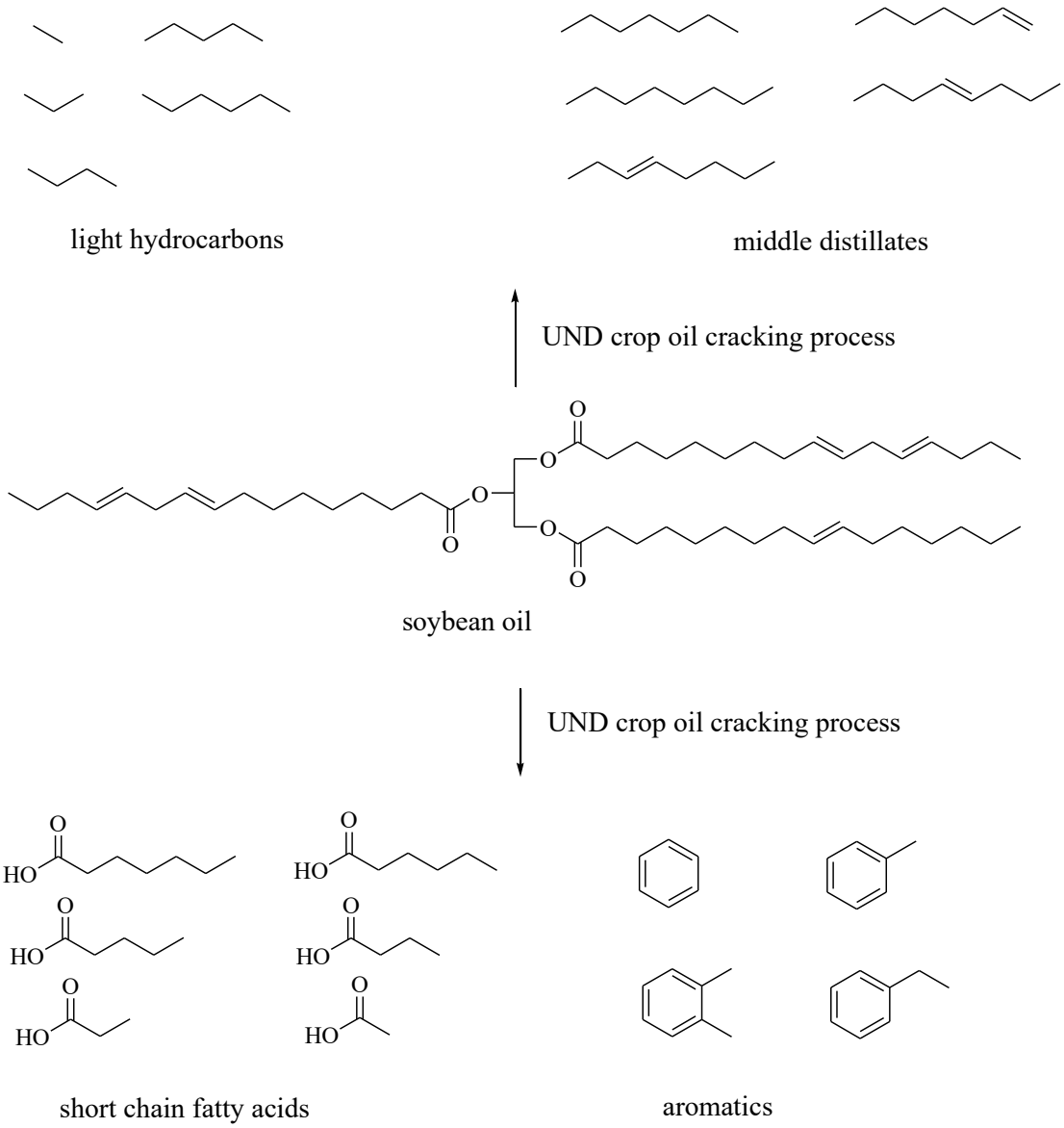

Figure 2.5. Products formed in UND crop oil cracking processes.

In order to solve the problem of the low glass transition temperatures of LVE homopolymers, LVEs can be copolymerized with other monomers to produce copolymers with various compositions of bio sources. Poly vinyl acetate and poly vinyl propionate, whose glass transition temperatures are 35 °C and 7 °C, are rubbery materials. Poly vinyl hexanoate and poly vinyl decanoate, both of which have glass transition temperatures below -25 °C, are viscous liquids at room temperature. It is

hypothesized that LVEs can be used to modify the thermomechanical and rheological properties of polymers with high stiffness, rigidity, and brittleness. Monomers, including styrene, methyl methacrylate, acrylic acid, and ethylene, were selected as comonomers in copolymerizations with LVEs in order to produce copolymers with improved flexibility and impact resistance, while also importing a degree of renewability. Figure 2.6 shows the comonomer systems selected for this work.

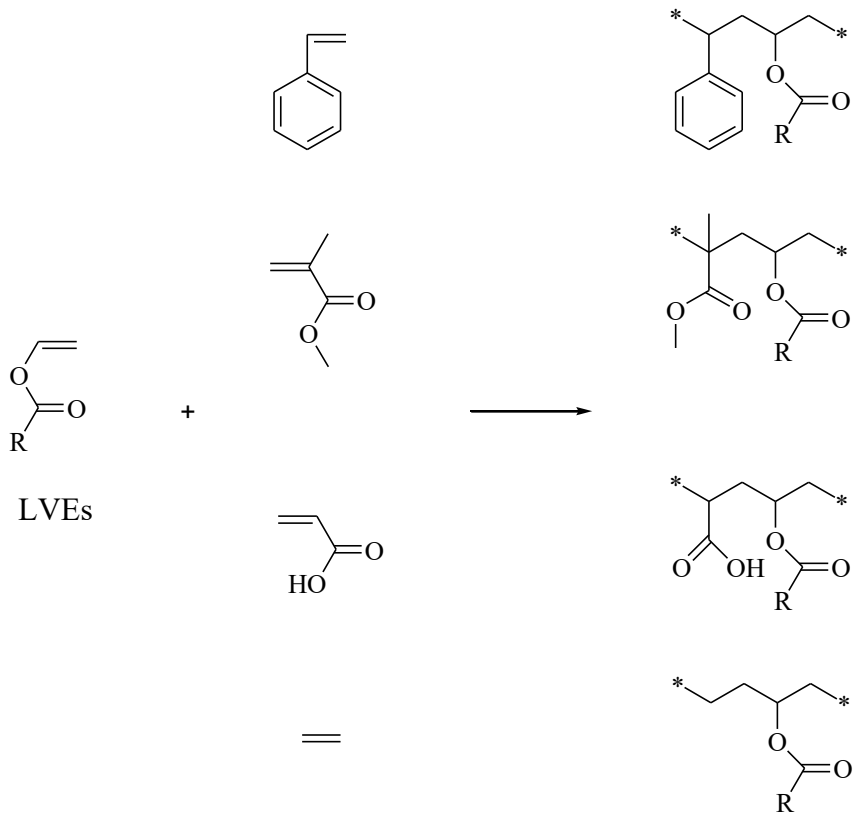

Figure 2.6. Copolymerizations of LVEs with comonomers.

Copolymers of LVEs with Monomers

Polystyrene (PS) and copolymers of styrene (St) with LVEs

PS is prepared commercially from St using bulk, solution, emulsion and suspension polymerizations. PS is used in a wide array of applications, including foams, cutlery, CD cases, and Petri dishes. Foamed PS has good thermal insulation

and damping performance and is often used in food containers and packing materials (Mishra et al., 2009A). In order to overcome its brittle nature, St is often copolymerized with butadiene to obtain high-impact-polystyrene (HIPS), or with acrylonitrile yielding acrylonitrile-styrene copolymers (SAN), or with both acrylonitrile and butadiene to get acrylonitrile-butadiene-styrene (ABS) copolymers, which are used in toy casings and sewer pipelines. St is derived from petroleum. The traditional method of producing St is via the alkylation of benzene to ethylbenzene followed the dehydrogenation of ethylbenzene (Mark et al., 1989E). But recently, a new method of St synthesis by the side-chain alkylation of toluene by methanol or other alcohol over a basic zeolite (Vasanthy et al., 1996) was reported. Therefore, St can also be obtained by the alkylation reaction of toluene from cracked crop oil by-product as well as LVEs.

Copolymerizations of St with LVEs, especially with VH and VD, were carried out with the goal of improving the rigidity and brittleness of PS. There has been little research conducted on the copolymerization of styrene with VE, with most work detailing the copolymerization of St with VA, particularly block copolymers of St with VA. Different polymerization methods, such as atom transfer radical polymerization (ATRP), reversible addition-fragmentation transfer (RAFT) polymerization, and cobalt-mediated radical polymerization (Paik et al., 1999, Xue et al., 2012, Kaneyoshi et al., 2007) were used. Some new catalytic systems were also studied, including electrochemistry based catalysts, UV-radiation, and iron complexes (Calafate et al., 1989, Ramelow et al., 1995, Huang et al., 2000, Xia et al., 1999, Daniel, N., 2002). However PS and its copolymers are commercially produced via free radical polymerizations. Therefore, free radical copolymerization was selected in this study. It was necessary to determine the copolymerization kinetics and the

thermomechanical properties of the resultant polymers in order to facilitate the future manufacturing of fully or partially biobased copolymers of St with LVEs.

Poly(methyl methacrylate) (PMMA) and copolymers of methyl methacrylate (MMA) with LVEs

MMA is also a very good candidate for copolymerization with LVEs. MMA is copolymerized to prepare PMMA by bulk, emulsion, solution, or suspension polymerization. PMMA is a widely used polymer in glazing materials and coatings because of its high strength, excellent optical properties, and high stiffness. Its brittleness, however, limits its applications. It has been determined that copolymerization with acrylic esters improved the impact resistance of MMA (Mishra et al., 2009B, Mark et al., 1989F, G, Chisholmet al., 2009). Thus, it is hypothesized that LVEs, which have similar chemical structures with acrylic esters, as shown in Figure 2.7, can be used to improve the flexibility and impact resistance of PMMA.

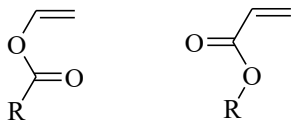

LVE acrylic esters

Figure 2.7. Chemical structures of LVE and acrylic ester.

Currently, the only LVE used in copolymerizations with MMA is VA (Dubé et al., 1995). Some of the available research focused on kinetic studies of copolymerization of MMA with VA in bulk, solution, and emulsion polymerizations (Scorah et al., 2001, Santos et al., 2000, Dossi et al., 2012, Steinmacher et al., 2010, Kubo et al., 1993, Ahmad et al., 2011, Md. Shahidu et al., 2012). Some studies

detailed the copolymerization using new catalysts (Zhu et al., 2007A, Granel et al., 1998, Zhu et al., 2007B). There was little research detailing the thermal and mechanical properties of random MMA-VA copolymers (Ahmad et al., 2011, Yang et al., 2008). Other researchers studied block copolymers of MMA with VA (Li et al., 2006, Dubé et al., 1997, Huang et al., 1998, Priyadarsi et al., 2002, Zou et al., 2000, Takashi et al., 1996). However, copolymers of MMA with other LVEs have not been reported in the literature.

Poly(acrylic acid) (PAA) and copolymers of acrylic acid (AA) with LVEs

AA is polymerized to produce poly acrylic acid (PAA) and related products, which are commonly used as adhesives, dispersants, and flocculating agents (Mark et al., 1989L). Ion-exchange resins and polyelectrolytes are also common applications (Van Krevelen et al., 2009). PAA salt (acrylic sodium polymer salt) is very useful as diaper additives because of its excellent water absorption properties. However, PAA is a brittle white solid that cannot be molded. Therefore, AA is usually copolymerized with other monomers, including acrylamide, acrylonitrile, and vinyl esters (Mark et al., 1989M), to yield versatile products used in the manufacturing of coatings and adhesives.

There has been some work reported detailing the copolymerizations of AA with LVEs, but it is limited to VA. Suspension copolymerizations of AA with VA were reported, the partition coefficients were determined (Silva et al., 2004) and copolymerization kinetics were modeled (Silva et al., 2010). The influences of surfactant on the polymerization mechanism during emulsion copolymerization were reported (Donescu et al., 1999, Tang et al., 1996). Solution copolymerization was another frequently reported method in the preparation of AA/VA copolymers, which

included the reactivity ratio determination (Zaldívar et al., 1998A), monomer conversion and copolymer composition evaluation (Zaldívar et al., 1998B), and mathematical modeling (Zaldívar et al., 1997). The solution copolymerization of AA and VA in the presence of crosslinker was applied in preparations of drug delivery gel (Ranjha et al., 2008). Some polymers, such as poly vinyl alcohol (PVA) and poly vinyl acetate, were used as crosslinking agents in reactions with AA or PAA to prepare proton exchange membranes for a fuel cell (Kim et al., 2005). Block copolymers consisting of AA and VA were also synthesized by taking advantage of the carboxyl groups of AA in order to obtain amphiphilic structures (Li et al., 2009, Can et al., 2006, Caneba et al, 2009).

Poly(ethylene-co-vinyl acetate) (EVA) and low density linear polyethylene (LLDPE)

EVA is a widely used commercial copolymer in shrink-wrap food packaging, adhesives, and coatings. EVA is usually produced by solution or emulsion copolymerization of ethylene (Et) with VA using free radical initiators. Commercial EVA products usually have 10% to 40% weight percent VA. Copolymers containing 2% to 5% weight percent VA behave similarly to polyethylene (PE), but show better clarity, higher impact strength, and better low temperature flexibility. Copolymers containing 7.5% to 12% weight percent VA have higher flexibility, higher puncture resistance, and exceptional impact strength. With even more VA, 15% to 18% weight percents, EVA exhibits rubbery characteristics (Mark et al., 1989H).

There is a great deal of information in the literature detailing EVA synthesis and characterization. The free radical copolymerization of EVA has been well studied, both experimentally (Scott et al., 1994, Araujo et al., 2001) and theoretically (Jonathan et al., 2002, Chien et al., 2007, Kiparissides et al., 2005). The reactivity

ratio of Et to VA, copolymerization kinetics and compositions of resultant EVA have also been analyzed by FT-IR (Xu et al., 2009), NMR (Souza et al., 1998), GC (German et al., 1971), high-temperature HPLC (Albrecht et al., 2009), and with 2D-HPLC (Ginzburg et al., 2010). In addition, the thermal mechanical properties, including glass transition temperature, melting temperature, deformation-stress, and stress-strain properties of EVA and crosslinked EVA have also been studied (Bugada et al., 1992, Gospodinova et al., 1998, Gladkikh et al., 2010, Rezaeian et al., 2009). However, there is no information in the literature detailing the copolymerization of Et and other LVEs including VP, VH, and VD. Some important properties of the resultant copolymers, such as the thermal and rheological properties, are still unknown.

Another very important reason for studying the synthesis and properties of copolymers of Et with other LVEs, especially with VH and VD, is that their structures are very similar to LLDPE, as shown in Figure 2.8. LLDPE is a widely used commodity polymer synthesized by the copolymerization of Et with α-olefins by coordinated copolymerization catalyzed by Ziegler-Natta catalysts. LLDPE has a long carbon backbone, similar to high density PE, but with short chain branches randomly distributed as shown in Figure 2.9. Depending on chosen comonomers, the short branches contain two carbons for 1-butene, four carbons for 1-hexene, and six carbons for 1-octene. As the molecular weights of the comonomers increase, some physical properties, such as toughness and tear strength, can be improved. The probable reason is that the increased length of short chain branches inhibit the folding of the PE molecular chain to form crystal lamella, and help to increase the number of interlamellar tie molecules (Mark et al., 1989J). LLDPE films, compared to traditional LDPE films, have higher tensile strength, puncture resistance, elongation, and

improved low temperature properties. LLDPE is used to manufacture films used to produce garbage bags, etc. For other applications, LLDPE can also be used for piping, tubing, wire, and cable insulators if they are processed by blow molding (Mark et al., 1989K).

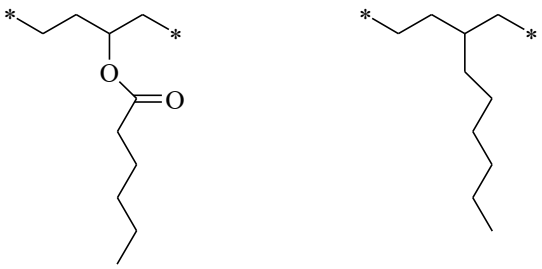

Figure 2.8. Chemical structures of LLDPE (1-octene) and poly(Et-*co*-VH).

Figure 2.9. The molecular structure of LLDPE with short branches.

It is hypothesized that ethylene-co-linear vinyl ester will behave in a manner similar to LLDPE and that longer side branches may lead to copolymers with improved properties compared to traditional EVA.

Characterization of Polymers

Traditional characterization methods used in chemistry can also be used in characterization of polymers, which include Fourier transform infrared spectroscopy (FT-IR), proton nuclear magnetic resonance (^{1}H-NMR), UV-vis spectroscopy, scanning electron microscope (SEM), high-performance liquid chromatography (HPLC), X-ray diffraction spectroscopy (XRD), etc. In addition, many methods have

been developed suitable for polymer analysis, such as gel permeation chromatography (GPC), differential scanning calorimetry (DSC), dynamic mechanical analysis (DMA), and rheometry.

Structural Analysis

Fourier Transform Infrared Spectroscopy (FT-IR)

Vibrations of chemical bonds that change the dipole moment of the molecules are IR active. Different functional groups have their specific absorption bands, from which the structures of molecules can be told. The position of a certain absorption band is specified by its wavenumber ($\bar{\nu}$), which is related to wavelength as shown in Equation 2.1.

$$\bar{\nu}\ (\mathrm{cm}^{-1}) = \frac{1}{\lambda\ (\mathrm{cm})}$$

Equation 2.1. Relation between wavelength and wavenumber.

At the same time, FT-IR is also able to be applied in quantitative analysis under certain conditions. According to the Beer-Lambert Law, as shown in Equation 2.2, the absorbance (A) or the peak height corresponds to the ratio of transmission of sample solution and solvent (I/I_0), and the product of the path length of light (l) and the concentration of solution (c). Therefore, the compositions of the samples can be determined by a simple mathematic calculation if l and c are constant.

$$A = -\lg\left(\frac{I}{I_0}\right) = -a \times l \times c$$

Equation 2.2. Beer-Lambert Law.

Proton-Nuclear Magnetic Resonance Spectroscopy (^{1}H-NMR)

^{1}H-NMR is a tool frequently used in the determination of the structures of organic compounds as well as polymeric materials. Hydrogen protons that are in different chemical environments have different resonance phenomena under an external magnetic field. The resonance signals captured using an NMR spectrometer form an NMR spectrum, from which the chemical structures of polymers and the composition of specific functional groups can be determined.

Average Molecular Weight (MWs) and Molecular Weight Distributions (MWDs)

MWs and MWDs are very important parameters in polymer research. MWs can be defined as number average molecular weight (M_n) and weight average molecular weight (M_w), whose mathematic expression are shown in Equation 2.3 and Equation 2.4. M_i is the mass of molecule, and N_i is the number of molecules with mass of M_i. The ratio of M_w to M_n is defined as the polydispersity index (PDI) which indicates the breadth of MWD.

$$M_n = \frac{\sum M_i \times N_i}{N_i}$$

Equation 2.3. Number average molecular weight.

$$M_w = \frac{\sum {M_i}^2 \times N_i}{\sum M_i \times N_i}$$

Equation 2.4. Weight average molecular weight.

Gel permeation chromatography (GPC), which is a type of size exclusion chromatography (SEC), is designed to determine the MWD of polymers based on

their hydrodynamic radius. Materials used in the column of a GPC have a porous structure. Molecules with smaller size diffuse into the pores more easily and stay in the pores longer than larger molecules when the analytes go through the column. Therefore, polymers with different MWs can be separated by their retention time.

Thermal Property

Differential scanning calorimetry (DSC) is one of the most important instruments to determine the thermal transitions (T_g) of polymers. For amorphous polymers, the molecular chains begin to move when the temperature reaches a certain value, which is defined as T_g. Amorphous polymers behave in a glass manner when the temperature is below T_g, but become rubbery after heated above T_g. Polymer molecules begin to flow at a certain temperature or in some temperature range, which is called the viscous flow temperature (T_f). The range between T_g and viscous flow temperature is defined as the rubber state. All these changes can be expressed by the thermal-mechanical curve of a polymer, as shown in Figure 2.10, in which ε is the strain of the polymer under constant stress. Different polymers have their own unique applications depending on their various thermal transitions. Rubbers, whose T_gs are usually lower than -50 °C are used because of their excellent elasticity at room temperature. However, PMMA having a T_g of 105 °C is applied as glazing materials due to its high strength at room temperature. Some polymers exhibit both crystalline and amorphous behavior. Typical DSC curves for polymer samples are shown in Figure 2.11, where T_g is the glass transition temperature, and T_m is the melting point. These semicrystalline polymers, such as PE, have both melt points and T_gs. Once the T_g of a designed polymer is known, its temperature range of application can be determined. The T_g and T_m of polymers are determined by measuring the heat

capacity changes when polymers are heated at a uniform rate.

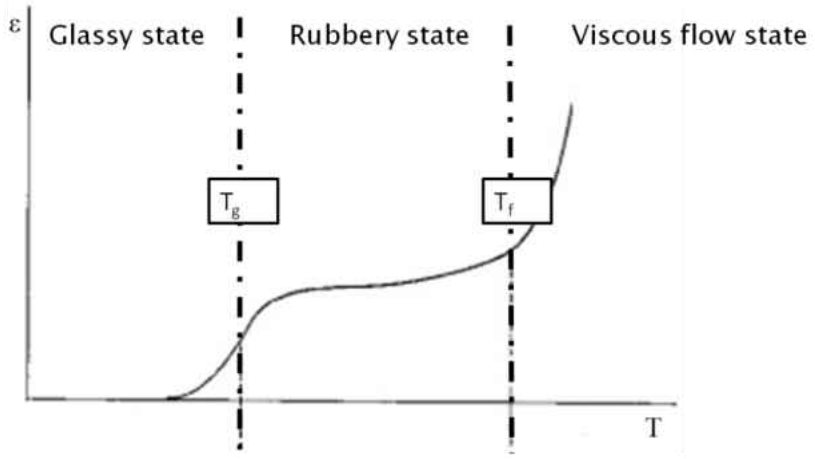

Figure 2.10. Thermal-mechanical curve of amorphous polymer.

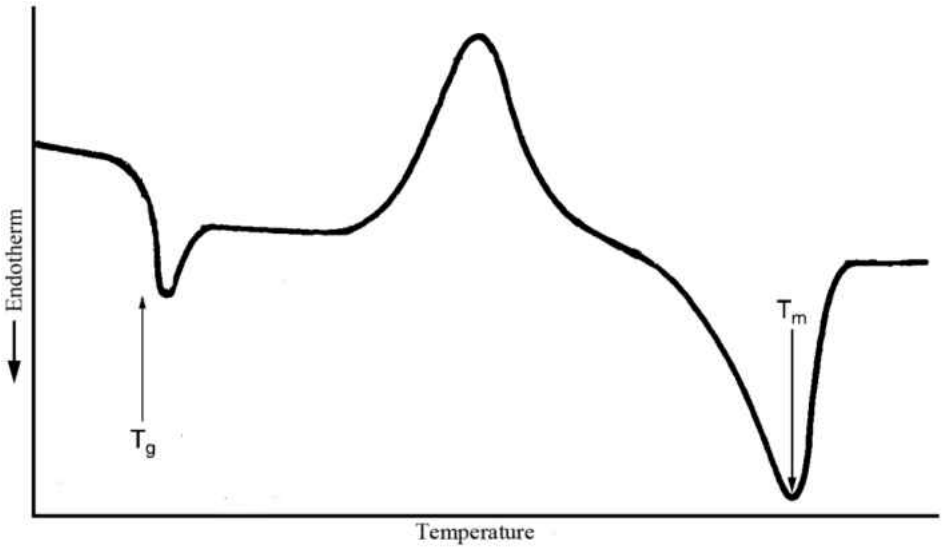

Figure 2.11. Typical DSC curve of semicrystalline polymer.

Thermomechanical Properties

Polymers exhibit both viscous and elastic behavior when subject to a stress. This behavior is known as viscoelasticity and can be measure using a dynamic mechanical analyzer. In order to measure this property, a sinusoidal deformation is applied to the sample. The stress and strain in the test can be expressed by Equation

2.5 and Equation 2.6. The storage modulus (E') refers to the amount of energy stored when the material undergoes a cyclic manner, which represents the elastic portion of the materials. Loss modulus (E") means the amount of energy dissipated as heat, which is the viscous portion. Both the storage modulus (E') and the loss modulus (E") are measured directly by dynamic mechanical analyzer and can be expressed using Equation 2.7 and Equation 2.8. The tan δ is calculated by dividing the loss modulus by the storage modulus (E"/ E').

$$\delta = \delta_0 \sin(\omega t + \delta)$$

Equation 2.5. Expression of stress under sinusoidal motion.

$$\varepsilon = \varepsilon_0 \sin(\omega t)$$

Equation 2.6. Expression of strain under sinusoidal motion.

$$E' = \frac{\delta_0}{\varepsilon_0} \cos \delta$$

Equation 2.7. Expression of storage modulus.

$$E'' = \frac{\delta_0}{\varepsilon_0} \sin \delta$$

Equation 2.8. Expression of loss modulus.

Both the storage modulus and the loss modulus are sensitive to the temperature. The storage modulus reduces rapidly and the loss modulus exhibits its highest value around the T_g. This is because the chains are able to slide relative to other chains at the T_g. The tan δ exhibits a peak at T_g. Therefore, the temperature

corresponding to the peak height of the tan δ is generally considered to be the T_g.

Rheological Properties

Rheology is the study of flow of non-Newtonian fluids. Although polymers are usually solid at room temperature, they become viscous melts above their T_f for amorphous polymers and above their T_m for semicrystalline polymers. Knowledge of polymer rheological properties is critical to the successful processing of that polymer. The viscosity (μ) of Newtonian flow is the ratio of shear stress (τ) and shear strain ($\dot{\gamma}$), as shown in Equation 2.9, which is a constant at a given temperature.

$$\tau = \mu\dot{\gamma}$$

Equation 2.9. Newtonian flow function.

However, most polymer melts are non-Newtonian fluids. Shear thinning and shear thickening fluids are the most common non-Newtonian fluids in polymer melts, whose behavior is expressed by Equation 2.10. K is the fluid consistency, and n is the flow index, in which $n<1$ for shear thinning fluid and $n>1$ for shear thickening fluid. Equation 2.10 can be modified to Equation 2.11, in which η_a is apparent viscosity. Therefore, the parameter η_a is a function of both $\dot{\gamma}$ and temperature.

$$\tau = K\dot{\gamma}^n$$

Equation 2.10. Non-Newtonian fluid function.

$$\tau = \eta_a\dot{\gamma}$$

Equation 2.11. Non-Newtonian fluid function.

A rheometer is a powerful instrument for studying the rheological properties of polymer melts. One of the most commonly used test modes is the response of polymer melts subject to oscillatory shear stresses. Shear storage (G') modulus and shear loss modulus (G"), which are expressed by Equation 2.12 and Equation 2.13, are obtained during the measurement. The tan δ is defined as the ratio of G" to G', as shown in Equation 14.

$$G' = \frac{\tau}{\dot{\gamma}} \cos\ \theta$$

Equation 2.12. Shear storage modulus of non-Newtonian fluid.

$$G'' = \frac{\tau}{\dot{\gamma}} \sin\ \theta$$

Equation 2.13. Shear loss modulus of non-Newtonian fluid.

$$\tan\ \delta = \frac{G''}{G'}$$

Equation 2.14. Damping of the material expressed as tan δ.

Shear storage modulus, shear loss modulus, and the apparent viscosity of polymer melts change with temperature, composition, MWs and molecular structures of the polymers.

Time-temperature superposition (TTS) is a rheological technique. It is impossible to measure the rheology of a polymer at very low shear rates due to time constraints. It is also impossible to measure the rheology of polymers at very high shear rates due to a number of limitations including centrifugal force and slip stick behavior. However, TTS helps to make an estimation of the rheology of polymers at

very low and high shear rates. For a rheological measurement, a series of shear storage and loss modulus curves ranging 5 frequency decades are obtained at different temperatures. The distance between the curves at different temperatures are termed shift factors (a_T). The obtained curves can be shifted to produce a master curve which ranges 10 frequency decades according to selected reference temperatures. If the reference temperatures are between T_g and T_g + 100°C, the Williams-Landel-Ferry (W-L-F) equations (Vinogradov et al., 1980A) can be used as a model to calculate the free volume of polymers according to Equation 2.15, where a_T is shift factor, C_1 and C_2 are constant for given polymers.

$$\log a_T = -\frac{C_1(T - T_g)}{C_2 + (T - T_g)}$$

Equation 2.15. W-L-F equation.

The free volume theory was first established by Fox and Flory. They considered the volume of a polymer to be composed of both occupied volume and unoccupied volume, which they termed free volume. The free volumes are distributed in the polymer as holes, which are used for the adjustment of polymer conformation. According to further developed free volume theory, the shift factor a_T can also be expressed using the Doolittle equation (Vinogradov et al., 1980B) shown as Equation 2.16, where B is a constant close to 1, and f_g is free volume fraction. Combining the W-L-F equation and the Doolittle equation yields Equation 2.17, where α_f is coefficient of expansion. Therefore, the free volume can be calculated from C_1 and C_2 after fitting master curves obtained with the W-L-F equation.

$$\log a_T = B\left(\frac{1}{f(T)} - \frac{1}{f_g}\right)$$

Equation 2.16. Doolittle equation.

$$\log a_T = -\frac{C_1(T - T_g)}{C_2 + (T - T_g)} = -\frac{\frac{B}{2.303 f_g}(T - T_g)}{\frac{f_g}{\alpha_f}(T - T_g)}$$

Equation 2.17. W-L-F equation combined Doolittle equation.

CHAPTER III

COPOLYMERS OF STYRENE WITH LVES

Chapter Abstract

Copolymers of styrene with a series of linear vinyl esters were prepared. The vinyl esters, including vinyl acetate, vinyl propionate, vinyl hexanoate, and vinyl decanoate ranged from 1 mol% to 19 mol%. Glass transition temperatures of the copolymers ranged from 53 °C to 87 °C. Dynamic mechanical analysis showed that the mole fractions of linear vinyl esters, length of side chains, and relative molecular weights had effects on the storage and loss moduli of the resultant thermoplastics. The mole fractions of linear vinyl esters and length of side chains were dominating effects when the number-average molecular weights of the copolymers were not above 1.0×10^4 g/mol.

Chapter Experimental

Materials

Azobisisobutyronitrile (AIBN), bought from Sigma-Aldrich, was recrystallized and dried before using. St, VA, and VP, purchased from Sigma-Aldrich, were purified by vacuum distillation. VH and VD from TCI America were washed with 2 wt % sodium hydroxide aqueous solutions to remove MEHQ inhibitors, washed by DI water until neutral pH, and then dried with anhydrous sodium sulfate before use. Commercial PS (M_n = 17 × 10^4 g/mol), which was used in the MWs and thermomechanical analysis as a reference, was bought from Sigma-Aldrich. HPLC grade tetrahydrofuran (THF) purchased from Sigma-Aldrich was used as received

Copolymerization Reactivity Ratio Estimation

In order to control the reaction time and feed ratio, it was necessary to determine the reactivity ratios of St with different LVEs. Comonomers were syringed into 5 mL vials with AIBN in different feed ratios. All vials were degassed by vacuum pump before the reactions. All vials were fixed in a water bath at 60 °C equipped with a shaker. The reactant was quenched and washed by cold ethanol, and then dried in a vacuum oven at 60 °C until constant weight. The cumulative compositions of all samples were determined by FT-IR, the details of which were described below. Fineman-Ross plots were applied to determine the reactivity ratios.

Composition Determination

A Nicolet 200 FTIR was used to determine the copolymer compositions. The copolymers were dissolved in THF to make 1 wt % polymer solutions. Uniform liquid films were formed by injection of polymer sample solution in a FT-IR KBr cell purchased from International Glass Inc. The spectrum of 1 wt % PS solution was applied as a baseline, in which there was no carbonyl peak around 1735 cm^{-1}. The spectrum of 1 wt % polyvinyl acetate (PVA), polyvinyl propionate (PVP), polyvinyl hexanoate (PVH), and polyvinyl decanoate (PVD) were used as standards. The carbonyl peaks of the standards were defined as 100%. A series of carbonyl peaks with various peak heights in between the spectrums of PS and homopolymers of different LVEs belonged to corresponding copolymers of St and LVE.

Copolymerization and Sample Handling

St and a series of LVEs along with 2 wt % initiator were charged into a three neck 500 mL flask with a stir bar and condenser. The flask was purged with N_2 to

remove O_2 and trace H_2O. All copolymerizations were carried out in an oil bath at 60 °C under nitrogen. Different reaction times were applied to keep the copolymerization conversion below 20% to prevent compositional drift. All reactions were quenched by pouring the reactant solution into ethanol. Solid samples were washed and immersed in ethanol to remove unreacted monomers and initiator, and then dried in a vacuum oven at 60 °C.

Measurement

The MWDs, along with M_ns and M_ws were determined by using a Varian 400 gel permeation chromatography (GPC) equipped with PL gel 5 μm MIXED-D and Varian Prostar refractive index detector. The GPC was calibrated using PS standard samples from Varian. HPLC grade THF, purchased from Fisher, was used as the mobile phase with the flow rates of 1 mL min^{-1}. T_gs were determined using a Perkin Elmer Jade DSC. A quick heating of 20 °C min^{-1} to 150 °C following by cooling at 10 °C min^{-1} was applied to erase thermal history. The 10 mg samples were then heated from 20 °C to 150 °C at a rate of 5 °C min^{-1}. Sample test bars with dimensions of 50 mm × 10 mm × 1.5 mm were prepared using a Carver press. Storage and loss modulus of all sample bars were analyzed using a Perkin Elmer Pyris Diamond dynamic mechanical analyzer (DMA) under bending test mode. A temperature sweep of 3 °C min^{-1} from 25 °C to 140 °C was conducted at a constant frequency of 1 Hz.

Chapter Results and Discussion

The Compositions of Poly(LVE-co-St) and Reactivity Ratios of St to LVEs

The mole fractions of LVE were determined using the Beer-Lambert Law. Representative spectrums of PS, PVH, and poly(VH-*co*-St) with varying mole

fractions are shown in Figure 3.1 of particular importance are the carbonyl peaks of polyvinyl hexanoate and poly(VH-*co*-St) with various mole fractions of VH. No peak was observed for PS because it lacks a carbonyl group. Therefore, the compositions of those copolymers could be determined using the Beer-Lambert law (Hirai et al., 1975, Chinal et al., 1961). The relationship between the mole fraction and peak height of absorption is expressed in the following Equation 3.1:

$$n_{PVE}\left(mol\%\right)=\frac{a_1^{'}\left(\frac{A_{PVE}}{A_{PS}}\right)-a_1}{\left(a_1^{'}-a_2^{'}\right)\left(\frac{A_{PVE}}{A_{PS}}\right)+\left(a_2-a_1\right)}\times\frac{1}{M_{LVE}}$$

Equation 3.1. Relationship between n_{PVE} and absorption.

In the equation, n_{PVE} is mole fraction of polyvinyl esters. A_{PVE} and A_{PS} are absorption of polyvinyl esters and PS obtained by transmittance ratios, which are I_{PVE}/I_{THF} and I_{PS}/I_{THF}. a_1', a_2', a_1, a_2 are constants derived from Beer-Lambert equation $A=a\times l\times c$, where l is the path length of infrared light, and c is the concentration of polymer solution. M_{LVE} is the molecular weight of LVE.

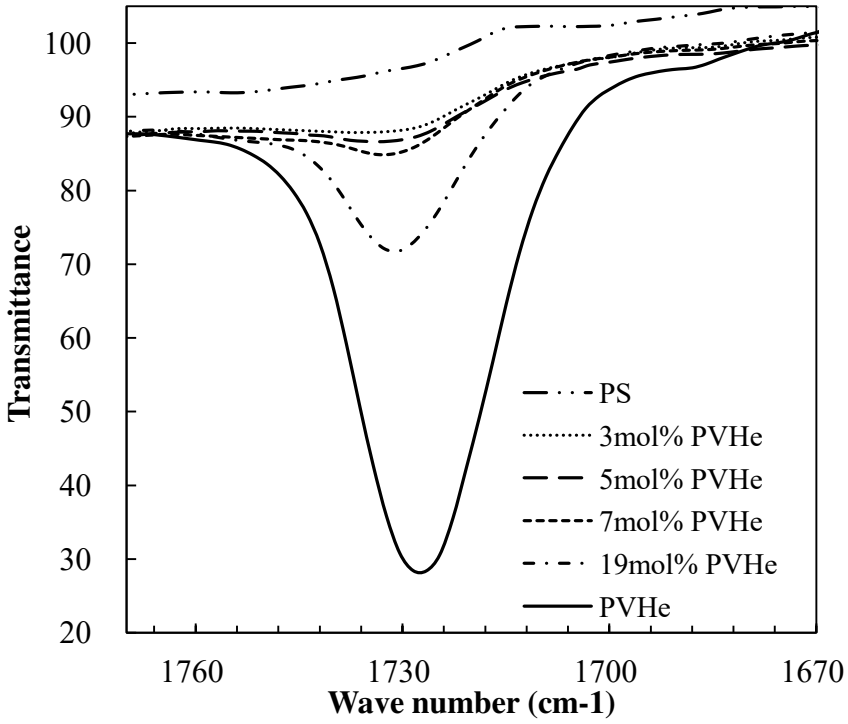

Figure 3.1. FT-IR spectrum of PS, poly(VH-*co*-St) and PVH at 1725cm^{-1}.

According to Figure 3.1, resultant copolymers of St with VH have mole fractions of VH ranging from 3 mol% to 19 mol%. The compositions of all resultant copolymers that obtained using the same method are showed in Table 3.1 along with the feed ratios of reactants. The resultant copolymers, including poly(VA-*co*-St), poly(VP-*co*-St), poly(VH-*co*-St), and poly(VD-*co*-St), contain LVEs ranging from 1 mol% to 19 mol%. The mole fractions of LVEs of poly(VA-*co*-St) series increased with increasing feed ratios of reactants as well as poly(VP-*co*-St), poly(VH-*co*-St) and poly(St-*co*-VD) series because St exhibited a much higher reactivity than all the LVE studied (Mark et al., 1989N). At the same time, the mole fractions of VH and VD are 5 mol% (run 8) and 12 mol% (run 13), which are higher than that of VA with 1 mol% (run 1) in copolymers with the same feed ratios of comonomers (0.5:0.5). This was attributed to the higher reactivity of VH and VD to St than that of VA. Table 3.2 presents the reactivity ratios of St to LVE, including VA, VP, VH, and VD. The

reactivity ratios were determined using the Fineman-Ross method. The monomer feed ratio of St to LVE is defined as F. The cumulative monomer ratio of St to the LVE in the resultant copolymer is defined as f which was determined from the FT-IR spectrums of poly(LVE-*co*-St) as mentioned above. Therefore the reactivity ratios of St (r_1) and certain LVE (r_2) can be obtained by equation 3.2 as shown below. An increasing trend is observed, which indicates the reactivity of LVE to St increases for those LVE have 2, 3, 6, and 10 carbons in fatty acid chains.

Table 3.1. Feed ratios, LVE compositions, M_n, M_w, PDI, and T_g of poly(LVE-*co*-St).

Run	Feed ratio (mol:mol)	LVE (mol%)	LVE (wt %)	M_n (10^{-4} g/mol)	M_w (10^{-4} g/mol)	PDI	$T_{g\text{-}M}$ (°C)[a]	$T_{g\text{-}C}$ (°C)[b]	ΔT_g (%)[c]
PS							87		
Poly(VA-St)	St:VA	VA							
#1	0.5:0.5	1	1	6.2	10.6	1.7	84	86	3
#2	0.3:0.7	4	3	3.1	5.6	1.8	81	85	5
#3	0.1:0.9	13	11	1.2	2.0	1.7	76	79	4
Poly(VP-St)	St:VP	VP							
#4	0.6:0.4	2	2	7.9	13.3	1.7	83	86	3
#5	0.4:0.6	4	4	3.3	6.0	1.8	80	85	5
#6	0.1:0.9	19	19	1.0	1.8	1.7	60	68	11
Poly(VH-St)	St:VH	VH							
#7	0.7:0.3	3	4	8.6	14.8	1.7	76	79	4
#8	0.5:0.5	5	6	5.5	10.0	1.8	74	76	3
#9	0.3:0.7	7	9	3.0	5.4	1.8	73	72	1
#10	0.1:0.9	19	24	1.1	1.8	1.7	54	53	2
Poly(VD-St)	St:VD	VD							
#11	0.7:0.3	8	14	8.7	15.2	1.8	67	69	2
#12	0.7:0.3	9	15	7.6	14.3	1.9	65	66	1
#13	0.5:0.5	12	21	5.6	10.0	1.8	66	64	4
#14	0.3:0.7	17	28	2.4	4.3	1.8	53	52	2

[a] Measured Glass Transition Temperature. [b] Calculated Glass Transition Temperature.

[c] Percentage of Difference between $T_{g\text{-}M}$ and $T_{g\text{-}C}$.

$$\frac{F(f-1)}{f} = r_1 \times \frac{F^2}{f} - r_2$$

Equation 3.2. Fineman-Ross Equation.

It was assumed there was no composition drift due to the low polymerization conversion. Run 12 with a conversion of 10%, is a repeat of run 11 with the conversion of 20%. The compositions and average molecular weights show no obvious difference which indicates no significant composition drift.

Table 3.2. Reactivity ratios of St with LVEs.

Monomer 1	Monomer 2	Reactivity ratios
VA	St	0.01/57
VP	St	0.01/55
VH	St	0.01/30
VD	St	0.01/14

The MWs and MWDs of poly(LVE-co-St)

The M_n, M_w and polydispersity index (PDI) are all presented in Table 3.1. The results show that the average molecular weights of each poly(LVE-*co*-St) series decreased with increasing mole fraction of LVE. Copolymers in run 2 and run 5 have M_n above 3×10^4 g/mol with as low as 4 mol% of LVE. However, the M_n of run 3 and run 6 dropped to nearly 1×10^4 g/mol with LVE mole fractions higher than 13 mol%. Comparatively, poly(VH-*co*-St) (run 9) with a M_n of 3×10^4 g/mol contains 7 mol% VH, which is nearly doubled the M_n of poly(St-*co*-VA) in run 2 and poly(VP-*co*-St) in run 5. For poly(VD-*co*-St) series, much higher LVE compositions and average molecular weights compared to poly(VA-*co*-St) and poly(VP-*co*-St) were observed. The M_n of poly(St-co-VD) was high as 8×10^4 g/mol with 8 mol% of VD, which is

twice as much as VA and VP in run 2 and run 5. The increasing of VD to 17 mol% results in the drop of M_n of poly(VD-*co*-St) to 2.4×10^4 g/mol, which is nearly as high as poly(VA-*co*-St) in run 2, and poly(VH-*co*-St) in run 9. These results indicate that poly(LVE-*co*-St) containing VH and VD can have much higher renewable content along with higher molecular weights than those of VA and VP. The PDI of all samples obtained were around 1.8, corresponding to low copolymerization conversions.

The T_gs of Poly(LVE-co-St)

The T_gs of all the copolymers measured using DSC are all listed in Table 3.1. The T_gs of resultant copolymers in each poly(LVE-*co*-St) series dropped with the increasing of compositions of LVE from 87 °C to as low as 53 °C. The trends of T_gs' decreasing accompany with the changing of LVE compositions for all poly(LVE-*co*-St) series are shown Figure 3.2.

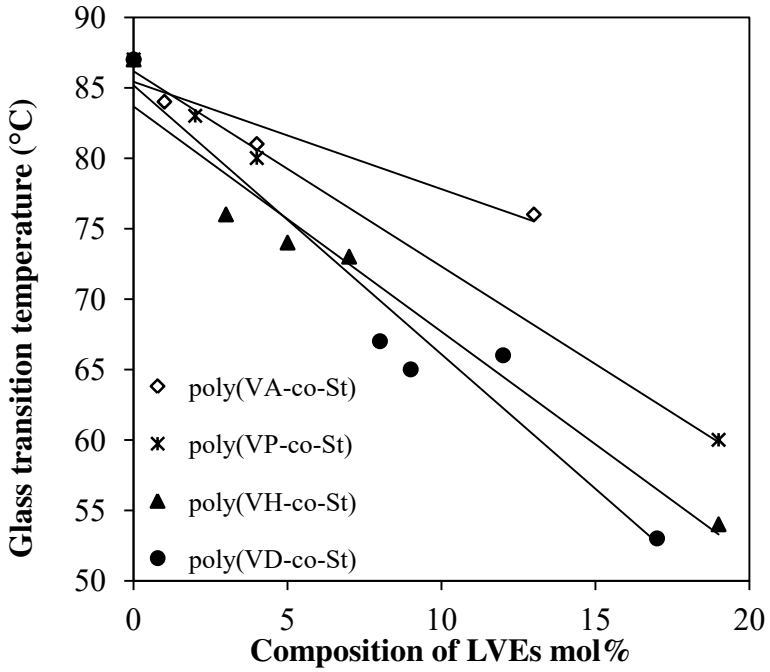

Figure 3.2. The T_gs versus LVE compositions.

The Flory-Fox equation, as shown below, was applied to calculate the theoretical T_gs of the resultant copolymers.

$$\frac{1}{T_g} = \frac{w_1}{T_{g1}} + \frac{w_2}{T_{g2}}$$

Equation 3.3. Flory-Fox Equation.

where T_g, T_{g1}, and T_{g2} are T_gs of resultant poly(St-*co*-VE), PS and PVE, w_1 and w_2 are weight fractions of PS and PVE in copolymers. A comparison of the measured T_gs with calculated values is shown in Table 3.1. The values of ΔT_g in Table 3.1 are defined as the percentage difference between $T_{g\text{-}M}$ and $T_{g\text{-}C}$. All the differences between $T_{g\text{-}M}$ and $T_{g\text{-}C}$ are less than 5% except run 6, which indicates a good agreement between experimental results and theoretical values.

The primary reason for the drop in each T_gs' series is the much lower T_g of the LVE homopolymers' than PS. As shown in Table 3.1, copolymers prepared from VD and VH have a larger decrease compared to those derived from VA and VP when the mole fractions of LVEs are less than 15%. A comparison of the T_gs of copolymers with similar mole fractions of LVE, such as run 2, run 5, run 7, and run 8 containing around 4 mol% of LVE, shows that copolymers of VH have lower T_g than those of VA and VP. This was explained by the fact that VH has a longer side chain of six carbons ($CH_3(CH_2)_4COO$-) in the copolymers than VA and VP which has side chain of two carbons (CH_3COO-) and three carbons (CH_3CH_2COO-). However, copolymers of VA and VP mentioned above have similar T_g due to their very similar side chain structures. A comparison of run 9, run 11 and run 12 shows a similar phenomenon, which was attributed to VH having a shorter side chain than VD ($CH_3(CH_2)_8COO$-).

Similar conclusions can also be drawn from the comparison of run 3 and run 13.

The effects of side chain length are not very obvious when the mole fractions of LVE are above 17 mol%. Run 6 and run 10 are poly(VP-*co*-St) and poly(VD-*co*-St) that both have 19 mol% of LVE and M_n of 1.0×10^4 g/mol, whose $T_{g\text{-}M}$ are only 5°C in difference. Run 10 and run 14 are poly(VH-*co*-St) and poly(VD-*co*-St) that have similar $T_{g\text{-}M}$ and LVE compositions. It is difficult to indicate that the drop of average molecular weighs is the main reason for the decreasing of glass transition temperatures. On one hand, poly(VA-*co*-St) in run 3 with the M_n of 1.2×10^4 g/mol still have the $T_{g\text{-}M}$ of 76 °C. On the other hand, PS which have M_ns of 3.0×10^4 g/mol and 0.3×10^4 g/mol have different T_gs, which are 100 °C and 40 °C (Stevens et al., 1998).

Dynamic Mechanical Analysis of Poly(LVE-co-St)

The storage moduli of poly(VH-*co*-St) and poly(VD-*co*-St) are shown in Figures 3.3 and Figure 3.4, respectively. The storage moduli of poly(VH-*co*-St) with VH compositions ranging from 3 mol% to 7 mol% decreased slightly from 10×10^{10} Pa to 8×10^{10} Pa. However, the modulus of poly(St-co-VH) with 19 mol% of VH dropped to 4.5×10^{10} Pa sharply as shown in Figure 3.3. The moduli of poly(VD-*co*-St) with 8 mol% and 12 mol% are 8×10^{10} Pa and 7×10^{10} Pa. An obvious decrease of the modulus to about 4.5×10^{10} Pa is observed for poly(VD-*co*-St) with 17 mol% of VD. A commercial PS with a M_n of 17×10^4 g/mol was also tested to serve as a reference, the modulus of which is about 12×10^{10} Pa. Copolymers with less than 10 mol% of VH and VD still have storage modulus as high as 8×10^{10} Pa, which are two third of the commercial PS. The slight drop of moduli in poly(VH-*co*-St) and poly(VD-*co*-St) was attributed to the fact that PS has a much

higher storage modulus than those of PVH and PVD which are both liquid at room temperature. The other important reason for the gradual decrease in storage modulus of run 8 and run 9 compared to run 7 is the much lower M_n. The sharp decline in the storage modulus of run 10 could also be attributed to the very high mole fraction of VH which makes the copolymer less elastic in addition to the extremely low molecular weight. A similar trend was also observed for run 11, run 12, run 13 and run 14. As the repeat of run 11, resultant copolymer of run 12 has very similar mole fractions of VD and M_n have nearly the same values in storage moduli.

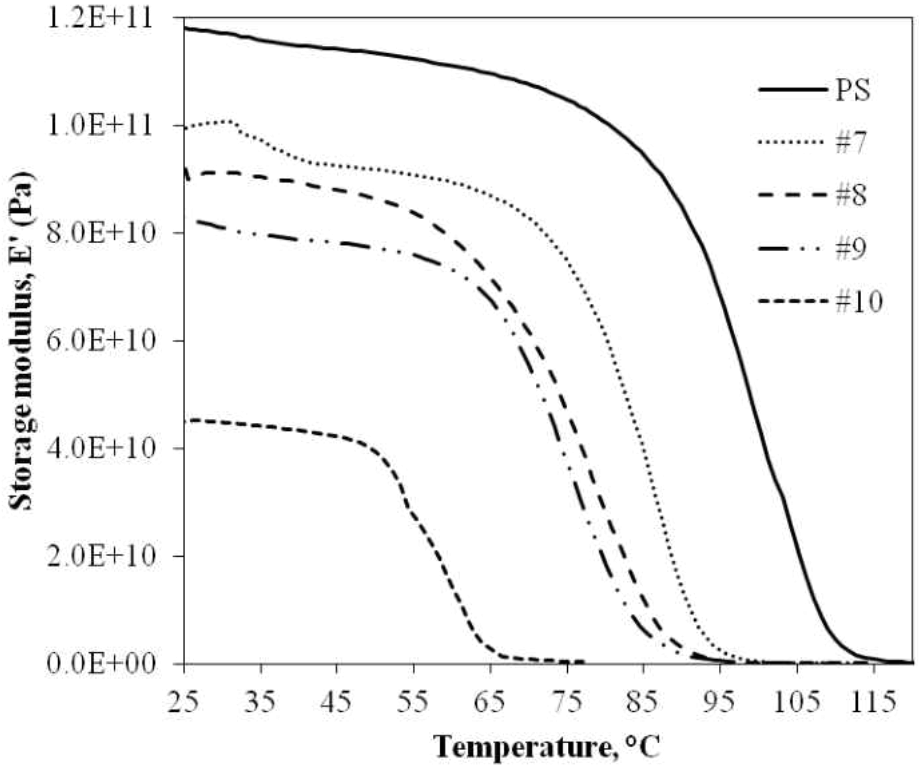

Figure 3.3. Storage moduli of poly(VH-*co*-St) series.

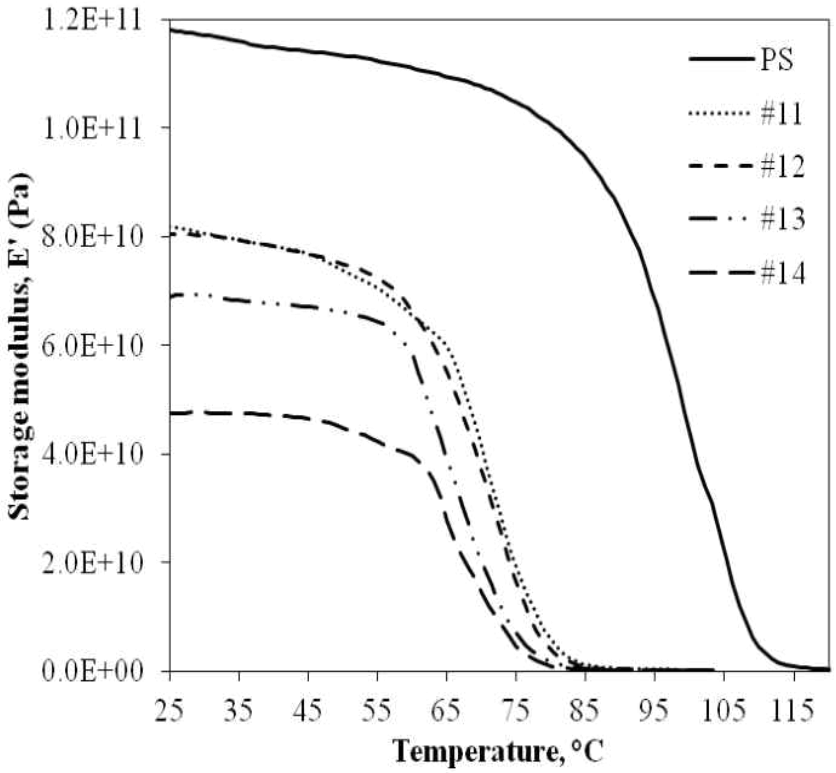

Figure 3.4. Storage moduli of poly(VD-*co*-St) series.

A comparison of run 9, run 11, and run 12 presented in Figure 3.5 shows that copolymers with similar mole fractions of VH and VD but different M_ns have similar storage moduli. The most probable reason is the reverse effect of molecular weight and mole fractions of LVE with various side chains. On one hand, the longer side chains of poly(VD-*co*-St) serve to decrease the elasticity of copolymers compared to $CH_3(CH_2)_4COO$- and poly(VH-*co*-St). However, the higher molecular weights of run 11 and run 12 contribute to a larger storage modulus. These opposing factors interact to adjust the resultant storage moduli of run 11 and run 12 which are comparable to run 9.

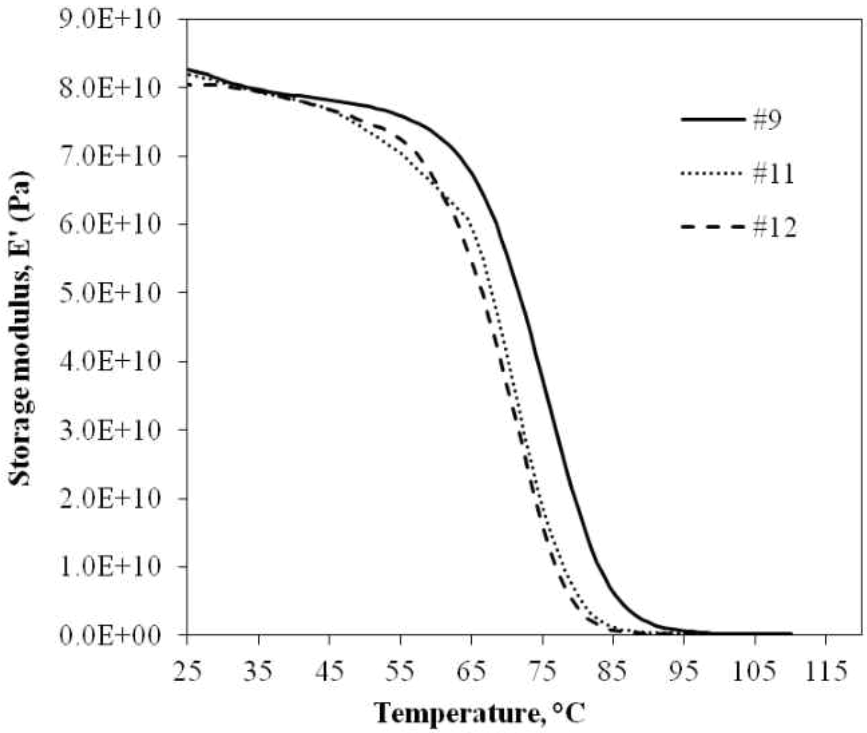

Figure 3.5. Storage moduli of poly(VH-*co*-St) and Poly(VD-*co*-St) with 7 mol% of LVEs.

The loss moduli of both poly(VH-*co*-St) and poly(VD-*co*-St) are shown in Figures 3.6 and Figure 3.7. The loss moduli increased gradually with increasing mole fractions of vinyl esters for both series due to the viscous properties of PVH and PVD. Although the molecular weights of run 9 and run 13 are significantly lower, their loss moduli are the highest among their series. It is probable that the effects of mole fractions of LVE on the loss moduli were stronger than that of the molecular weights when the mole fractions of LVE were less than 12%. However, run 10 and run 14, with LVE contents higher than 15 mol%, showed a marked decrease in loss modulus. This large decrease was attributed to the reduction in molecular weights. The peak maximum of all the curves shifted to lower temperatures which corresponds to the decline of T_g of both poly(VH-*co*-St) and poly(VD-*co*-St). But the shift is not very distinct because those samples have similar mole contents of LVE.

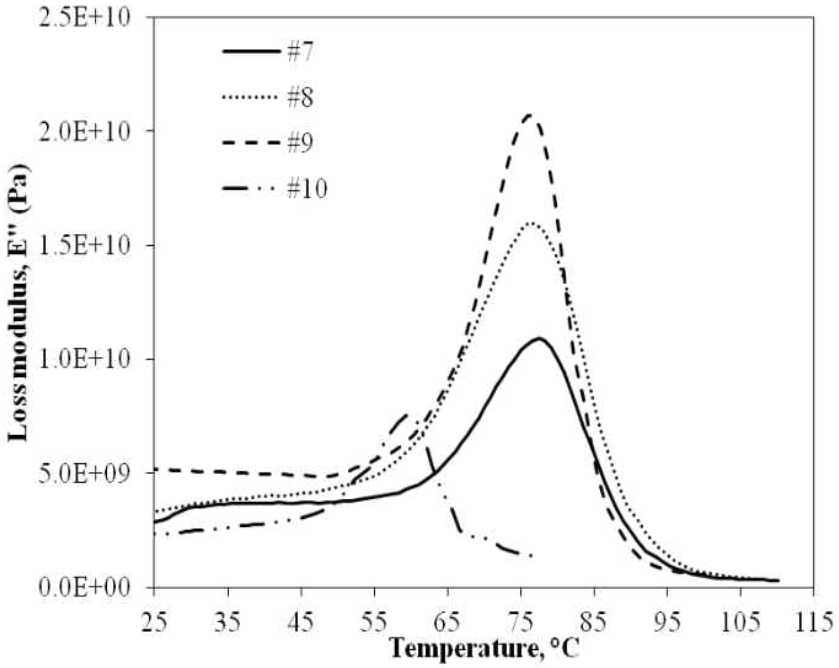

Figure 3.6. Loss moduli of poly(VH-*co*-St) series.

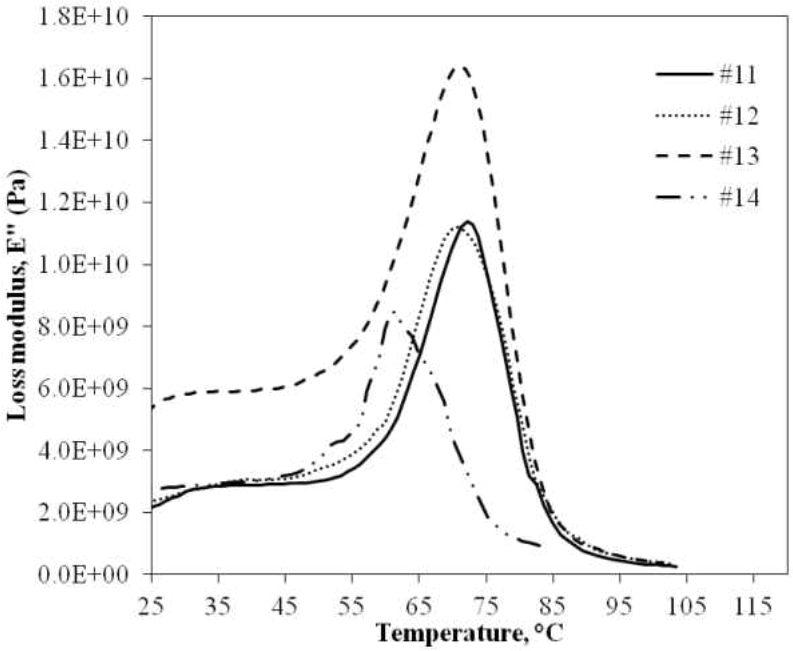

Figure 3.7. Loss moduli of poly(VD-*co*-St) series.

A comparison of loss moduli of poly(VH-*co*-St) and poly(VD-*co*-St), each with around 7 mol% LVE, is shown in Figure 3.8. Copolymer run 9 with lower

molecular weight has a larger loss modulus than either run 11 or run 12. PVH which is more viscous than PVD had a greater effect on the loss modulus when they are at similar mole fractions.

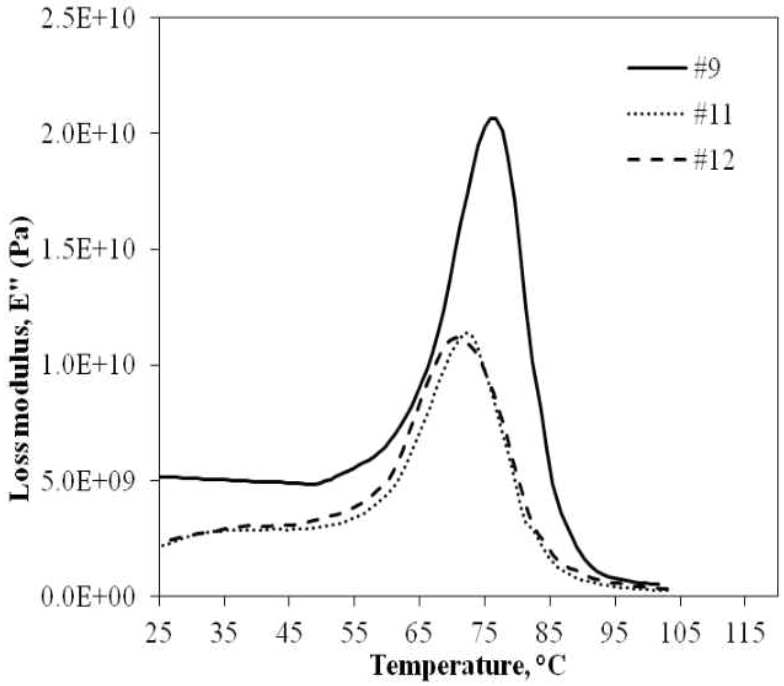

Figure 3.8. Loss moduli of poly(VH-*co*-St) and poly(VD-*co*-St) with 7 mol% of LVEs.

In addition to poly(VH-*co*-St) and poly(VD-*co*-St), DMA test of poly(VA-*co*-St) and poly(VP-*co*-St) were carried out under the same conditions. The moduli of run 1 and run 4, which had have very low LVE contents, are about 9×10^{10} Pa. DMA test of run 2, run 3, run 5, and run 6 did not get reliable moduli data due to the extremely high brittleness of the resultant copolymers. Therefore, the resultant copolymers were not suitable for commodity applications compared to poly(VH-*co*-St) and poly(VD-*co*-St) with similar molecular weights.

Chapter Conclusions

A series of copolymers of St with LVE of varying molecular weights were prepared. The reactivity ratios of the various LVE with styrene were determined. Thermal property studies of these thermoplastics showed that the T_gs of PS was reduced from 87 °C to 53 °C by incorporation of LVE from 1 mol% to 19 mol%. The M_n of the copolymers became smaller with greater incorporation of LVE due to the reactivity ratio difference between St and LVE. DMA analysis found that relative molecular weights, the contents of LVE, and the length of side chains would all have an effect on the storage and loss modulus of the copolymers.

CHAPTER IV

COPOLYMERS OF MMA WITH LVES

Chapter Abstract

A series of copolymers of methyl methacrylate (MMA) with linear vinyl esters (LVEs), including vinyl acetate (VA), vinyl propionate (VP), vinyl hexanoate (VH), and vinyl decanoate (VD), were synthesized by free radical copolymerizations at 60 °C. The LVE composition was varied from 3 mol% to 41 mol% in the resultant copolymers. The glass transition (T_gs) of the copolymers ranged from 60 °C to 108 °C. The storage moduli (E') of the copolymers decreased as the LVE composition increased from 4×10^9 Pa to 1.5×10^9 Pa. Copolymers containing VD exhibited a more obvious reduction in storage moduli and a larger shift of the tan δ peak. The rheological property analysis of the copolymers at different temperatures showed that the shear storage and loss moduli of poly(LVE-*co*-MMA) (G' and G") were mostly dominated by MWs. Short side chains did not have an obvious impact on the shear moduli or complex viscosities.

Chapter Experimental

Materials

Azobisisobutyronitrile (AIBN), purchased from Sigma-Aldrich, was recrystallized and dried before use. MMA, VA, and VP from Sigma-Aldrich were purified by vacuum distillation. VH and VD from TCI America were pretreated with 2 wt % sodium hydroxide aqueous solutions to remove inhibitors, and washed to neutral pH using deionized water. The monomers were then dried using anhydrous sodium

sulfate. $CDCl_3$ (99.96% atom D) purchased from Sigma Aldrich was used as received. HPLC grade tetrahydrofuran (THF) from Sigma-Aldrich was used as received.

Copolymerization and Sample Handling

MMA and LVEs, including VA, VP, VH, and VD, with 2 wt % initiators were charged in a 500 mL three-neck flask equipped with magnetic stirring and refluxing. The flask was purged with N_2 to remove O_2 and trace H_2O. Copolymerizations were carried out in an oil bath at 60 °C under nitrogen flow. Compositional drift was prevented by controlling the copolymerization conversion to below 20%. The reaction was quenched by pouring the mixtures into ethanol. The resultant copolymers were washed and immersed in ethanol to remove most of the unreacted monomers, and dried in a vacuum oven at 60 °C.

Measurement

The copolymers synthesized were dissolved in $CDCl_3$ (99.96% atom D). The compositions were determined using a Brücker Advanced 500 NMR spectrometer. The number-average molecular weight (M_n), weight-average molecular weight (M_w), and molecular weight distribution (MWD) were determined using a Varian 400 gel permeation chromatography (GPC) equipped with a PL gel 5 μm MIXED-D and Varian Prostar refractive index detector. The GPC was calibrated using polystyrene standard samples from Varian. THF was used as the mobile phase with a flow rate of 1 mL min^{-1}. Thermomechanical properties were analyzed using dynamic mechanical analysis (DMA). Sample bars with dimensions of 50 mm × 10 mm × 1.5 mm were prepared using a Carver press. Storage moduli and tan δ of all samples were obtained using a Perkin Elmer Pyris Diamond dynamic mechanical analyzer using bending test

mode. A temperature sweep of 2 °C min^{-1} from 10 °C to 150 °C was conducted at a constant frequency of 1 Hz. The rheological measurements were carried out using an AR 2000 paralleled-plate rheometer with a 1.5 mm gap under a nitrogen flow. Both the cell compliance and geometry compliance were calibrated using instrument software. Samples were loaded on to the paralleled-plates and trimmed after they were heated to the measurement temperatures. The oscillatory frequency sweeps were completed at temperatures of 180 °C, 200 °C, and 220 °C for all samples. An oscillatory stress sweep was carried out before each run to ensure a linear viscosity range.

Chapter Results and Discussion

Structural Characterization

A variety of LVEs with varying MWs were used in this research. There are 2, 3, 6, and 10 carbon atoms on the fatty acid chains of VA, VP, VH, and VD respectively. The resultant random copolymers, including poly(VA-*co*-AA), poly(VP-*co*-AA), poly(VH-*co*-AA), and poly(VD-*co*-AA), are shown in Figure 4.1. The chemical shifts of poly(LVE-*co*-MMA) (^{1}H-NMR, 500MHz, $CDCl_3$, δ ppm) are given by: poly(VA-*co*-MMA), 5.0 (mH, -C$\underline{H}$-), 2.0 (1H, -CO-C$\underline{H}_3$), 1.7 (2H, -C$\underline{H}_2$-), 3.6 (1H, -O-C$\underline{H}_3$), and 1.5 (1H, -C$\underline{H}_3$); poly(VP-*co*-MMA), 5.0 (mH, -C$\underline{H}$-), 2.3 (3H, -CO-C$\underline{H}_2$-CH_3), 1.0 (1H, -CO-CH_2-C$\underline{H}_3$), 1.7 (2H, -C$\underline{H}_2$-), 3.6 (1H, -O-C$\underline{H}_3$), and 1.5 (1H, -C$\underline{H}_3$); poly(VH-*co*-MMA), 5.0 (mH, -C$\underline{H}$-), 1.0 (1H, -CO-$(CH_2)_4$-C$\underline{H}_3$), 3.6 (1H, -O-C$\underline{H}_3$), and 1.3~2.3 (mH, -CO-$(C\underline{H}_2)_4$-CH_3, -C$\underline{H}_2$-, and -C$\underline{H}_3$); poly(VD-*co*-MMA), 5.0 (mH, -C$\underline{H}$-), 1.0 (1H, -CO-$(CH_2)_8$-C$\underline{H}_3$), 3.6 (1H, -O-C$\underline{H}_3$), and 1.3~2.3 (mH, -CO-$(C\underline{H}_2)_8$-CH_3, -C$\underline{H}_2$-, and -C$\underline{H}_3$).

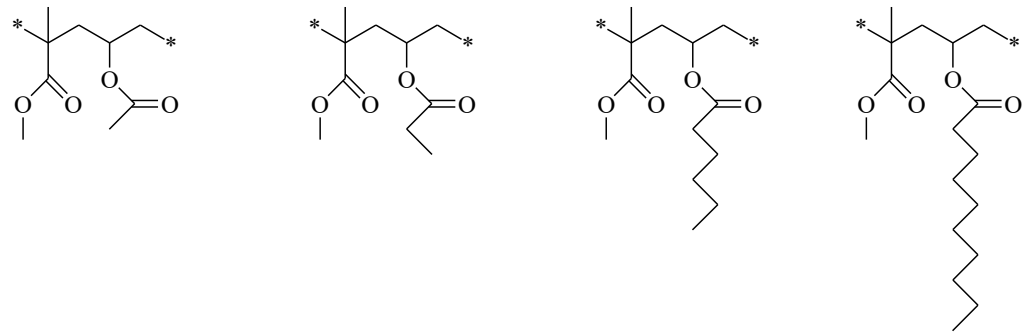

poly(VA-*co*-MMA) poly(VP-*co*-MMA) poly(VH-*co*-MMA) poly(VD-*co*-MMA)

Figure 4.1. The chemical structures of poly(LVE-*co*-MMA).

Composition, MWs, and MWDs of Poly(LVE-co-MMA)

The ^{1}H-NMR spectrums were used to estimate the compositions of MMA and LVEs. Integration of hydrogen on methyl of MMA (δ = 3.6 ppm, 1H, -CO-C<u>H</u>$_3$) and hydrogen on methine of LVEs (δ = 4.5~5.5 ppm, mH, -C<u>H</u>-) were carried out to determine the molar ratios of MMA to LVE. Table 4.1 shows the feed ratio, LVE compositions, MWs and T_gs of the polymers produced for this work. The compositions of LVEs in the poly(LVE-*co*-MMA) are lower than their initial monomer feed compositions due to the lower reactivity ratios of LVEs than MMA. The reactivity ratios of MMA to LVEs were r_{MMA}=5.2/r_{VA}=0.06, r_{MMA}=7.4/r_{VP}=0.06, r_{MMA}=0.18/r_{VA}=0.06, and r_{MMA}=0.32/r_{VA}=0.06, which were calculated using the Fine-Loss method as discussed in Chapter 3. These values are different from the literature values (Mishra et a., 2009C) due to the relatively high copolymerization conversion (around 20%).

Table 4.1. Feed ratios, LVE compositions, M_n, M_w, PDI, and T_g of poly(LVE-*co*-MMA).

	Feed ratio (mol:mol)	C_{LVE}* mol%	C_{LVE} wt%	M_n ($\times 10^5$ g/mol)	M_w ($\times 10^5$ g/mol)	PDI (M_w/M_n)	$T_{g\text{-}M}$ (°C)	$T_{g\text{-}C}$ (°C)
PMMA		0	0	3.2	5.6	1.8	120	
poly(VA-co-MMA)								
VA-1	0.5:0.5	12	10	1.8	3.2	1.8	108	110
VA-2	0.7:0.3	27	24	1.1	2.2	1.9	94	93
VA-3	0.9:0.1	41	37	0.6	1.4	2.0	78	81
poly(VP-co-MMA)								
VP-1	0.5:0.5	12	12	1.6	3.1	2.0	103	101
VP-2	0.7:0.3	25	25	0.9	2.1	2.2	84	82
VP-3	0.9:0.1	40	40	0.6	1.3	2.3	60	63
poly(VH-co-MMA)								
VH-1	0.1:0.9	5	7	2.7	6.6	1.8	104	105
VH-2	0.3:0.7	8	11	2.3	4.1	1.8	94	96
VH-3	0.5:0.5	10	14	1.9	3.5	1.8	90	88
VH-4	0.7:0.3	19	25	1.1	2.2	2.0	70	67
poly(VD-co-MMA)								
VD-1	0.1:0.9	3	6	2.7	4.7	1.7	100	99
VD-2	0.3:0.7	6	11	2.2	4.3	2.0	90	84
VD-3	0.5:0.5	8	15	1.7	3.3	2.0	80	77
VD-4	0.7:0.3	12	21	1.2	2.5	1.9	60	57

* C_{LVE} is the mole fractions of LVEs in copolymers.
$T_{g\text{-}M}$ is the measured T_g, and $T_{g\text{-}C}$ is the predicted T_g.

The MWs of poly(VA-*co*-MMA), poly(VP-*co*-MMA), poly(VH-*co*-MMA), and poly(VD-*co*-MMA) series all decreased with increasing LVE compositions. At the same time, all the MWs were lower than homoPMMA produced under similar conditions (M_n=3.2 × 10^5 g/mol, M_w=5.6 ×10^5 g/mol). This is attributed to the lower reactivity ratios of LVEs compared to MMA (Mishra et al., 2009C). The M_ns of poly(LVE-*co*-MMA) ranged from 2.7 × 10^5 g/mol to 5.6 × 10^5 g/mol with LVE compositions varying from 3 mol% to 41 mol%. Considering that disproportionation (Odian, 1993) is the dominant termination mechanism of PMMA, the PDI values around 2.0 for all poly(LVE-*co*-MMA) indicates the MWDs are close to their

theoretical value.

Thermomechanical Properties of Poly(LVE-co-MMA)

Comparisons of the storage moduli of PMMA with all poly(LVE-*co*-MMA) series are shown in Figures 4.2 (a-d). Generally, the storage moduli decreased with increasing LVE compositions. This behavior was attributed to the side chains of LVEs behaving like plasticizers in the copolymers, making the copolymers less rigid. According to Figure 4.2 (a), the storage moduli of poly(VA-*co*-MMA) series decreased from around 3.0×10^9 Pa to 2.0×10^9 Pa with increasing VA compositions and declining M_n. The reduction in storage modulus of VA-3 is not obvious although VA-3 (C_{VA} = 41 mol%, $M_n = 0.6 \times 10^5$ g/mol) has a much higher VA composition and lower M_n compared to VA-1 and VA-2. The comparisons of poly(VP-*co*-MMA) series, poly(VH-*co*-MMA) series, and poly(VD-*co*-MMA) exhibited similar phenomena. The storage moduli reduced from about 3.5×10^9 Pa to 1.5×10^9 Pa for poly(VP-*co*-MMA) as shown in Figure 4.2 (b). A decrease from 4.0×10^9 Pa to 2.0×10^9 Pa are shown for poly(VH-*co*-MMA) as presented in Figure 4.2 (c). The decrease from 4.0×10^9 Pa to 1.5×10^9 Pa for are poly(VD-*co*-MMA) series as presented in Figure 4.2 (d).

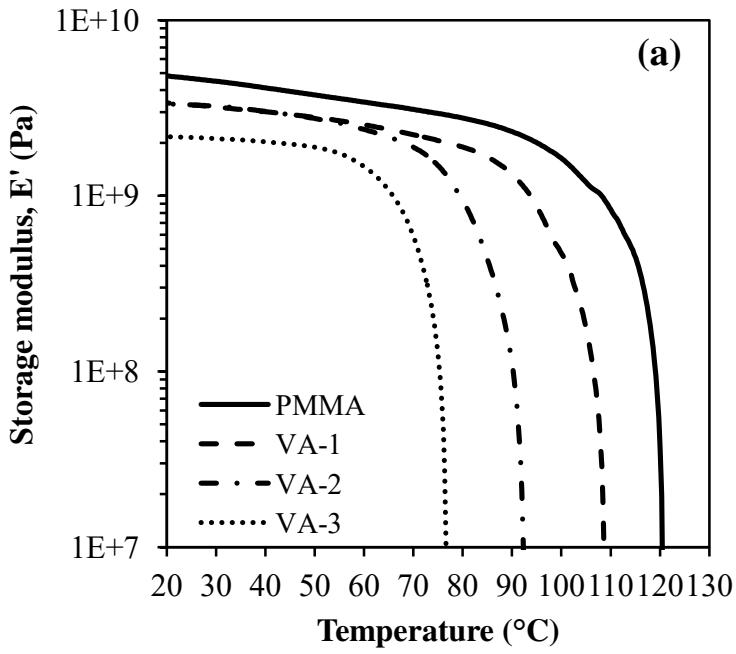

Figure 4.2 (a). Storage moduli of poly(VA-*co*-MMA) series.

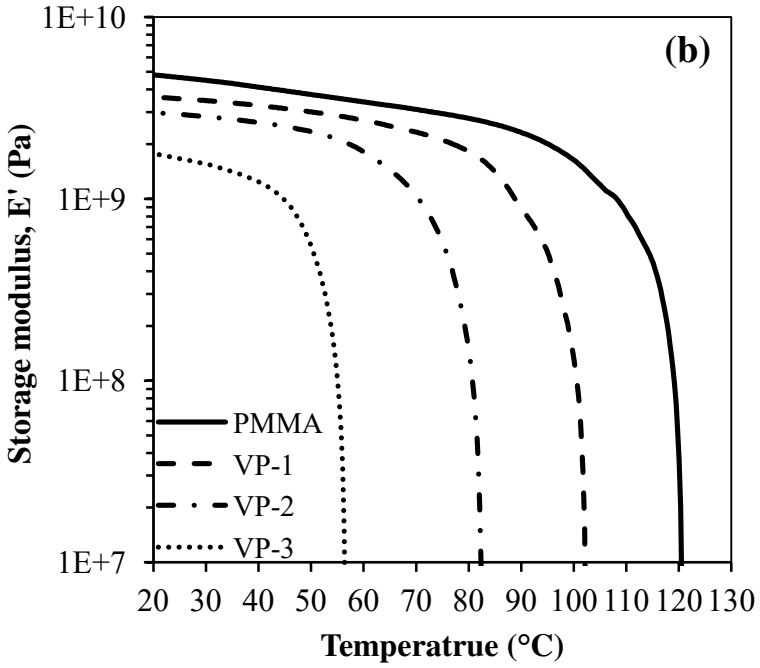

Figure 4.2 (b). Storage moduli of poly(VP-*co*-MMA) series.

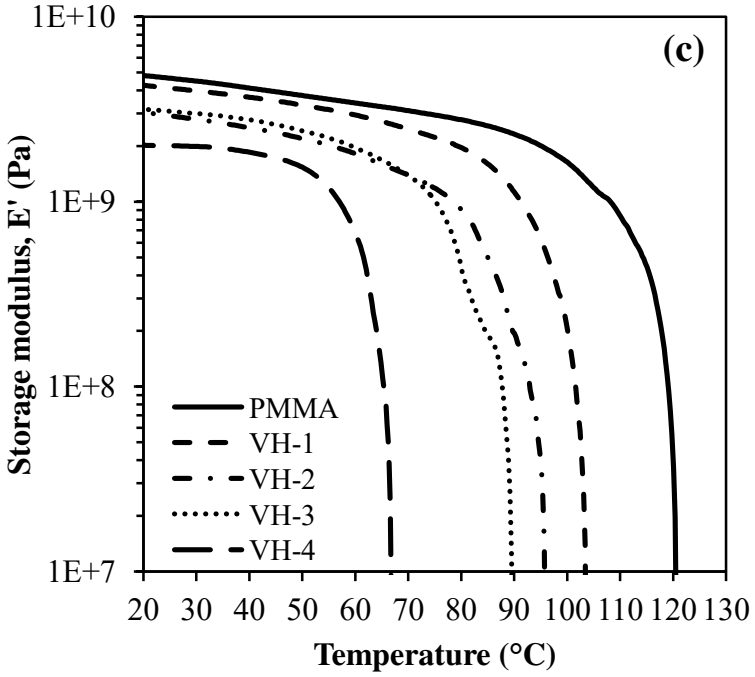

Figure 4.2 (c). Storage moduli of poly(VH-*co*-MMA) series.

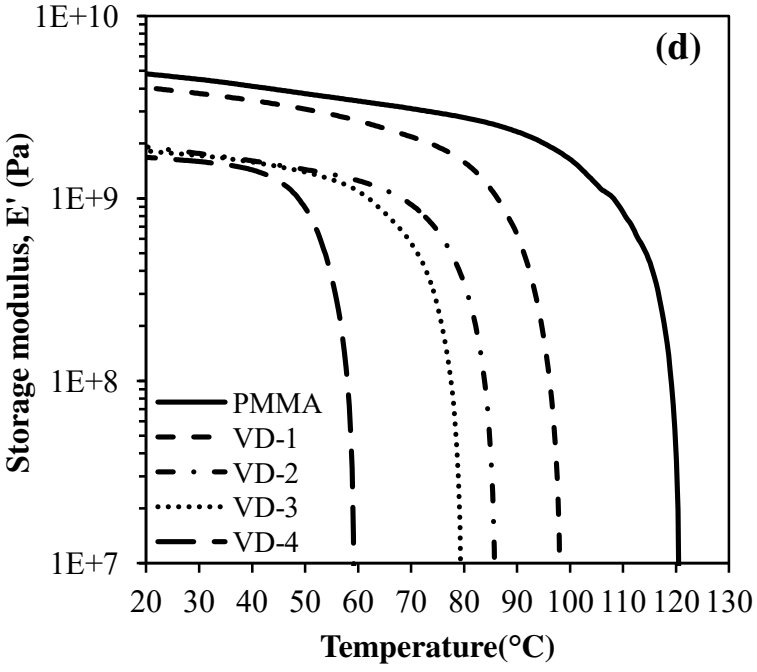

Figure 4.2 (d). Storage moduli of poly(VD-*co*-MMA) series.

A comparison of the storage moduli of VA-1, VP-1, VH-3, and VD-3, which have similar M_ns (around 1.7×10^5 g/mol), is made in Figure 4.3 (a). The low

temperature storage moduli of VA-1, VP-1, and VH-3 are quite similar (around 3.0 × 10^9 Pa), while VD-3 is significantly lower (around 1.5 × 10^9 Pa). Although VD-3 has a lower LVE composition (C_{VD} = 8 mol%) than the others (C_{VA}, C_{VP} and C_{VH} ≈ 12 mol%), its low temperature storage modulus is rough half. The longer side chain of VD-3 (-O-CO-$(CH_2)_8$-CH_3) reduces the elasticity of the copolymer. Another comparison of storage moduli of VA-2, VP-2, VH-4, and VD-4, which have similar M_ns (around 1.0 × 10^5 g/mol), are presented in Figure 4.3 (b). This shows a more obvious trend of decrease. As mentioned in Figure 4.3 (a), the longer chain of VD lead to a greater decline in the storage modulus even when the VD composition in VD-4 (C_{VD} = 12 mol%) is not as high as those of VA-2 (27 mol%), VP-2 (25 mol%), and VH-4 (19 mol%). The storage moduli of all the resultant copolymers ranged from 4 × 10^9 Pa to 2 × 10^9 Pa, which indicates the resultant materials still have enough strength for transparent boards and containers when beneath their glass transition temperatures.

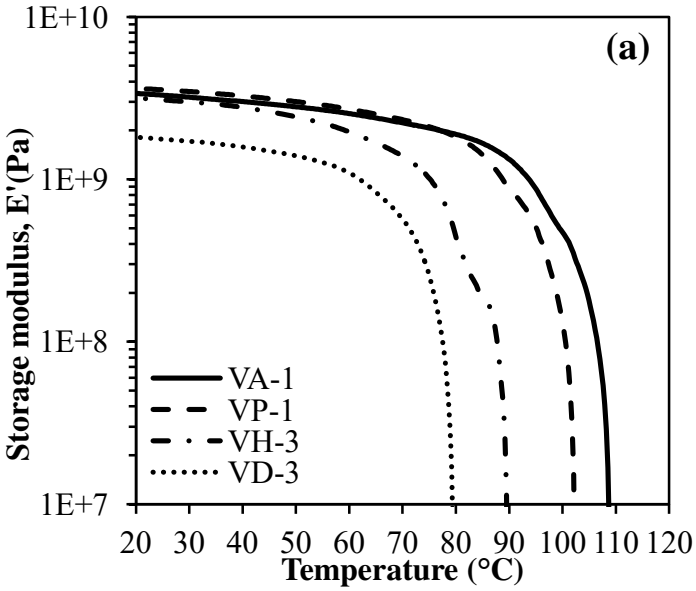

Figure 4.3 (a). Storage moduli of VA-1, VP-1, VH-3, and VD-3.

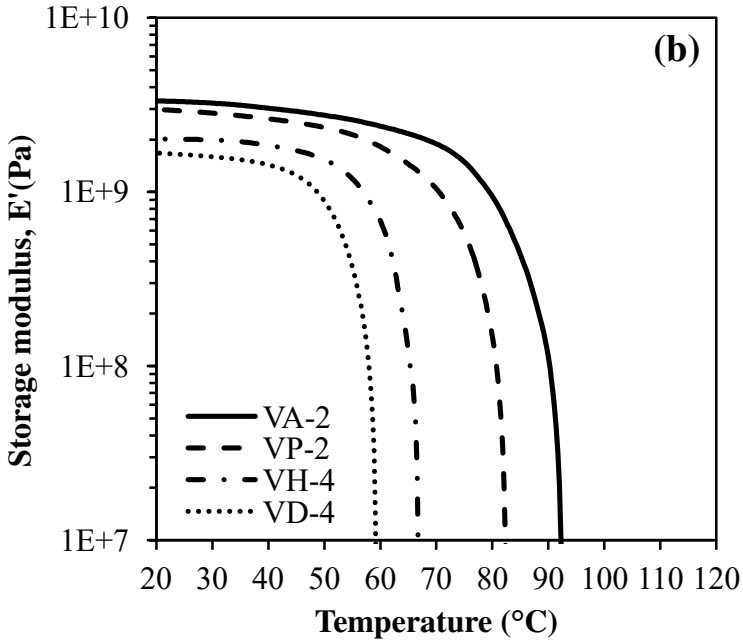

Figure 4.3 (b). Storage moduli of VA-2, VP-2, VH-4, and VD-4.

The tanδ distributions of all poly(LVE-*co*-MMA) series are presented in Figure 4.4 (a-d). The T_gs of the resultant copolymers are listed in Table 4.1. The T_gs decreased gradually from 120 °C with increasing LVE composition for each poly(LVE-*co*-MMA) series. The T_gs reached as low as 60 °C for poly(VP-*co*-MMA) and poly(VD-*co*-MMA). The motions of the polymer chains were facilitated by incorporation of more flexible side chains, which resulted in the shifts of T_gs to lower temperatures.

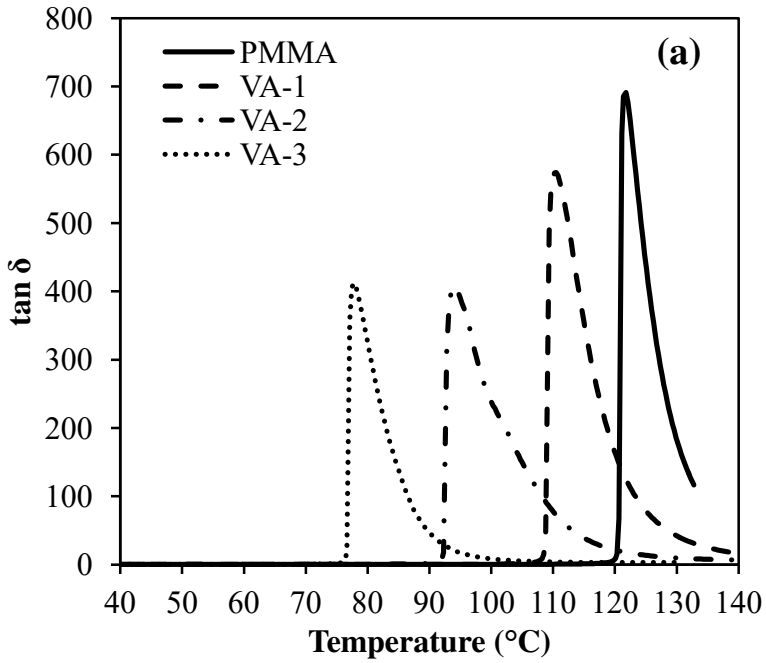

Figure 4.4 (a). tan δ distribution of poly(VA-*co*-MMA) series.

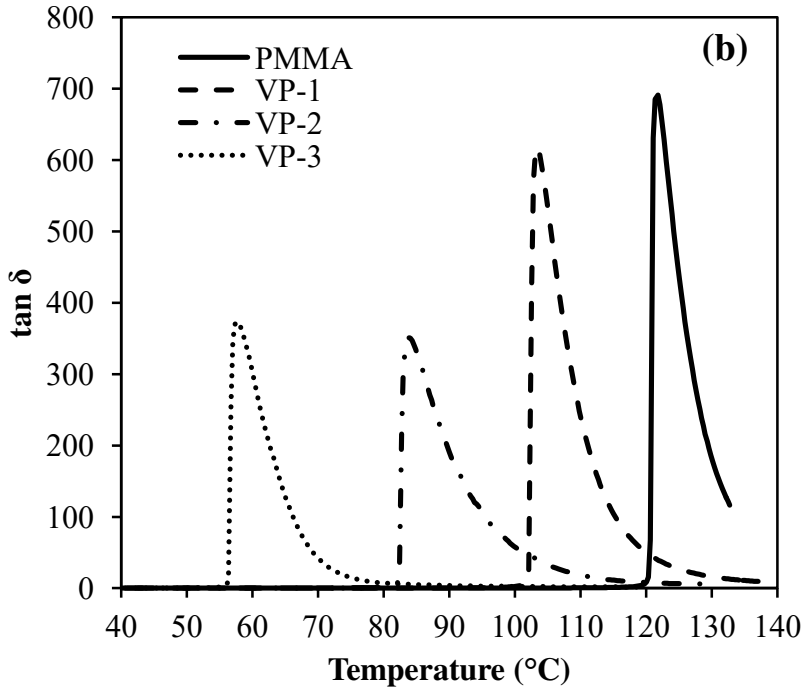

Figure 4.4 (b). tan δ distribution of poly(VP-*co*-MMA) series.

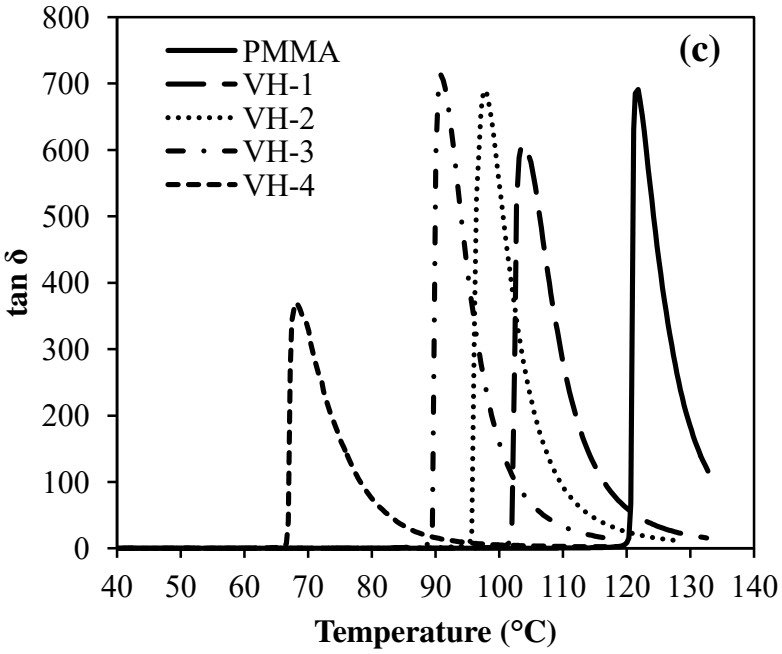

Figure 4.4 (c). tan δ distribution of poly(VH-*co*-MMA) series.

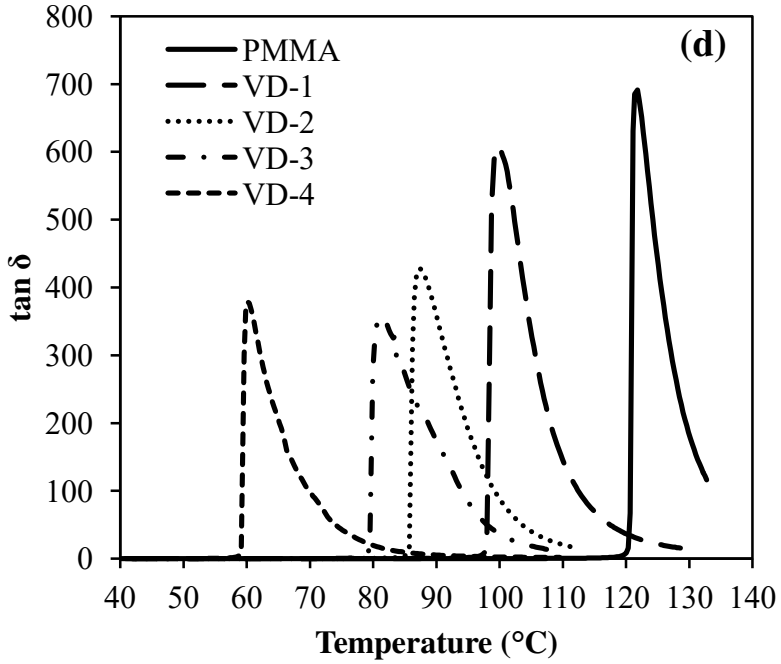

Figure 4.4 (d). tan δ distribution of poly(VD-*co*-MMA) series.

A comparison of tan δ distributions of VA-1, VP-1, VH-3, and VD-3, which have similar M_ns (around 1.7×10^5 g/mol), is shown in Figure 4.5 (a). The shift in T_gs

to lower temperatures can be observed according to the order of VA-1, VP-1, VH-3, and VD-3. For VA-1, VP-1, and VH-3, which have similar LVE compositions (C_{LVE} = 12 mol%), the reduction of T_gs is attributed to the increase of side chain lengths from 2 to 6 carbon atoms. The increase of side chain length resulted in larger distances between polymer backbones, which lead to the increase of free volumes of the copolymers. It can be seen more clearly from the T_g of VD-3. VD-3, which had a lower LVE composition (C_{VP} = 8 mol%) still had the lowest T_g in this comparison. Another comparison of VA-2, VP-2, VH-4, and VD-4, which had similar M_ns (around 1.1×10^5 g/mol), is made in Figure 4.5 (b). The T_g of VH-4 (C_{VH} = 19 mol%) was lower than those of VA-2 (C_{VA} = 27 mol%) and VP-2 (C_{VP} = 25 mol%). VD-4 (C_{VD} = 12 mol%), which had a much lower LVE composition still but showed the lowest T_g in the comparison. This shows that VD has the largest effect on increasing free volume.

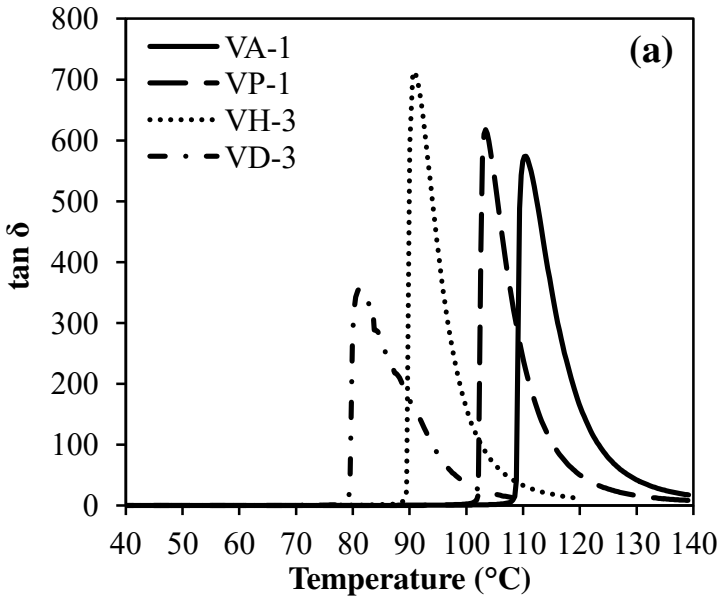

Figure 4.5 (a). tan δ distribution of VA-1, VP-1, VH-3, and VD-3.

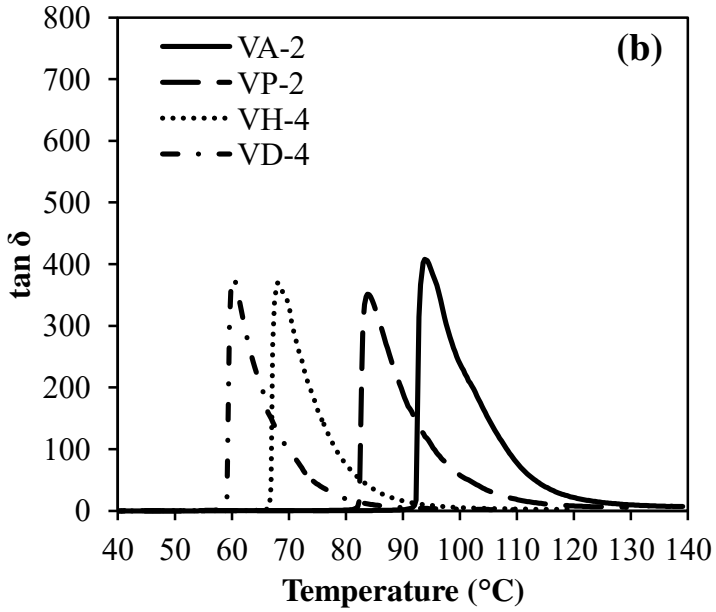

Figure 4.5 (b). tan δ distribution of VA-2, VP-2, VH-4, and VD-4.

A quick comparison of the T_gs of VP-3 (T_g = 60 °C, VP = 40 mol%, and M_n = 0.6 × 10^5 g/mol,) and VD-4 (T_g = 60 °C, VD = 12 mol%, and M_n = 1.2 × 10^5 g/mol) also shows that much lower LVE compositions are needed for poly(VD-*co*-MMA) than poly(VP-*co*-MMA) to lead to similar reduction in the T_g. The longer side chain of poly(VD-*co*-MMA) had a greater impact on the T_gs of the copolymers.

Rheological Properties of Poly(LVE-co-MMA)

Shear Storage and Loss Moduli of Poly(LVE-co-MMA)

The shear storage and loss moduli of poly(VA-*co*-MMA), poly(VP-*co*-MMA), poly(VH-*co*-MMA), and poly(VA-*co*-MMA) series as a function of frequency at 180 °C, are shown in Figure 4.6 (a-d). The shear storage and loss moduli of PMMA at 180 °C were used as reference data for the comparison. In general, the shear storage and loss moduli decreased gradually with increasing MWs and LVE compositions. Reductions in MWs tend to result in declines in the shear moduli. These reductions were also due to the side chains of poly(LVE-co-MMA)

which increased the distance between the copolymer backbones. This facilitated the flow of molecules compared to the more efficient packing of homoPMMA molecules.

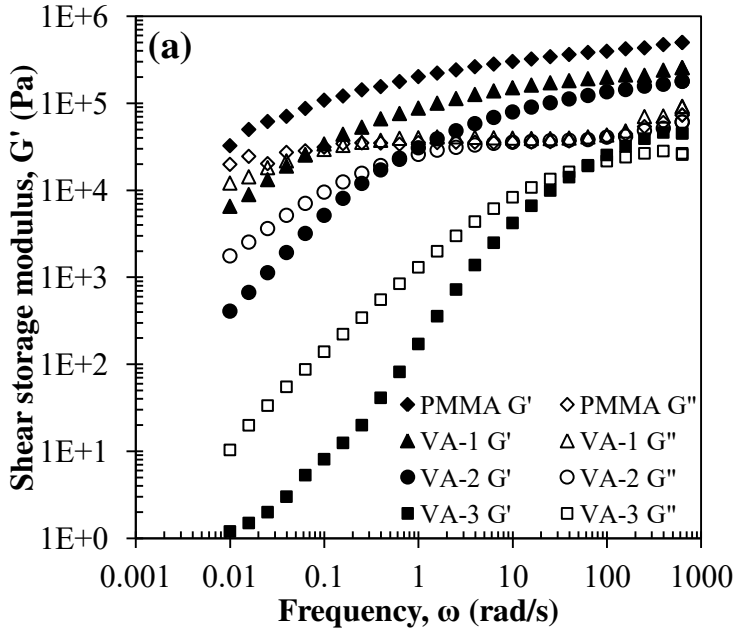

Figure 4.6 (a). Shear storage and loss moduli of poly(VA-*co*-MMA) series at 180 °C.

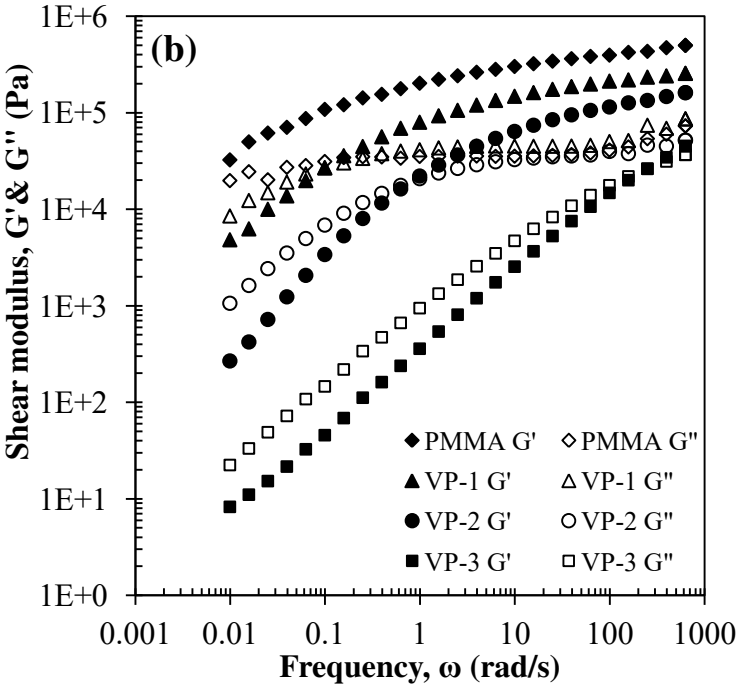

Figure 4.6 (b). Shear storage and loss moduli of poly(VP-*co*-MMA) series at 180 °C.

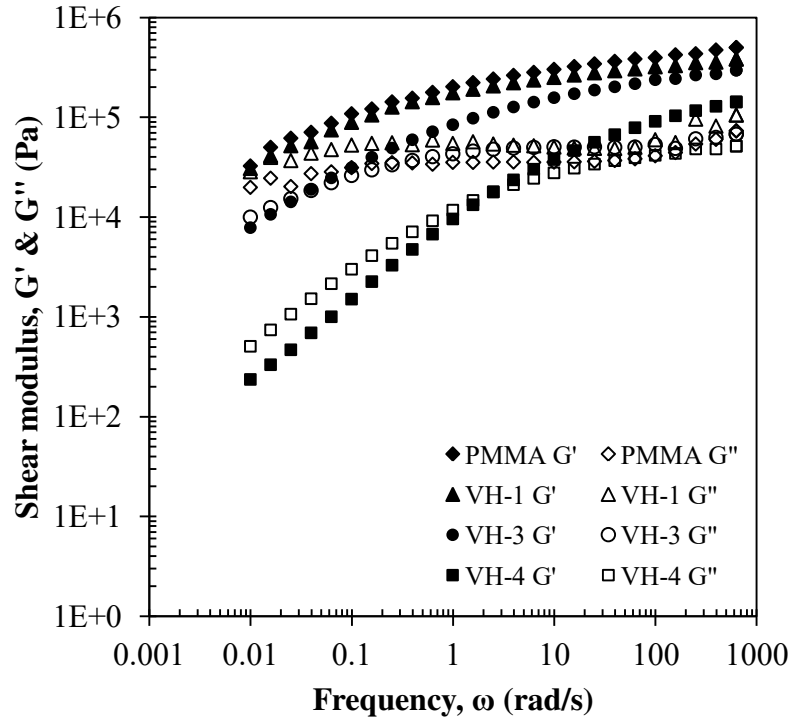

Figure 4.6 (c). Shear storage and loss moduli of poly(VH-*co*-MMA) series at 180 °C.

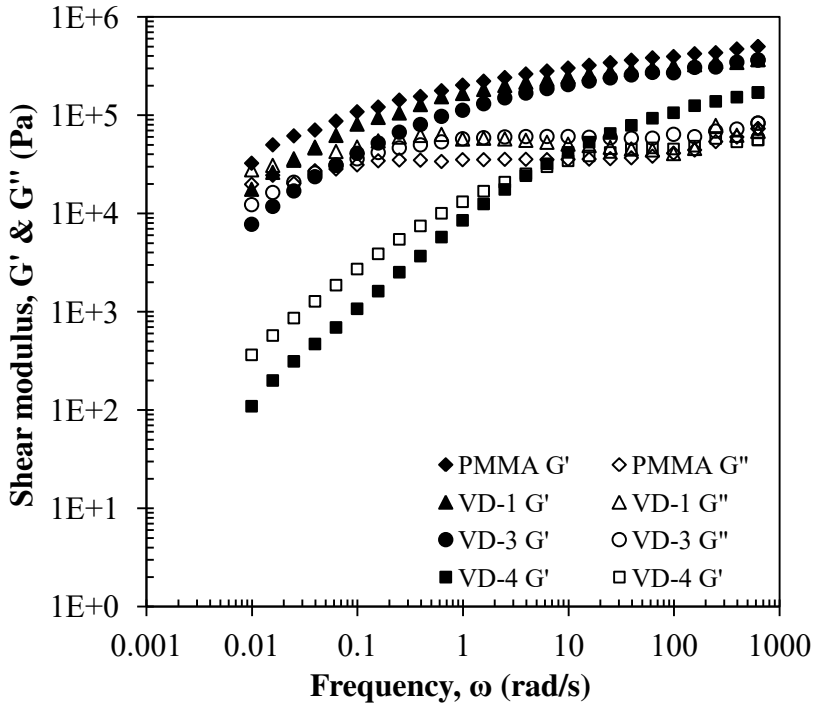

Figure 4.6 (d). Shear storage and loss moduli of poly(VD-*co*-MMA) series at 180 °C.

The copolymer MWs and LVE compositions are difficult to control in free radical copolymerizations. Therefore, samples with similar copolymer MWs and LVE compositions were selected to make comparisons. VH-1 (C_{VH} = 5 mol%, M_n = 2.7 × 10^5 g/mol) and VD-1 (C_{VD} = 3 mol%, M_n = 2.7 × 10^5 g/mol), have low LVE compositions and a slightly lower MWs compared to PMMA (M_n = 3.2 × 10^5 g/mol), however, their shear storage and loss moduli are very close to those of PMMA as shown in Figure 4.6 (c) and (d). This is probably because of the dominating role MWs play in determining the shear flow behavior of polymer melts. Samples VA-1 (C_{VA} = 12 mol%, M_n = 1.8 × 10^5 g/mol), VP-1 (C_{VP} = 12 mol%, M_n = 1.6 × 10^5 g/mol), VH-3 (C_{VH} = 10 mol%, M_n = 1.9 × 10^5 g/mol), and VD-3 (C_{VD} = 8 mol%, M_n = 1.7 × 10^5 g/mol) which have similar MWs, show shear storage moduli around 1 × 10^4 Pa compared to the shear modulus of PMMA which was around 3 × 10^4 Pa at low shear rates. At higher shear rates the shear storage moduli approached that of PMMA. The shear loss moduli of VA-1, VP-1, VH-3, and VD-3 are nearly the same when the frequency is above 1 rad/s. Although the LVE compositions of VA-1, VP-1, VH-3, and VD-3 are around 10 mol%, there were no large reductions in shear storage and loss moduli compared to those of homoPMMA when the MWs of the copolymers were around 1.7 × 10^5. Therefore, MWs have an obvious impact on the shear flow in this situation. As the MWs decreased and the LVE compositions increased, very obvious declines in the shear moduli are observed in each poly(LVE-*co*-MMA) series. This is particularly pronounced at low shear rate. The research on linear lower density polyethylene with different side chain length also had the similar phenomena that MWs was the dominant factor on shear moduli (Wei el al., 2007).

In order to determine the effect of side chains on the rheological properties of poly(LVE-*co*-MMA), comparisons of shear storage and loss moduli of

poly(LVE-*co*-MMA) with similar MWs were made using master curves obtained at 200 °C using the Arrhenius model as shown in Equation 4.1, where a_T is the shift factor obtained by fitting the data with Arrhenius model, E_a is the activation energy of molecular flow, and T_{ref} is the reference temperature. The master curves were obtained by using shear moduli curves at 200 °C as the reference and manually shifting the shear moduli curves at 180 °C and 220 °C until the curves overlapped by inspection. Table 4.2 shows the E_as determined for the poly(LVE-*co*-MMA) copolymers

$$\lg a_T = \frac{E_a}{R}\left(\frac{1}{T_{ref}} - \frac{1}{T}\right)$$

Equation 4.1. Arrhenius mode of temperature time superposition (TTS).

Table 4.2. Arrhenius activation energy of flow for poly(LVE-*co*-MMA).

	C_{LVE}* (mol%)	M_n ($\times 10^5$ g/mol)	E_a (KJ/mol)
VA-1	12	1.8	350
VP-1	12	1.6	297
VH-3	10	1.9	202
VD-3	8	1.7	155
VA-2	27	1.1	259
VP-2	25	0.9	184
VH-4	19	1.1	144
VD-4	12	1.3	120

Master curves of VA-1 (C_{VA} = 12 mol%, $M_n = 1.8 \times 10^5$ g/mol), VP-1 (C_{VP} = 12 mol%, $M_n = 1.6 \times 10^5$ g/mol), VH-3 (C_{VH} = 10 mol%, $M_n = 1.9 \times 10^5$ g/mol), and VD-3 (C_{VD} = 8 mol%, $M_n = 1.7 \times 10^5$ g/mol) were developed and are shown in Figure 4.7 (a) and (b). There was no large difference in shear storage or loss moduli of VA-1,

VP-1, and VH-3. A gap was observed between the shear storage and loss moduli of VD-3 and VA-1, but the difference was small. The most probably reason for the phenomena was the similar MWs of these copolymers. There was no obvious difference in behavior of samples with different LVEs. The E_a declined as the side chain lengths increased however. This indicates that it was easier to initiate the flow of poly(LVE-*co*-MMA) with longer side chains. This was attributed to the flexible side chains increasing the distance between the main backbones of the polymers. The side branches were significantly below the critical length and therefore did not participate in chain entanglements. This limited the effect of the side chains to increasing the separation between the main chains and serving as plasticizers.

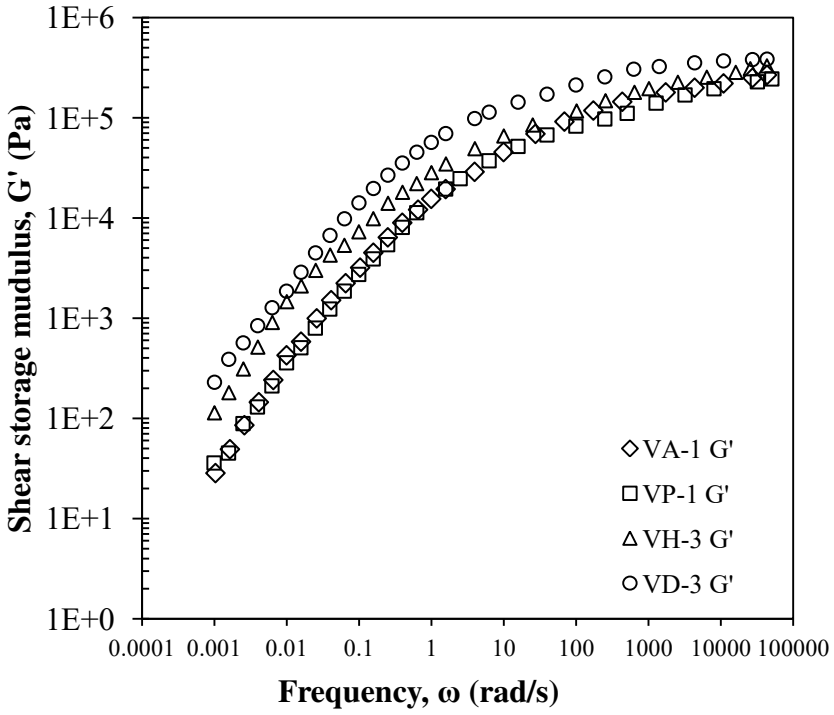

Figure 4.7 (a). Shear storage modulus master curves of VA-1, VP-1, VH-3, and VD-3 at 200 °C.

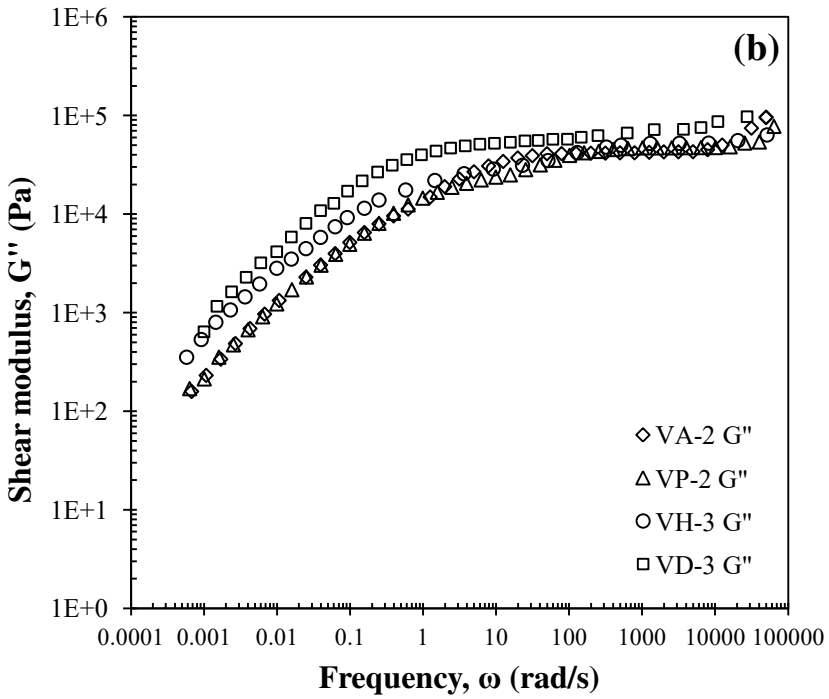

Figure 4.7 (b). Shear loss modulus master curves of VA-1, VP-1, VH-3, and VD-3 at 200 °C.

Another series of master curves were constructed for VA-2 (C_{VA} = 27 mol%, M_ns = 1.1 × 10^5 g/mol), VP-2 (C_{VP} = 25 mol%, 0.9 × 10^5 g/mol), VH-4 (C_{VH} = 19 mol%, 1.1 × 10^5 g/mol), and VD-4 (C_{VD} = 12 mol%, 1.3 × 10^5 g/mol) and are shown in Figure 4.8 (a) and (b). These copolymers had similar MWs but dissimilar comonomer ratios. As can be seen in Figure 4.8 (a) and (b), the master curves of these samples were very similar. Therefore, the influence of the LVE molecular weight on the G' and G'' was determined to be negligible. The largest impact on both G' and G'' was the MWs of the copolymers. However, the molecular weights of the different LVEs did play a role in the E_a, with higher molecular weight LVEs leading to polymers with reduced E_a. The research of the E_a of isotactic poly(propylene), α-poly(butene), and a series linear low density polyethylene also had the similar trend (Stadler et al., 2007).

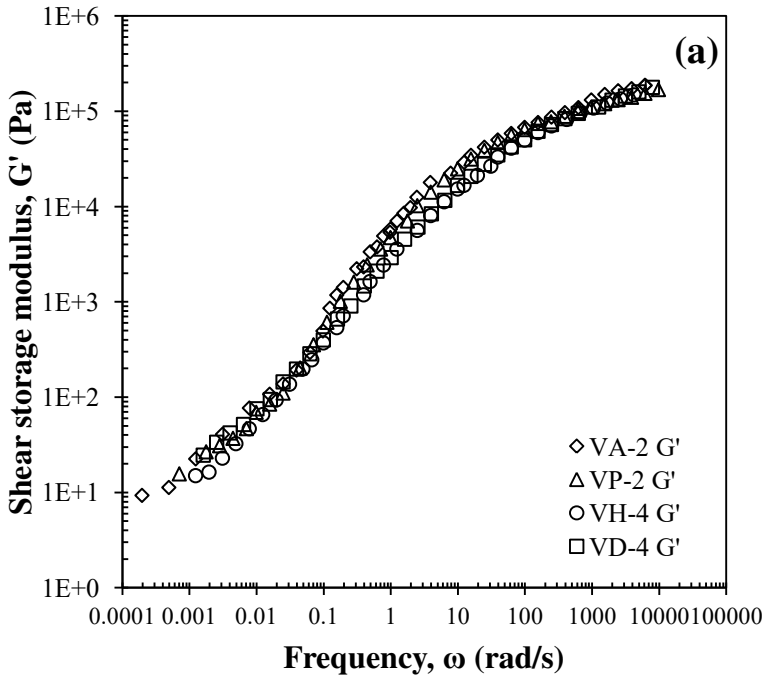

Figure 4.8 (a). Shear storage modulus master curves of VA-2, VP-2, VH-4, and VD-4 at 200 °C.

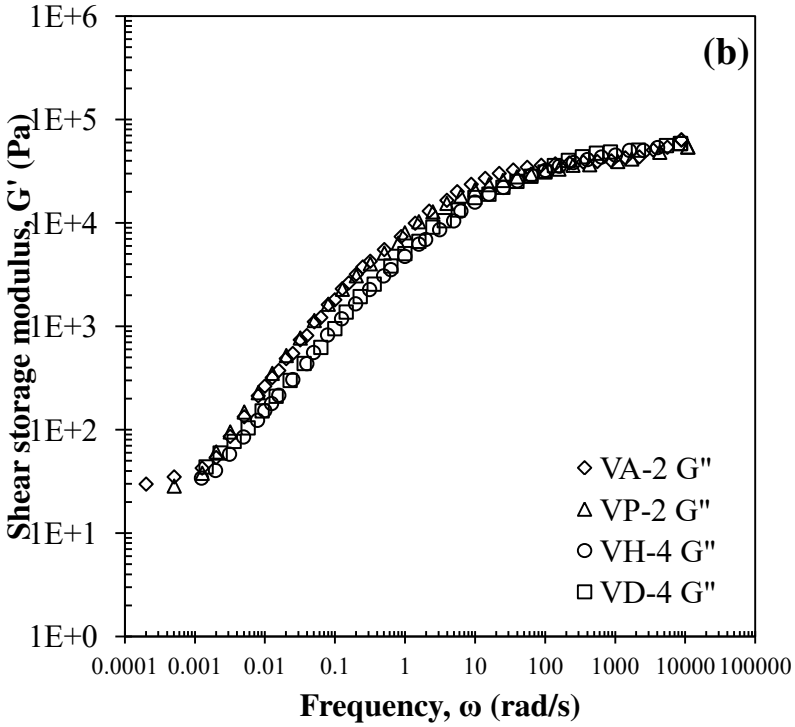

Figure 4.8 (b). Shear loss modulus master curves of VA-2, VP-2, VH-4, and VD-4 at 200 °C.

Complex Viscosity of Poly(LVE-co-MMA)

The complex viscosities of poly(VA-*co*-MMA), poly(VP-*co*-MMA), poly(VH-*co*-MMA), and poly(VA-*co*-MMA) series at 180°C are shown in Figure 4.9 (a-d). The complex viscosity of PMMA at 180°C was applied as the reference for the comparison. Figure 4.9 (a-d) shows the effects of comonomer construction on the complex viscosities of poly(LVE-*co*-MMA). In each figure, the complex viscosity of virgin PMMA is shown as a reference. It can be seen in Figure 4.9 (a) that the η_0^* decreased significantly as the comonomer ratio increased. A significant portion of this decrease can be attributed to the decrease in MWs from VA-1 to VA-3. It is also well known that the low shear viscosity of a polymer can be related to its MWs using Equation 4.3:

$$\eta_0^* = k \times MW^{3.4}$$

Equation 4.3. Relationship between MW and complex viscosity at low shear rate.

where k is a polymer dependent constant and MW is the weight average molecular weight. Using this relationship it can be seen that tripling the MWs, as occurred between VA-3 and VA-1, should lead to an approximately 40 fold increase in η_0^*, if all other factors were held constant. However, the η_0^* showed an increase of approximately 3 orders of magnitude. The additional decrease in η_0^* beyond that predicted by MW, was attributed to the increase in comonomer content. The increase in branch content increased the spacing between main chains, leading to decreased η_0^*. This behavior was also reflected in a reduction in the flow activation energy.

Similar behavior was observed for poly(VP-*co*-MMA) as can be seen in Figure 4 (a-d). Greater decreases in η_0^* were observed than can be attributed solely to

decreases in copolymer MW. Again, the enhanced reduction in η_0^* was attributed to the effect of increased branching.

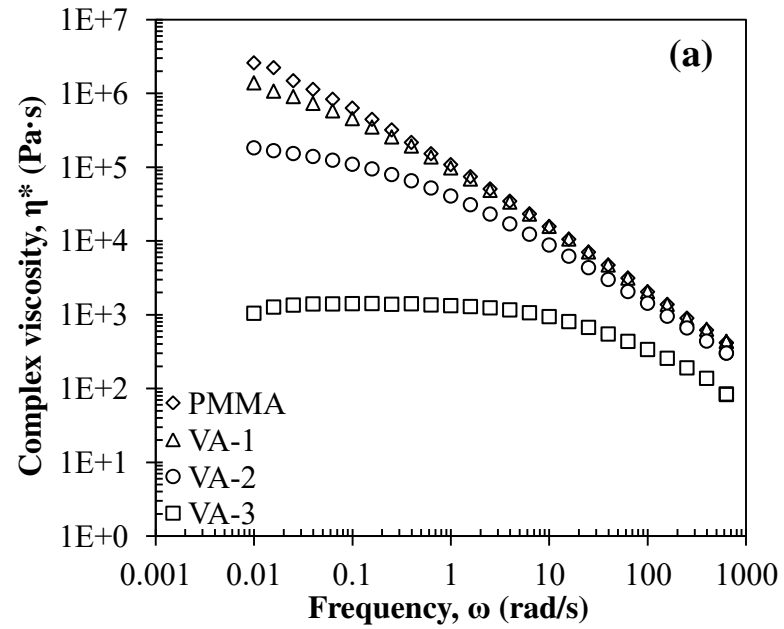

Figure 4.9 (a). Complex viscosities of poly(VA-*co*-MMA) series at 180 °C.

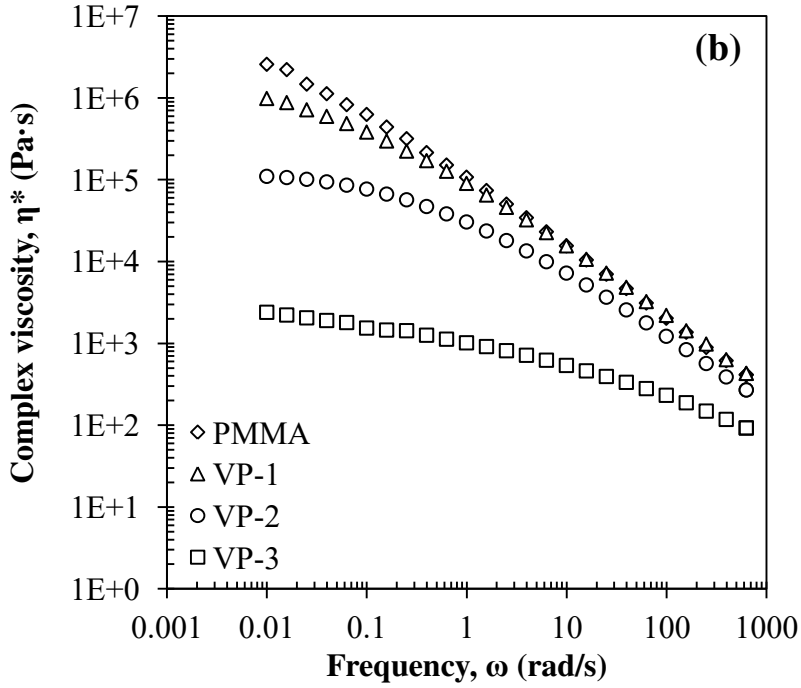

Figure 4.9 (b). Complex viscosities of poly(VP-*co*-MMA) series at 180 °C.

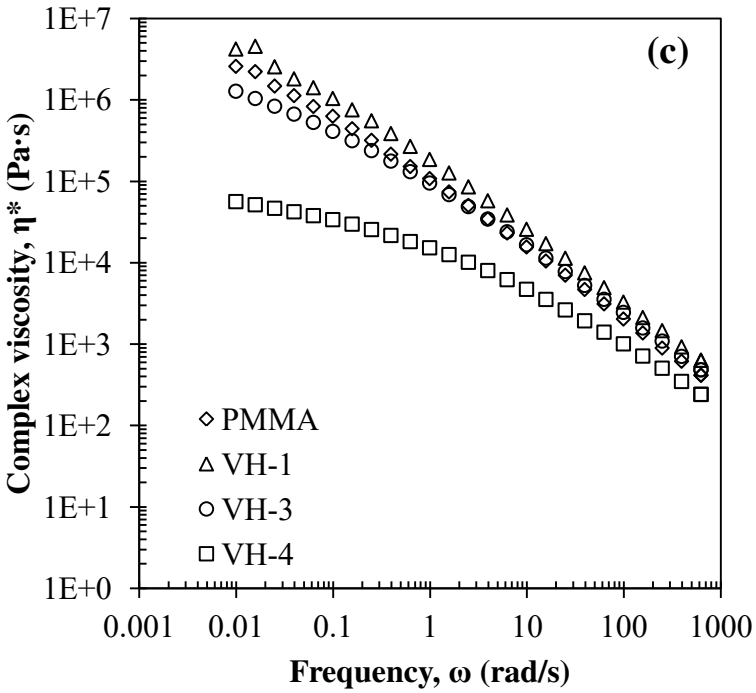

Figure 4.9 (c). Complex viscosities of poly(VH-*co*-MMA) series at 180 °C.

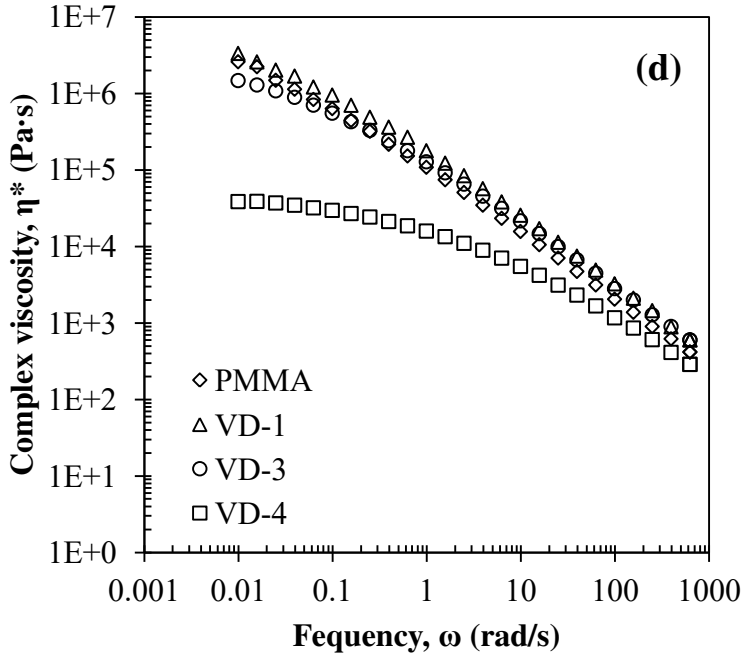

Figure 4.9 (d). Complex viscosities of poly(VD-*co*-MMA) series at 180 °C.

A comparison of the complex viscosity of poly(LVE-*co*-MMA) with similar

MWs, including VA-1, VP-1, VH-3, and VD-3, is shown in Figure 4.10 (a). The complex viscosity of PMMA at 180°C was used as a reference. These samples have similar MWs (approximate 1.6×10^5 g/mol) and C_{LVE} (approximate 10 mol%). It can be seen that the complex viscosities in Figure 4.10 (a) are very similar. This indicates that branch lengths did not play a large role in η_0^* at the comonomer concentration. However, in Figure 4.10 (b) the samples shown have similar MWs but the mole fractions of comonomer trend down with increasing LVE molecular weights. Sample VD-4 had a significantly lower η_0^* than VA-2, despite having a similar MWs and a lower C_{LVE}. This indicates that at higher comonomer ratios the branch lengths did indeed influence the η_0^*. Commercial LLDPE has the similar phenomena, which the complex viscosity was dominated by MWs (Garofalo et al., 2012).

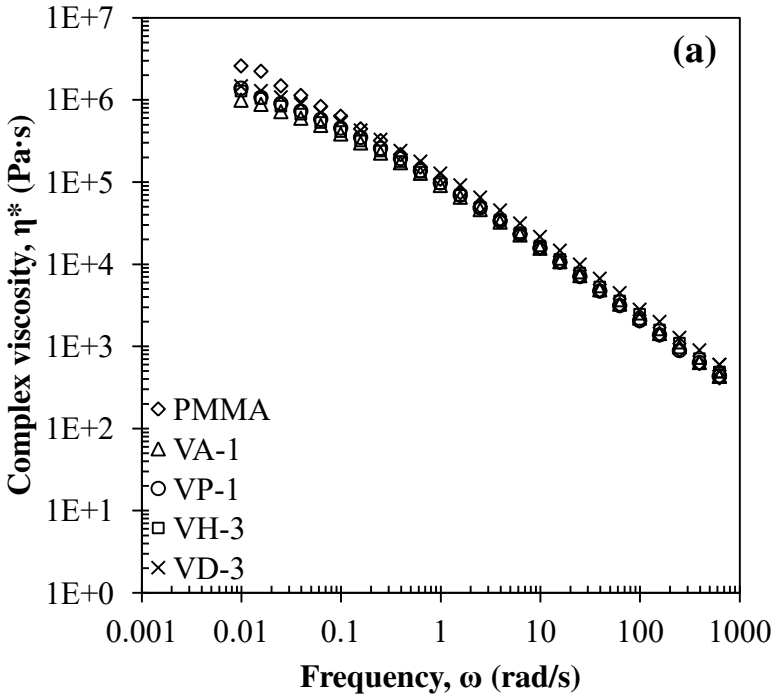

Figure 4.10 (a). Complex viscosities of VA-1, VP-1, VH-3, and VD-3 at 180 °C.

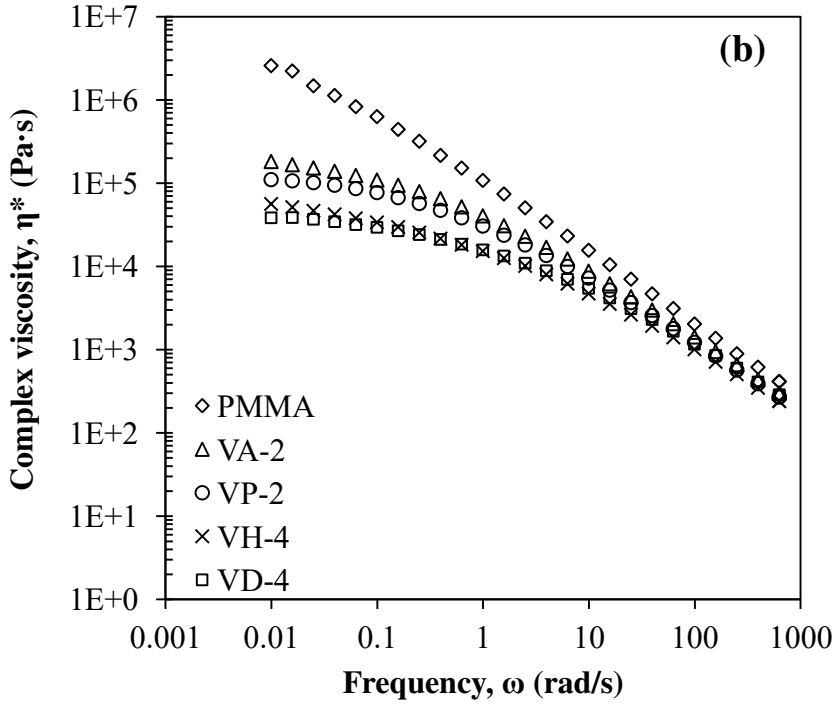

Figure 4.10 (b). Complex viscosities of VA-2, VP-2, VH-4, and VD-4 at 180 °C.

Chapter Conclusions

A series of poly(LVE-*co*-MMA) were prepared by free radical bulk copolymerizations. The resultant copolymers had LVE compositions varying from 3 mol% to 41 mol%. The storage moduli and T_gs of the resultant copolymers decreased with increasing LVE compositions. Copolymers with VD exhibited larger reductions of storage moduli and shifts in tan δ. Meanwhile, the G' and G" were dominated by the MWs of the copolymers, but the LVE compositions and molecular weights also influenced the rheological responses. Increases in LVE compositions led to decreases in G', G", and η_0^*, while increasing LVE molecular weight led to further decreases. Finally, as hypothesized, the introduction of LVEs decreased the stiffness of homoPMMA, potentially leading to application for poly(LVE-*co*-MMA) as transparent flexible board.

CHAPTER V

COPOLYMERS OF ACRYLIC ACID WITH LVES

Chapter Abstract

A series of amphiphilic copolymers with varying compositions of acrylic acid (AA) and linear vinyl esters (LVEs), including vinyl propionate (VP), vinyl hexanoate (VH), and vinyl decanoate (VD), were synthesized by solution copolymerizations. The average molecular weights (MWs) of the resultant copolymers varied due to the different reactivity ratios of AA and LVEs. The thermomechanical studies determined the glass transition temperatures (T_gs) of the copolymers ranged from 40 °C to 70 °C by incorporation of LVEs from 7 mol% to 42 mol%. The storage moduli of the copolymers were also impacted by the compositions and chain lengths of LVEs. The incorporation of VD, which provided longer side chains than VP and VH, had a more significantly effect on the T_gs and storage moduli of resultant copolymers. Rheological property analysis indicates that the MWs were the dominant factor influencing the shear flow behaviors of copolymer melts. But the influence of the LVE side chain lengths on the shear flow became more obvious when the MWs were lower than 0.8×10^5 g/mol.

Chapter Experimental

Materials

Benzoyl peroxide (BPO), purchased from Sigma-Aldrich, was recrystallized to remove impurities prior to use. Anhydrous ethanol (99.5%), purchased from Fisher Scientific, was pretreated with anhydrous sodium sulfate to remove residual water.

AA and VP from Sigma-Aldrich were purified by vacuum distillation. VH and VD from TCI America were pretreated with 2 wt % sodium hydroxide aqueous solutions to remove inhibitors, and washed to neutral pH. The monomers were then dried with anhydrous sodium sulfate to remove water.

Copolymerization and Sample Handling

A 500 mL flask equipped with stirring and refluxing was purged with N_2 to remove O_2 and trace H_2O before copolymerizations. AA and LVEs, including VP, VH, and VD, along with 1 gram initiator per 100 mL of solution were charged into the flask to form a 50 vol% aqueous solution. All copolymerizations were carried out in an oil bath at 60 °C under nitrogen protection. Compositional drift was prevented by controlling the copolymerization conversion to below 20%. All reactions were quenched by pouring the reactants into deionized water. The resultant copolymers were washed and immersed in deionized water to remove most of the unreacted monomers. The collected solids were then dried in a vacuum oven at 50 °C before any measurements were made.

Measurement

The structural characterizations of copolymers were carried out using a Nicolet 200 Fourier transform Infrared spectrometer (FT-IR) equipped with an attenuated total reflection (ATR) accessory, using a zinc selenide (Zn-Se) crystal. The measurement range was from 4000 cm^{-1} to 400 cm^{-1}. The compositions of all poly(LVE-*co*-AA) samples were determined by potentiometric titration with NaOH in aqueous solutions of 0.05 M NaCl. The molecular weight distribution (MWD), number-average molecular weight (M_n), and weight-average molecular weight (M_w)

were determined using a Varian 400 gel permeation chromatograph (GPC) equipped with a PL gel 5 μm MIXED-D and Varian Prostar refractive index detector. The GPC was calibrated using polystyrene standard samples from Varian. HPLC grade tetrahydrofuran (THF), purchased from Fisher, was used as the mobile phase with a flow rate of 1 mL min^{-1}. The thermomechanical properties were analyzed using dynamic mechanical analysis (DMA). Sample bars with dimensions of 50 mm × 10 mm × 1.5 mm were prepared using a Carver press. The storage moduli and tan δ of all samples were determined using a Perkin Elmer Pyris Diamond dynamic mechanical analyzer under bending test mode. Temperature sweeps of 2 °C min^{-1} from -20 °C to 120 °C were conducted at a constant frequency of 1 Hz. The rheological measurements were carried out using an AR2000 parallel-plate rheometer with a 1.5 mm gap under nitrogen protection. Both the cell compliance and geometry compliance were calibrated using instrument software. Samples were loaded onto the parallel-plates and trimmed after heating to the measurement temperature. The oscillatory frequency sweeps were completed at a temperature of 140 °C in consideration of the intramolecular dehydration of carboxyl groups that may occur above 150°C (Abdelaal et al., 2012). An oscillatory stress sweep was carried out before each run to ensure a linear viscosity range.

Chapter Results and Discussion

Structural Characterization

The chemical structures of the random copolymers are shown in Figure 5.1. The differences in structure are due to lengths of fatty acid chains. There are 3, 6, and 10 carbon atoms on the fatty acid chains of VP, VH, and VD respectively. A representative FT-IR spectrum is shown in Figure 5.2. The characteristic vibrations,

including the -C=O stretching absorption band of AA and/or LVEs from 1650 cm^{-1} to 1730 cm^{-1} and the C-H stretching absorption band at 2950 cm^{-1} of $–CH_3$ and $–CH_2$-, were observed using ATR/FT-IR. The –OH absorption band was overlapped by C-H stretching absorption, but the composition was determined quantitatively using the titration method previously described.

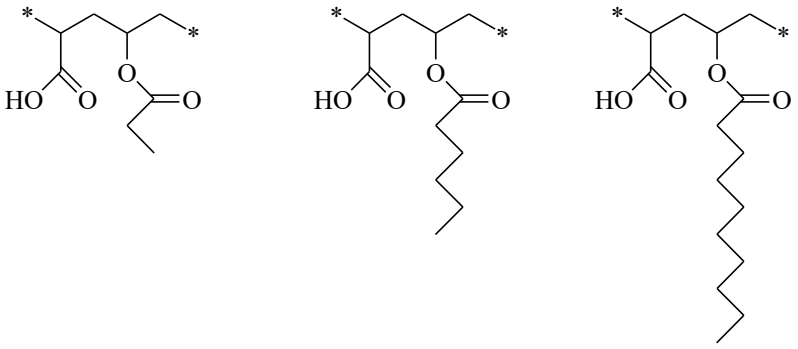

poly(VP-*co*-AA) poly(VH-*co*-AA) poly(VD-*co*-AA)

Figure 5.1. The chemical structures of poly(LVE-*co*-AA).

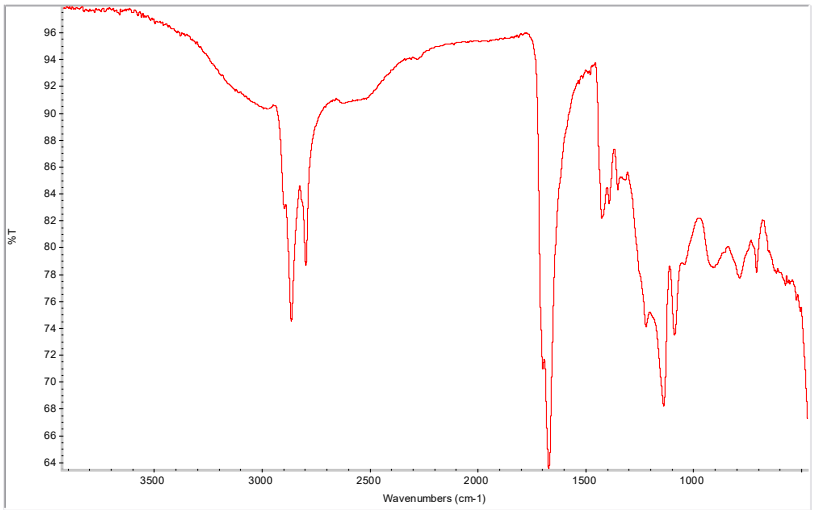

Figure 5.2. The FT-IR spectrum of poly(VD-*co*-AA) (VD-4).

Composition, Molecular weights and Molecular Weight Distributions

The compositions (C_{LVE}), M_n, M_w, PDI and T_g of the poly(LVE-*co*-AA)

samples synthesized in this work are shown in Table 5.1. The reactivity ratios of AA and VA in a solution copolymerization using ethanol as the solvent were previously reported as r_{AA} = 2.4 and r_{VA} = 0.04 by Zaldívar et al (Zaldívar et al., 1997). VD was expected to have a lower reactivity because the LVE compositions of VD in poly(VD-*co*-AA) were lower than those of VP in poly(VP-*co*-AA) and VH in poly(VH-*co*-AA) when the feed ratios are the same. The reactivity ratios estimated at high copolymerization conversion (25%) were r_{AA}/r_{VP}= 1.2/0.01, r_{AA}/r_{VH}= 1.5/0.01, and r_{AA}/r_{VD}= 5.4/0.01. The decrease of MWs in each poly(LVE-*co*-AA) series are also attributed to the different reactivity ratios between AA and LVEs. The polydispersity indexes (PDI) of all poly(LVE-*co*-AA) were close to 2.3. This relatively narrow PDI indicates that the compositional drift was not significant.

Table 5.1. Feed ratio, LVE compositions, M_n, M_w, PDI, and T_g of poly(LVE-*co*-AA).

	Feed ratio (mol:mol)	C_{LVE} [a] mol%	C_{LVE} wt%	M_n ($\times 10^{-5}$ g/mol)	M_w ($\times 10^{-5}$g/mol)	PDI [b]	T_{g-M} (°C)	T_{g-C} (°C)
poly(VP-*co*-AA)								
VP-1	0.3:0.7	21	27	1.2	2.8	2.3	69	70
VP-2	0.5:0.5	30	37	1.0	2.3	2.3	59	60
VP-3	0.7:0.3	42	50	0.8	1.9	2.2	53	53
poly(VH-*co*-AA)								
VH-1	0.3:0.7	19	32	1.2	2.5	2.2	61	58
VH-2	0.5:0.5	26	41	1.0	2.3	2.3	55	51
VH-3	0.7:0.3	35	52	0.8	2.0	2.3	48	43
poly(VD-*co*-AA)								
VD-1	0.3:0.7	7	17	1.2	2.7	2.2	56	53
VD-2	0.5:0.5	11	25	0.8	1.9	2.3	50	46
VD-3	0.7:0.3	16	34	0.6	1.5	2.3	41	35

[a] C_{LVE} is LVE composition expressed by mole fraction. [b] PDI = M_w/M_n

Dynamic Mechanical Analysis of Poly(LVE-co-AA)

The storage moduli of poly(VP-*co*-AA) with varying C_{LVE} are shown in Figure 5.3 (a). HomoPAA was not tested because PAA degrades before it softens. Therefore samples could not be prepared by melt processing. The storage moduli decreased from about 9×10^9 Pa to 3×10^9 Pa as the VP compositions increased from 21 mol% to 42 mol%. The reduction in storage modulus was attributed to the increase in side branch content. These branches increased the distance between main polymer chains softening the polymer. Similar trends were observed for poly(VH-*co*-AA) and poly(VD-*co*-AA) series. The storage modulus of poly(VH-*co*-AA) decreases from 5×10^9 Pa to 1×10^9 Pa as shown in Figure 5.3 (b), while the storage modulus of poly(VD-*co*-AA) decreased from 3.5×10^9 Pa to 7×10^8 Pa as presented in Figure 5.3 (c). These effects were also attributed to the incorporation of side chains of 6 or 10 carbon atoms.

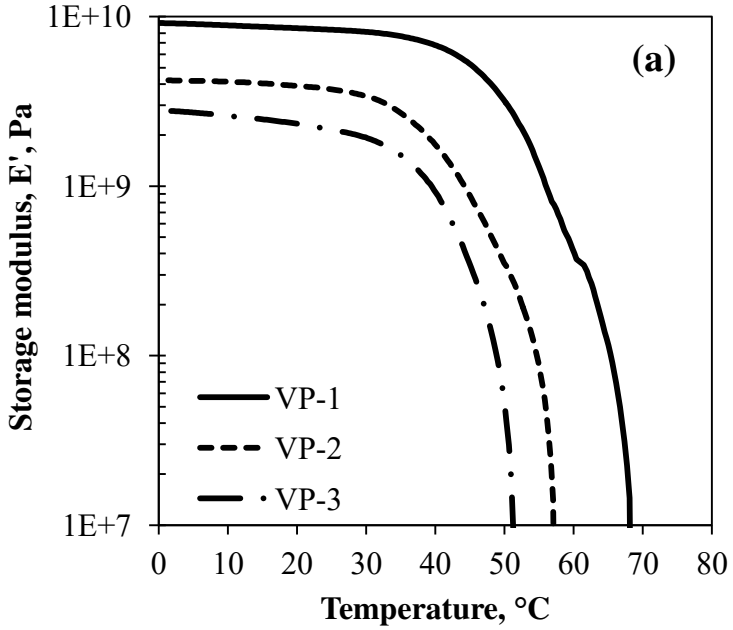

Figure 5.3 (a). Storage moduli of poly(VP-*co*-AA) series.

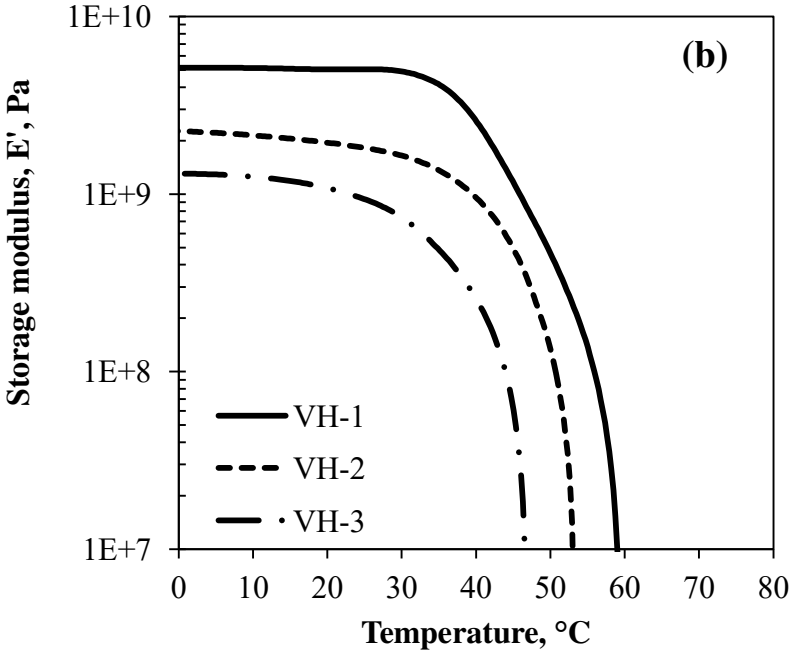

Figure 5.3 (b). Storage moduli of poly(VH-*co*-AA) series.

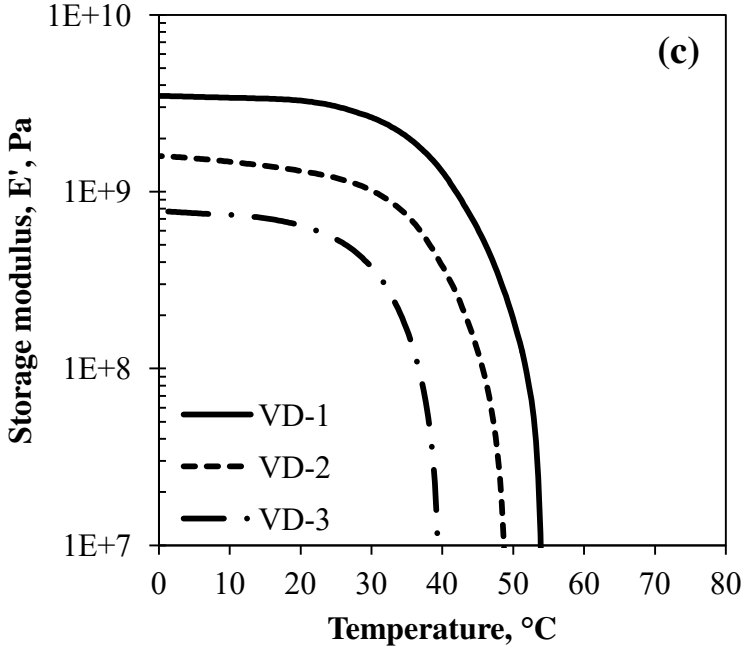

Figure 5.3 (c). Storage moduli of poly(VD-*co*-AA) series.

In order to determine the effect of varying side chain lengths on the storage modulus, a comparison of VP-1, VH-1, and VD-1 was made in Figure 5.4 (a). VP-1

(C_{VP} = 21 mol%, M_n = 1.2 × 10^5 g/mol), VH-1 (C_{VH} = 19 mol%, M_n = 1.2 × 10^5 g/mol), and VD-1 (C_{VD} = 7 mol%, M_n = 1.2 × 10^5 g/mol) have similar M_ns but different LVE compositions. The resultant storage moduli declined with increasing LVE molecular weight. This was despite the fact that VD-1 had a much lower C_{LVE} than either VP-1 or VH-1. This reduction in storage modulus was mostly attributed to the increase of LVE molecular weights. In other words, VD, which has a side chain of 10 carbon atoms, had a larger impact on the reduction of the storage moduli compared to VP and VH although LVE composition of VD-1 was only one third of VP-1 and VH-1. The longer side chain further increased the distance between chains, resulting in a more efficient plasticizing effect. VH-1 had a lower storage modulus than VP-1, but the impact of its side chain was not as pronounced as VD.

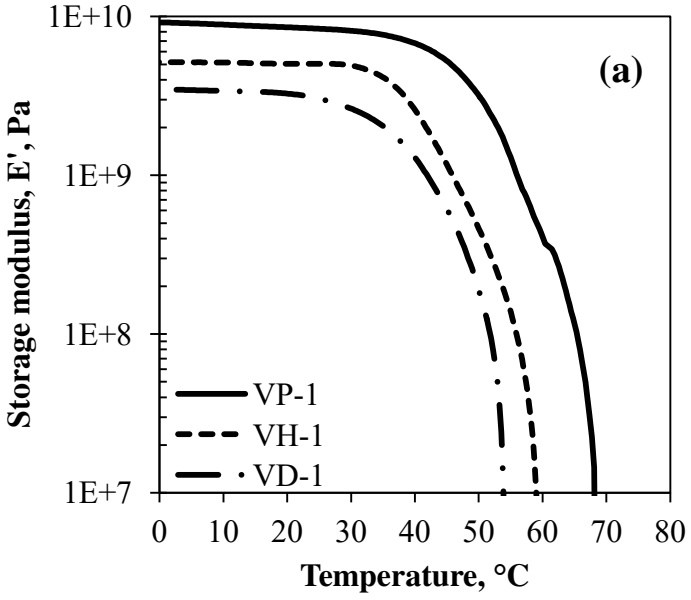

Figure 5.4 (a). Comparison of storage moduli of VP-1, VH-1, and VD-1.

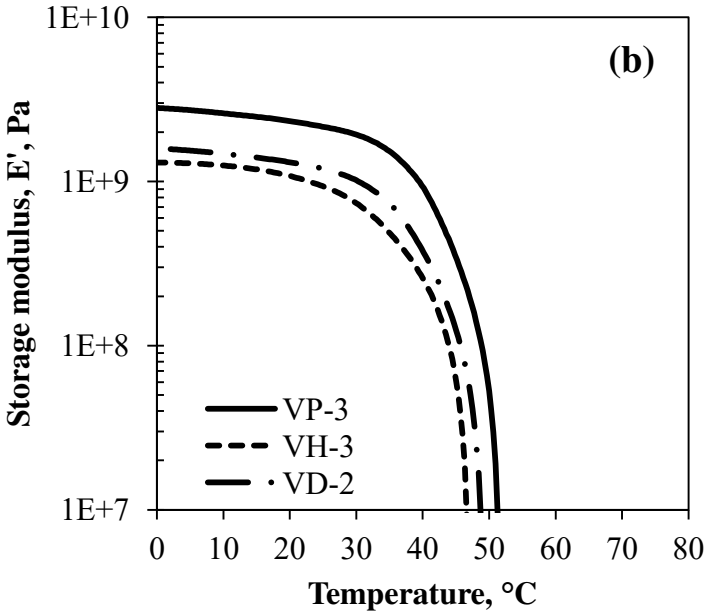

Figure 5.4 (b). Comparison of storage moduli of VP-3, VH-3, and VD-2.

The storage moduli of VP-3 (C_{VP} = 42 mol%, M_n = 0.8 × 10^5 g/mol), VH-3 (C_{VH} = 35 mol%, M_n = 0.8 × 10^5 g/mol) and VD-2 (C_{VD} = 11 mol%, M_n = 0.8 × 10^5 g/mol) are shown in Figure 5.4 (b). These polymers all had similar MWs but the C_{LVE} decreased from 42 mol% to 35 mol% to 11mol%. Despite this reduction in C_{LVE} the storage modulus of VP-3 was significantly higher than that of VH-3 or VD-2. However, the storage moduli of VH-3 and VD-2 were similar. This occurred despite the fact that the C_{LVE} of VD-2 was less than the C_{LVE} of VH-3. This was attributed to the fact that the side chains of VD-2 were much longer than VH-3, which lead to a much larger reduction of storage modulus. Therefore, both mole fractions and the side chain lengths of LVEs have impact on the storage moduli of poly(LVE-*co*-AA). The impact is more obvious for LVEs that have longer side chain length.

The T_gs of all poly(LVE-*co*-AA) were determined by DMA. The tan δ distributions of poly(VP-*co*-AA) series, poly(VH-*co*-AA) series, and poly(VD-*co*-AA) series are shown in Figure 5.5 (a-c). The peak values of tan δ, which were used to

determine T_gs, in each series shifted to lower temperatures with an increase in LVE composition. By introducing more flexible side chains to copolymers, the energy required for the motions of polymer backbones become lower. The reductions in T_gs were in good agreement with that predicted by the Fox-Flory equation, which are $T_{g\text{-}C}$ as listed in Table 5.1.

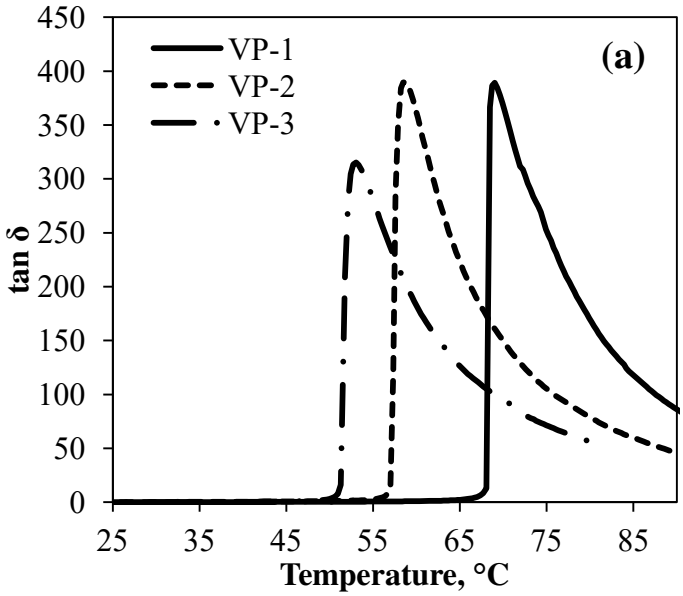

Figure 5.5 (a). tan δ distribution of poly(VP-*co*-AA) series.

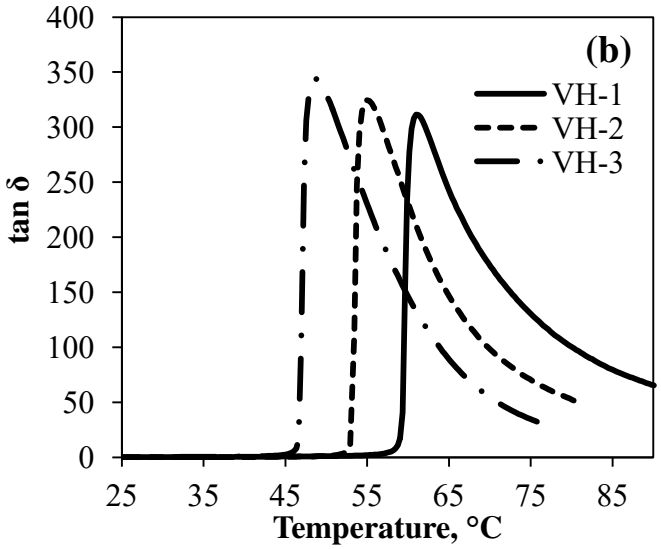

Figure 5.5 (b). tan δ distribution of poly(VH-*co*-AA) series.

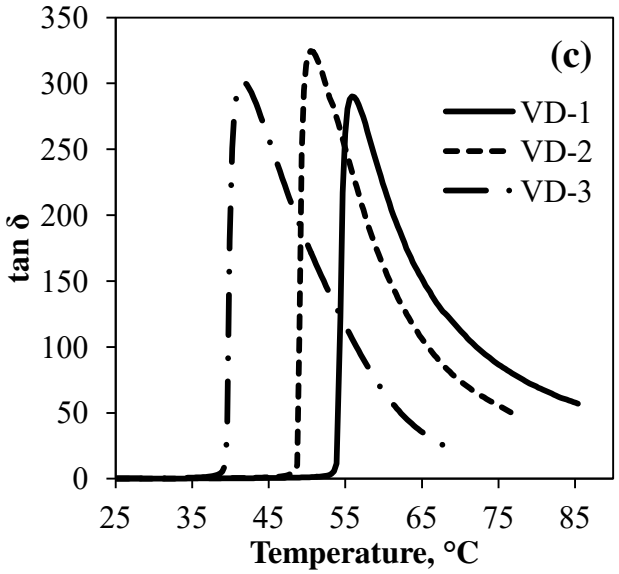

Figure 5.5 (c). tan δ distribution of poly(VD-*co*-AA) series.

The effect of branch length on the copolymer T_g was determined by comparing VP-1, VH-1, and VD-1, as shown in Figure 5.6 (a) and VP-3, VH-3, and VD-2, as shown in Figure 5.6 (b). The T_gs decreased gradually for VP-1 (C_{VP} = 21 mol%, M_n = 1.2 × 10^5 g/mol), VH-1 (C_{VH} = 19 mol%, M_n = 1.2 × 10^5 g/mol), and VD-1 (C_{VD} = 7 mol%, M_n = 1.2 × 10^5 g/mol) which have similar M_ns but different LVE compositions as shown in Figure 5.6 (a). It is obvious that VD had a larger impact on the T_gs of poly(LVE-*co*-AA) than VP or VH due to the fact that VD-1 had less LVE composition than VP-1 or VH-1 but exhibited a lower T_g. Because of the larger branch lengths, the free volume of VD-1 was larger than that of VP-1 and VH-1, leading to greater reductions in the T_gs.

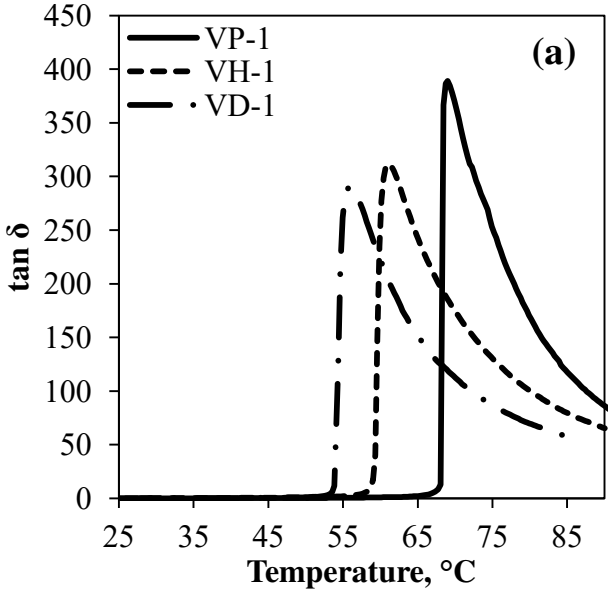

Figure 5.6 (a). Comparison of tan δ distribution of VP-1, VH-1, and VD-1.

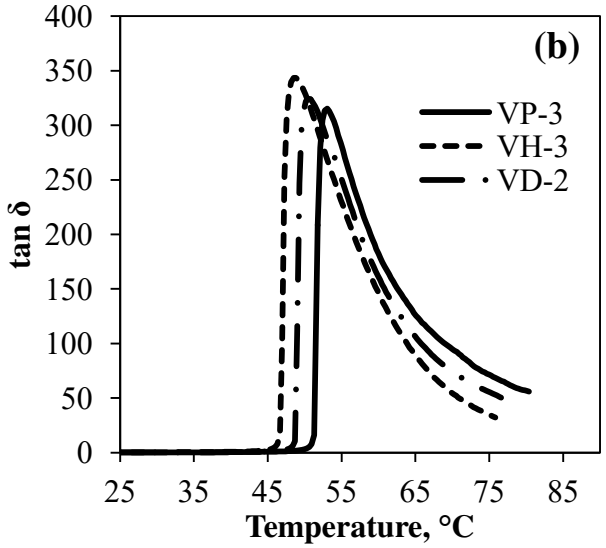

Figure 5.6 (b). Comparison of tan δ distribution of VP-3, VH-3, and VD-2.

A comparison of the tan δ distributions of VP-3 (C_{VP} = 42 mol%, M_n = 0.8 × 10^5 g/mol), VH-3 (C_{VH} = 35 mol%, M_n = 0.8 × 10^5 g/mol), and VD-2 (C_{VD} = 11 mol%, M_n = 0.8 × 10^5 g/mol) is shown in Figure 5.6 (b). The T_g of VP-3 was close to that of VH-3. The impact of side chain length was not very obvious in this case as both VP-3

and VH-3 had more than 30 mol% of LVE. It is believed that the impact of chain lengths was weaker than the LVE compositions when the resultant poly(LVE-*co*-AA) had high LVE compositions (more than 30 mol%). The T_g of VD-2 was between those of VP-3 and VH-3. The free volumes of poly(LVE-*co*-AA) were a function of both the side chain lengths and the LVE compositions. Although the side chain of VD-2 is much longer than VP-3 and VH-3, but VP-3 and VH-3 have much higher LVE mole fractions than VD-2. Therefore, both LVE compositions and side chain lengths impacted on the T_gs of poly(LVE-*co*-AA).

Rheological Property Analysis of Poly(LVE-co-AA)

Shear Storage and Loss Moduli of Poly(LVE-co-AA)

The rheological properties of the poly(LVE-*co*-AA) samples synthesized in this work were studied using a parallel plate rheometer. The shear storage and loss moduli of poly(VP-*co*-AA) samples with varying comonomer contents are shown in Figure 5.7. The measuring temperature did not exceed 140 °C in order to avoid the degradation of AA. In general, the storage and loss moduli decreased for VP-1, VP-2, and VP-3 at the same shear rate. The increase in side branches further separated the main chains, facilitating the macromolecular motions of the polymer chains. The side chains not only increased the distance between backbones but also disrupted intermolecular hydrogen bonding of the carboxyl groups. At lower shear rates, the gap between the shear storage moduli of VP-1(G' $\approx 10^5$ Pa) was two orders of magnitude larger than that of VP-3 (G' $\approx 10^3$ Pa). The gap between the shear loss modulus of VP-1 (G" $\approx 10^4$ Pa) and VP-3 (G' $\approx 10^3$ Pa) at low shear rate was one order of magnitude as shown in Figure 5.7 (b). Although the gap between shear storage modulus of VH-1 (G' $\approx 10^4$ Pa) and VH-3 (G' $\approx 10^2$ Pa) at low shear rate is also two

orders of magnitude, the gap between shear loss modulus of VH-1 (G' ≈ 10^4 Pa) and VH-2 (G' ≈ 10^4 Pa) is two order of magnitude, which was larger the that of VP-1 and VP-3, as shown in Figure 5.8 (a) and (b). This indicates that the shear moduli were reduced by incorporation of more LVEs. The gap between shear storage modulus of VD-1 (G' ≈ 10^4 Pa) and VD-3 (G' ≈ 10 Pa), and shear loss modulus of VD-1 (G' ≈ 10^4 Pa) and VD-3 (G' ≈ 10 Pa) was even larger, as shown in Figure 5.9 (a) and (b), which indicates that VD was more effective at reducing the shear storage moduli at low shear rates.

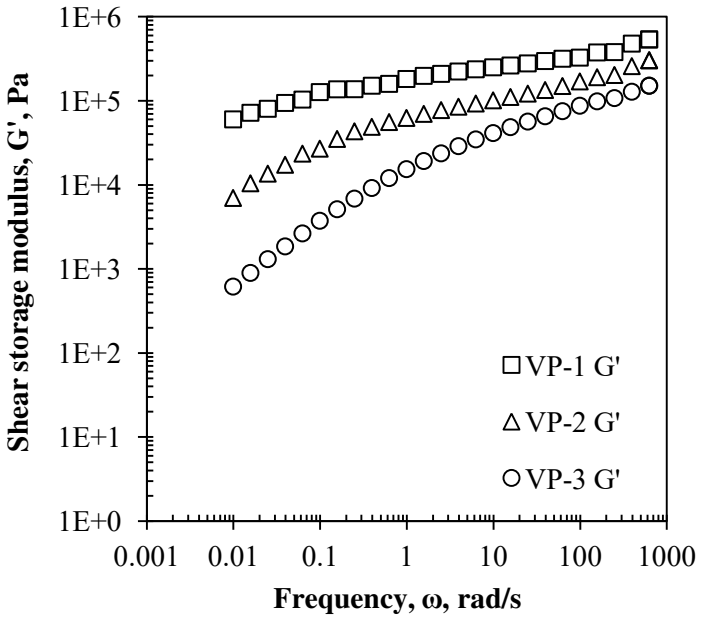

Figure 5.7 (a). Shear storage moduli of poly(VP-*co*-AA) at 140 °C.

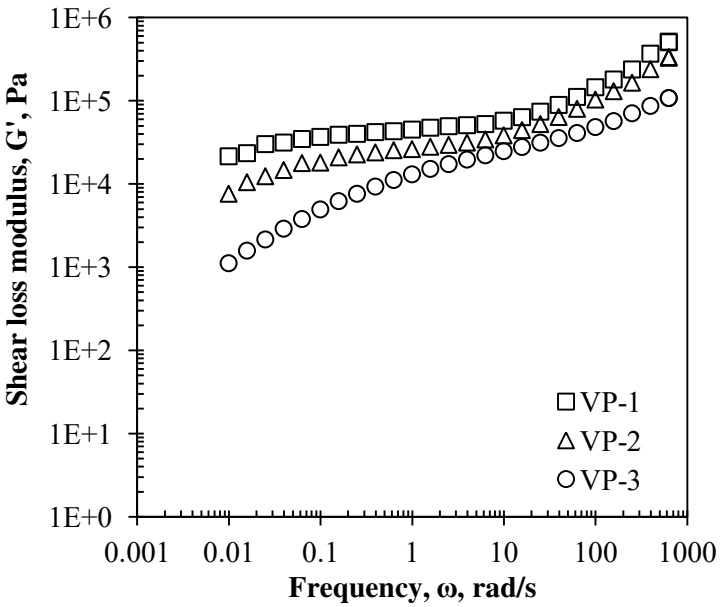

Figure 5.7 (b). Shear loss moduli of poly(VP-*co*-AA) series at 140 °C.

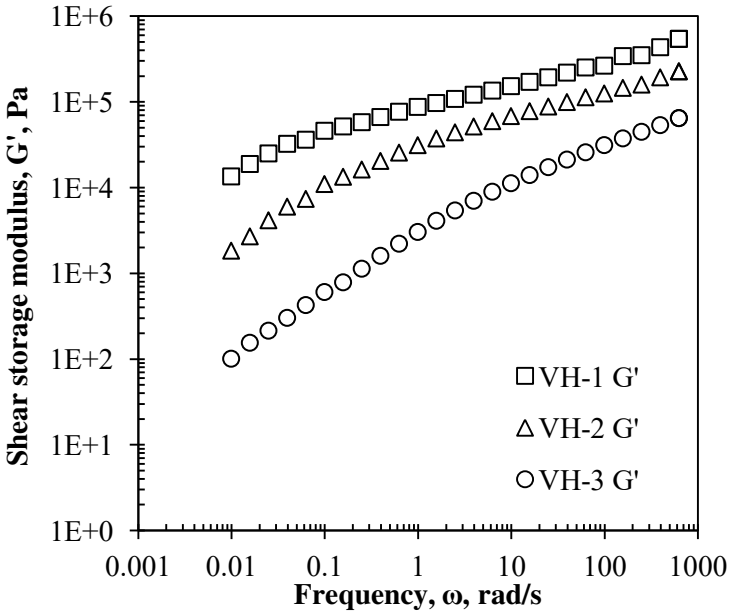

Figure 5.8 (a). Shear storage moduli of poly(VH-*co*-AA) series at 140 °C.

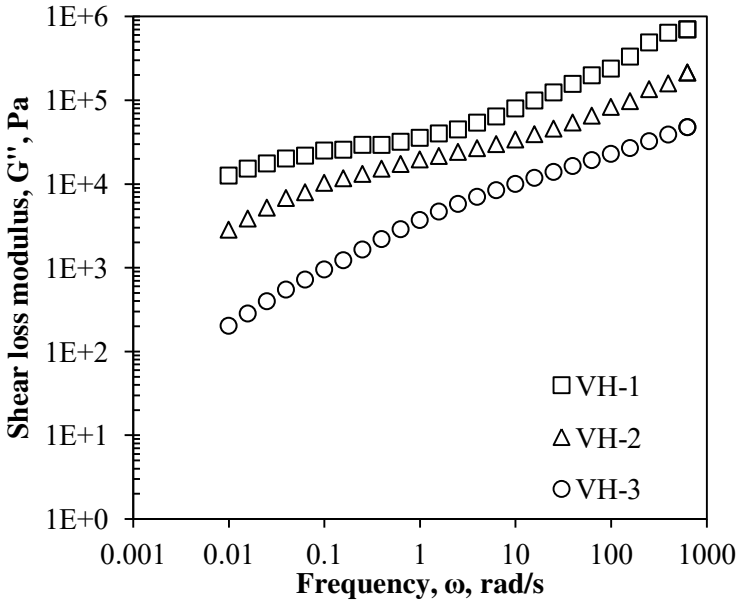

Figure 5.8 (b).Shear loss moduli of poly(VH-*co*-AA) series at 140 °C.

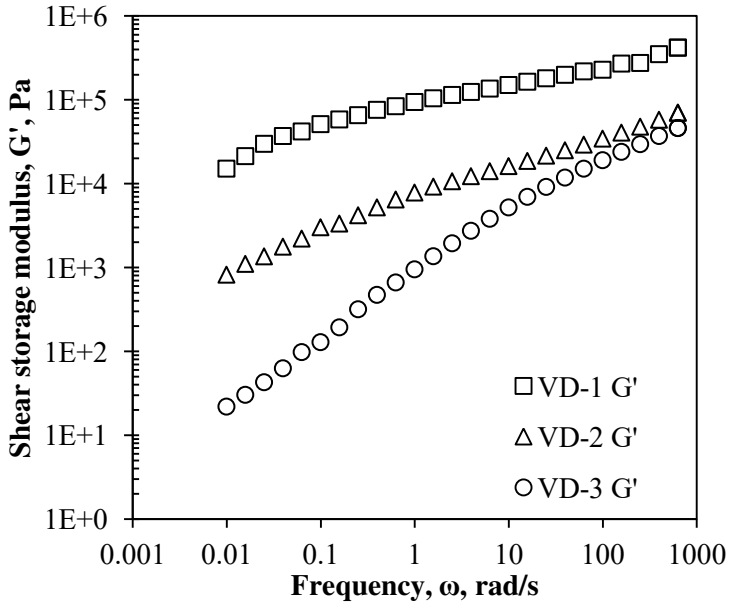

Figure 5.9 (a). Shear storage moduli of poly(VD-*co*-AA) series at 140 °C.

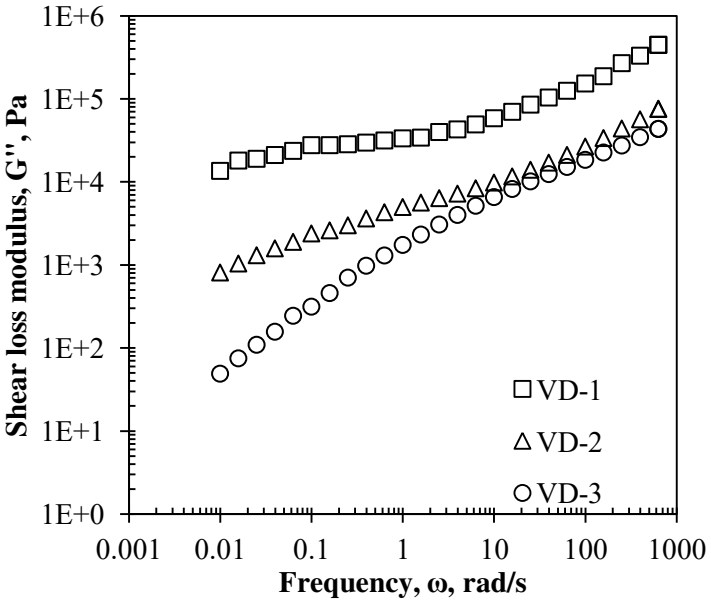

Figure 5.9 (b). Shear loss moduli of poly(VD-*co*-AA) series at 140 °C.

An attempt to determine the effect of the LVE concentration on the shear storage and loss moduli is made of VP-1, VH-1, VD-1, and VD-2 is shown in Figure 5.10 (a) and (b). The copolymers in this comparison, which are VP-1 (C_{VP} = 21 mol%, M_n = 1.2 × 10^5 g/mol), VH-1 (C_{VH} = 19 mol%, M_n = 1.2 × 10^5 g/mol), and VD-1(C_{VD} = 7 mol%, M_n = 1.2 × 10^5 g/mol), have very similar MWs but different LVE mole fractions. The shear storage and loss moduli are very similar for VP-1, VH-1, and VD-1. Therefore, it is believed that molecular weights play a more important role in determing the shear flow behavior of polymer melts when MWs are as high as 1.2 × 10^5 g/mol. Neither the LVE compositions nor side chain lengths had an obvious impact on the shear moduli in this comparison. VP-1 exhibited a shear storage modulus, which was an order of magnitude higher than VH-1 and VD-1 at low shear rates, as seen in Figure 5.10 (a), but there is no obvious differences of the shear loss moduli of VP-1, VH-1, and VD-1 as shown in Figure 5.10 (b). It is notcied that VH-1 and VD-1 have similar shear storage and loss moduli. The most probable reason is

that VH-1 and VD-1 have similar MWs. On the other hand, VH-1had a 12 mol% higher LVE composition than VD-1 but shorter side chains. However, VD-2 (C_{VD} = 11 mol%, $M_n = 0.8 \times 10^5$ g/mol), which had a lower M_n, shows lower shear moduli compared to the other three copolymers in this comparison. On one hand, this decrease may have been caused by the increase of VD mole fraction. On the other hand, the shear modulus is strongly dependent on the M_ns of the samples.

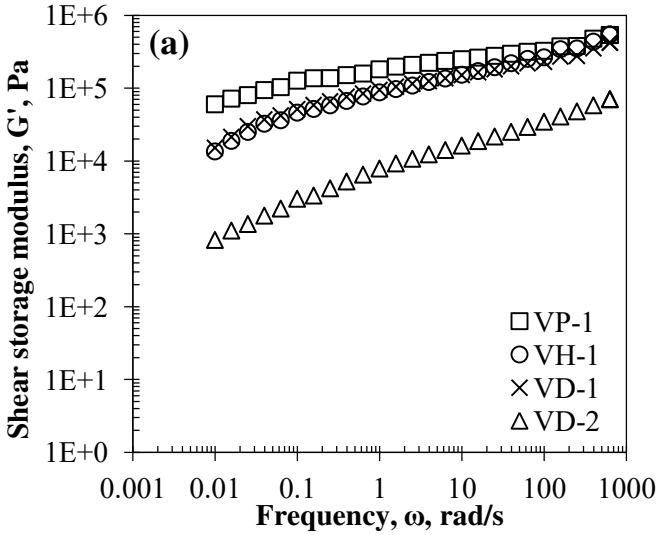

Figure 5.10 (a). Shear storage moduli of VP-1, VH-1, VD-1, and VD-2 at 140 °C.

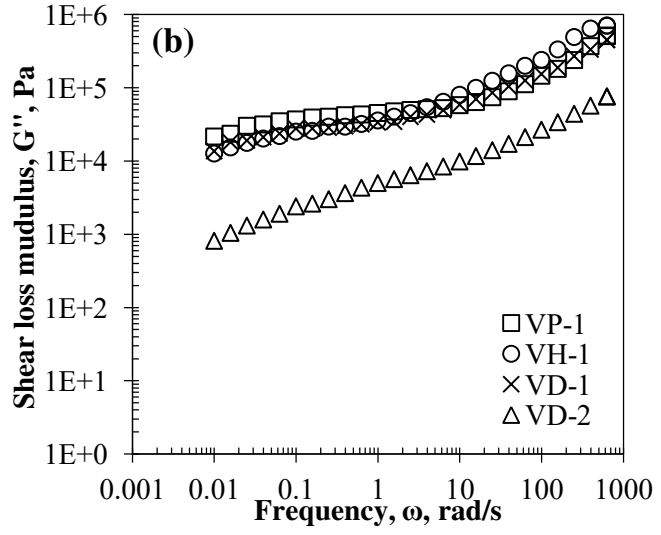

Figure 5.10 (b). Shear loss moduli of VP-1, VH-1, VD-1, and VD-2 at 140 °C.

Another comparison of shear storage and loss moduli was made among VP-3, VH-3, VD-2, and VD-3, which have lower M_ns, as shown in Figure 5.11 (a) and (b). In this situation, VP-3 (C_{VP} = 42 mol%, M_n = 0.8 × 10^5 g/mol), VH-3 (C_{VH} = 35 mol%, M_n = 0.8 × 10^5 g/mol), VD-2 (C_{VD} = 11 mol%, M_n = 0.8 × 10^5 g/mol) have very similar M_ns but varying LVE compositions. The shear moduli of VP-3 was an order of magnitude higher than VH-3 at low shear rates. This was attributed to the differeces in side chain lengths when MWs (0.8 × 10^5 g/mol) decline to two thirds as much as those of VP-1, VH-1, and VD-1 (1.2 × 10^5 g/mol) from last comparison. In other words, the effect of side chain lengths becomes more obvious when MWs are lower. The more flexible side chain of VH-1 facilitated the motion of macromolecules in the melt state more effectively than VP-1. The shear moduli of VD-2, which had only one third LVE composition as VH-3, lay between the shear storage and loss moduli of VP-3 and VH-3 as shown in Figure 5.11 (a) and (b). The 10 carbon atoms side chain of VD-2 helped to reduce the shear modulus significantly, particularly VD-2 had only one third the LVE compositions asVH-3. Another comparison of both the shear storge and loss moduli of VH-3 and VD-3 showed no large differences, as can be seen in Figure 10 (a) and (b). The most important reason is that the difference of M_ns between VH-3 and VD-3 (C_{VD} = 16 mol%, M_n = 0.6 × 10^5 g/mol) was smaller (0.2 × 10^5 g/mol) compared to the difference between VH-1 and VD-2 (0.4 × 10^5 g/mol) as shown in Figure 9 (a) and (b). But the small gap between the shear moduli of VH-3 and VD-3 resulted mostly from the differences in the side chain lengths.

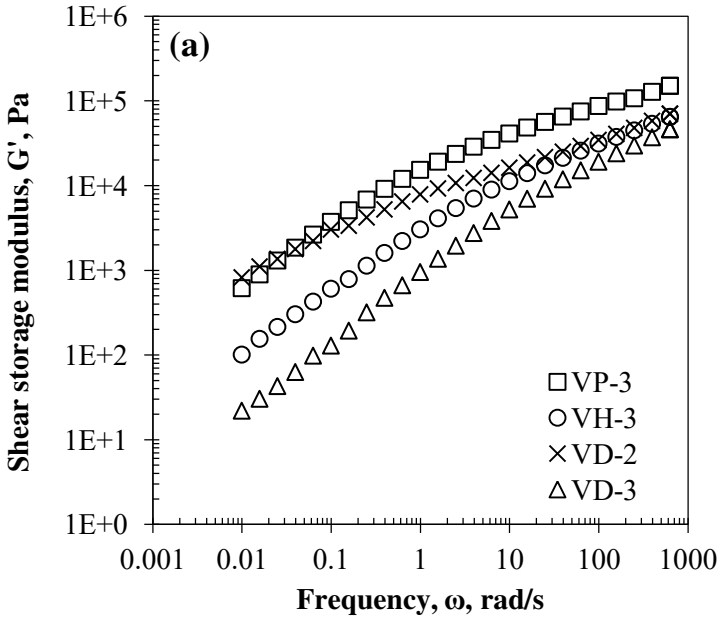

Figure 5.11 (a). Shear storage moduli of VP-3, VH-3, VD-2, and VD-3 at 140 °C.

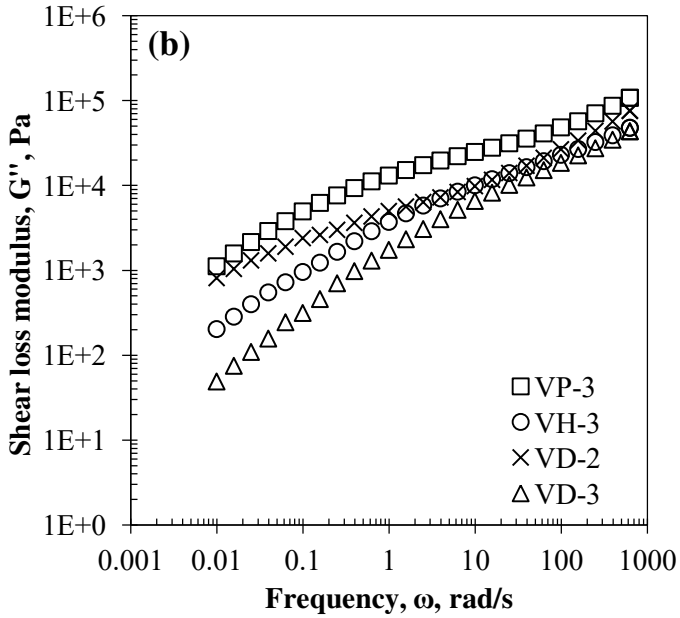

Figure 5.11 (b). Shear loss moduli of VP-3, VH-3, VD-2, and VD-3 at 140 °C.

Complex Viscosity Analysis of Poly(LVE-co-AA)

The complex viscosities of poly(VP-*co*-AA), poly(VH-*co*-AA), and poly(VD-*co*-AA) series are presented in Figure 5.12 (a-c). It can be seen that the

viscosities of the copolymers decreased with increasing LVE compositions. The declines in the complex viscosities are attributed to decreasing MWs and the LVE branches weakening the interactions between poly(LVE-*co*-AA) backbones.

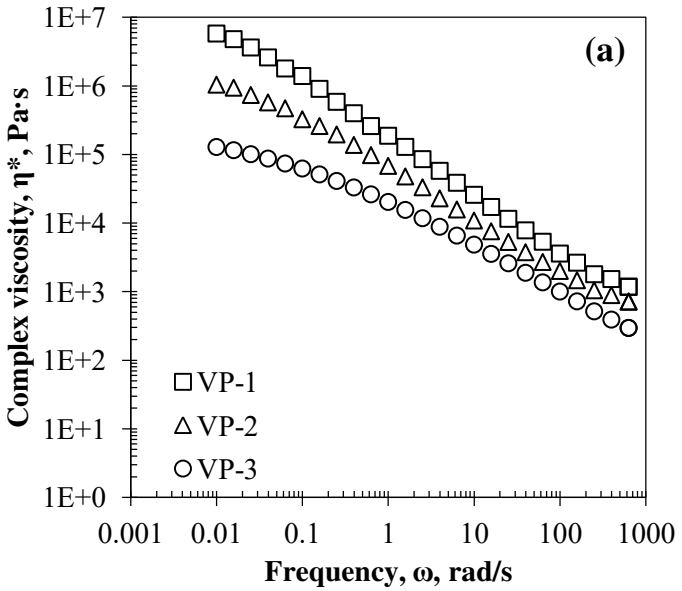

Figure 5.12 (a). Complex viscosities of poly(VA-*co*-AA) series at 140 °C.

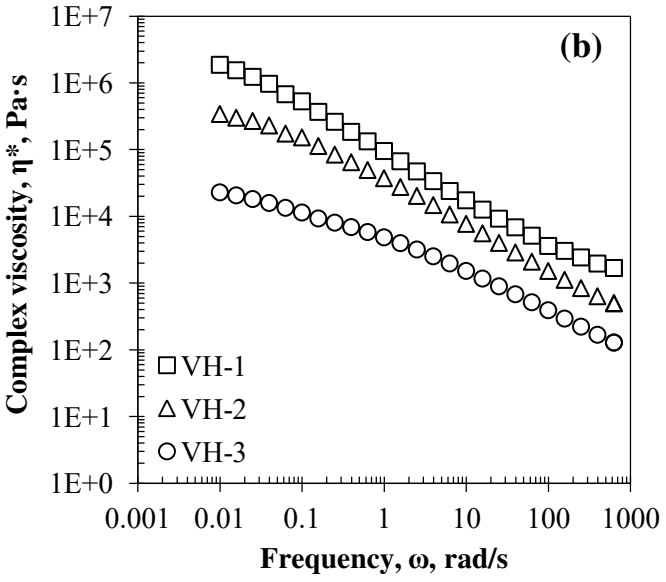

Figure 5.12 (b). Complex viscosities of poly(VH-*co*-AA) series at 140 °C.

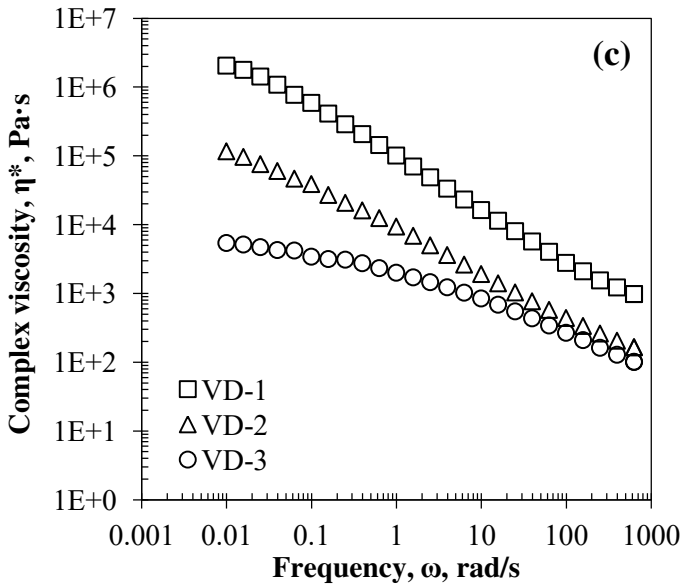

Figure 5.12 (c). Complex viscosities of poly(VD-*co*-AA) series at 140 °C.

A comparison of the complex viscosities of VP-1, VH-1, VD-1, and VD-2 is presented in Figure 5.13 (a). Copolymers in this comparison, including VP-1 (C_{VP} = 21 mol%, M_n = 1.2 × 10^5 g/mol), VH-1 (C_{VH} = 19 mol%, M_n = 1.2 × 10^5 g/mol), and VD-1(C_{VD} = 7 mol%, M_n = 1.2 × 10^5 g/mol), had similar complex viscosity due to their similar M_ns, even though VP-1, VH-1, and VD-1 had different LVE compositions and side chain lengths. VD-2 (C_{VD} = 11 mol%, M_n = 0.8 × 10^5 g/mol), whose M_n is significantly lower than the others, exhibited an obvious decrease in complex viscosity. Another comparison of complex viscosity of copolymers, as shown in Figure 5.13 (b), includes VP-3 (C_{VP} = 42 mol%, M_n = 0.8 × 10^5 g/mol), VH-3 (C_{VH} = 35 mol%, M_n = 0.8 × 10^5 g/mol), VD-2 (C_{VD} = 11 mol%, M_n = 0.8 × 10^5 g/mol), and VD-3 (C_{VD} = 16 mol%, M_n = 0.6 × 10^5 g/mol), also shows that M_ns had the largest impact on the complex viscosity. The results are compatible with those mentioned in the shear moduli analysis.

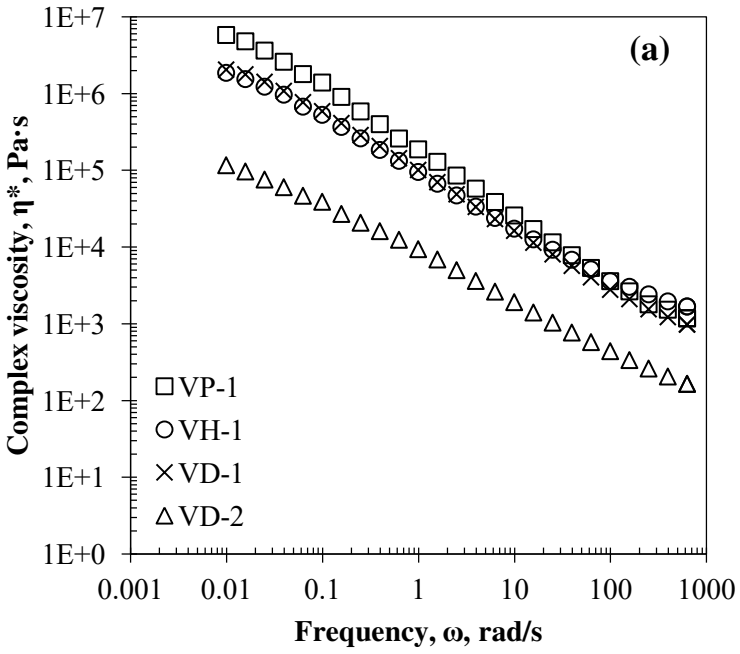

Figure 5.13 (a). Complex viscosities of VP-1, VH-1, VD-1, and VD-2 at 140 °C.

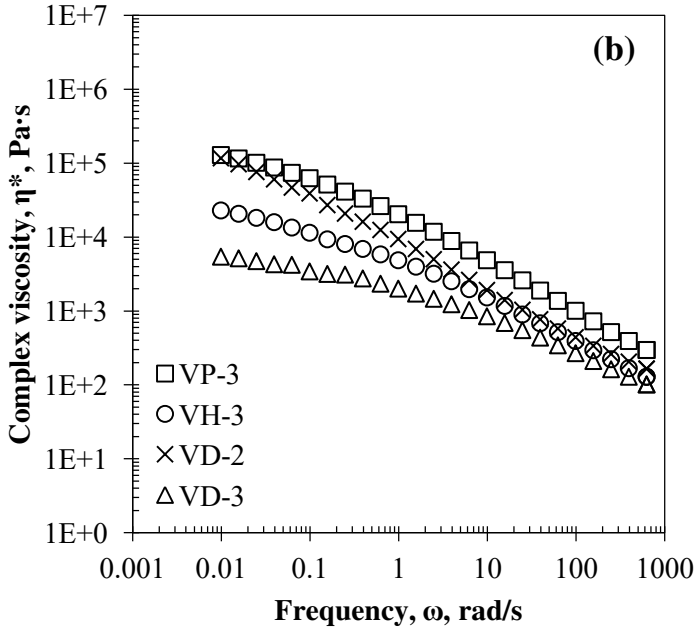

Figure 5.13 (b). Complex viscosities of VP-3, VH-3, VD-2, and VD-3 at 140 °C.

Chapter Conclusions

Amphiphilic copolymers with various mole fractions of AA and LVEs,

including VP, VH, and VD, were synthesized using solution copolymerization. The MWs of the obtained poly(LVE-*co*-AA) decreased with increasing LVE composition because of the differences in reactivity ratios. The thermomechanical property analysis indicates that the T_gs and storage moduli of copolymers are impacted by the side chain lengths and compositions of LVE. Rheological property analysis shows that the shear flow behaviors are mainly affected by the MWs of copolymers. But the lengths of the side chains also have an impact on shear flow when MWs are low. The poly(LVE-*co*-AA) synthesized have both the flexible and adhesive natures due to the introduction of LVE and the carboxyl group of AA, which make the copolymer potential in application of flexible adhesive board.

CHAPTER VI

COPOLYMERS OF ETHYLENE WITH LVES

Chapter Abstract

Copolymers of ethylene (Et) with linear vinyl esters (LVEs), including vinyl butyrate (VB), vinyl hexanoate (VH), and vinyl decanoate (VD), were synthesized using solution copolymerizations. The LVE compositions did not change significantly when the ethylene pressure ranged from 800 psi to 1100 psi. The MWs of poly(LVE-*co*-Et) decreased when the ethylene pressure decreased. The PDI also declined with the decrease of ethylene pressure.

Chapter Experimental

Materials

VB, VH, and VD, purchased from TCI America were washed with 2 wt% sodium hydroxide aqueous solutions to remove inhibitors, washed with DI water till neutral and then dried using anhydrous sodium acetate. Benzoyl peroxide (BPO) from Sigma-Aldrich was recrystallized before use. The solvents tert-butyl alcohol (TBA) and HPLC grade tetrahydrofuran (THF) from Sigma-Aldrich were used as received. Ethylene, purchased from PRAXAIR, was used as received.

Copolymerization and Sample Handling

The copolymerizations were carried out in a 300 mL autoclave reactor equipped with gas inlet pipeline, safety purge, mechanical agitation, and a heating jacket. A desired volume of LVEs were charged with 30 mL of TBA. The initiator was

chosen to be 3.0 wt % of the charged LVE. After purging with N_2 to remove O_2 and trace H_2O for 10 minutes, the reactor was charged with ethylene and heated to 65 °C. The ethylene pressure was controlled between 800 psi to 1100 psi. The temperatures and pressures were kept constant during the copolymerizations. The reaction times were 8 hours for the copolymerizations of 10 mL of LVEs and 6 hours for the copolymerizations of 5 mL of LVEs. Cooling water was pumped into the jacket to quench the polymerizations. All the reactants were poured in ethanol. Solids were washed with ethanol, dried in fumehood, and then dried in vacuum oven at 60 °C.

Structural Characterization

The structure characterizations of the copolymers were carried out using a Nicolet 200 Fourier transform Infrared spectrometer (FT-IR) equipped with an attenuated total reflection (ATR) accessory. A zinc selenide (Zn-Se) crystal was used as the crystal material. The measurement range was from 4000 cm^{-1} to 400 cm^{-1}.

Composition Determination

A Nicolet 200 FTIR was used to estimate the copolymer compositions. The synthesized copolymers were dissolved in THF to make 1 wt % polymer solutions. Uniform liquid films were formed by injection of polymer sample solution into a FT-IR KBr cell purchased from International Glass Inc. The spectrum of LDPE solid was employed as a reference, in which there was no carbonyl peak around 1735 cm^{-1}. The spectrum of 1 wt % polyvinyl butyrate (PVB), polyvinyl hexanoate (PVH), and polyvinyl decanoate (PVD) were used as 100% carbonyl group standards for each corresponding poly(LVE-*co*-Et). A series of carbonyl peaks with various peak heights in between the spectrums of LDPE and homopolymers of different LVEs were

exhibited for poly(LVE-*co*-Et) with different LVE compositions. The LVE compositions were determined using the Beer-Lambert Law as mentioned in Chapter 3.

MWs and MWDs Determination

The MWDs, along with number-average molecular weight (M_ns) and weight-average molecular weight (M_ws), were determined using a Varian 400 gel permeation chromatography (GPC) equipped with a PL gel 5 μm MIXED-D and Varian Prostar reflection index detector. The GPC was calibrated using PS standard samples supplied by Varian. HPLC grade THF, purchased from Fisher, was used as the mobile phase with a flow rate of 1 mL/min.

Chapter Results and Discussions

Structure Characterization of Poly(LVE-co-Et)

The structures of the resultant random copolymers, including poly(VP-*co*-Et), poly(VH-*co*-Et), and poly(VD-*co*-Et), are shown in Figure 6.1. The characteristic vibrations, including the -C=O stretching absorption band of the LVEs from 1650 cm^{-1} to 1730 cm^{-1} and the C-H stretching absorption band from 2950 cm^{-1} to 2760 cm^{-1} of $–CH_3$ and $–CH_2$-, were observed using ATR/FT-IR. A comparison of the FT-IR spectrum of EVA and poly(VD-*co*-Et) is shown in Figure 6.2.

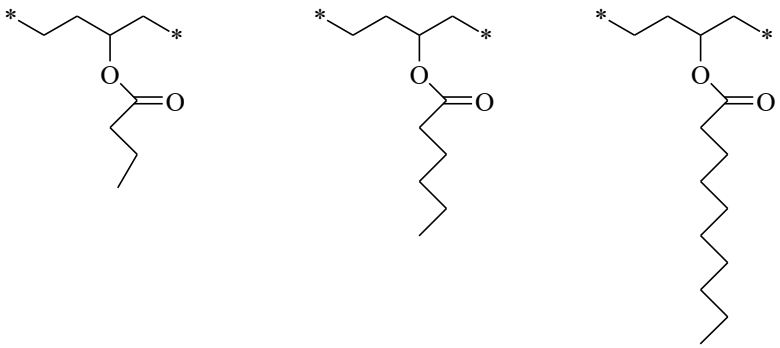

poly(VB-*co*-MMA) poly(VH-*co*-MMA) poly(VD-*co*-MMA)

Figure 6.1. The chemical structures of poly(LVE-*co*-Et).

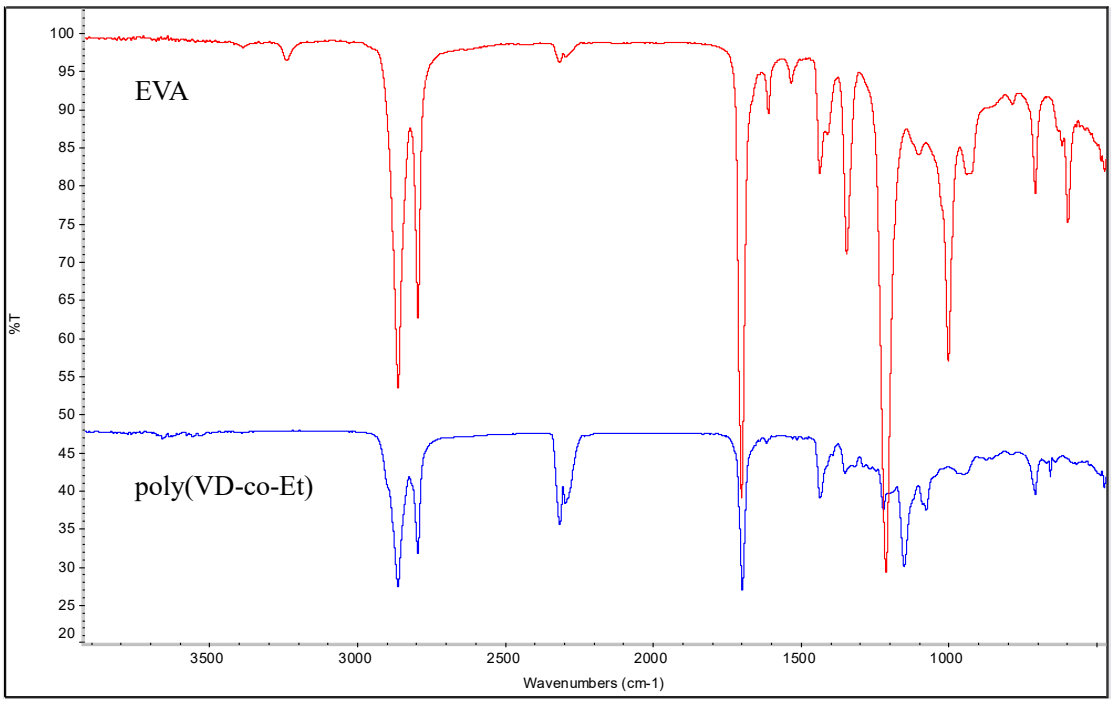

Figure 6.2 The chemical structures of commercial EVA and poly(VD-*co*-Et).

Compositions, MWs, and MWDs of Poly(LVE-co-Et)

The VB compositions of poly(VB-*co*-Et) range from 13 mol% to 18 mol%. The VH compositions of poly(VH-*co*-Et) ranged from 12 mol% to 15 mol%. The VD compositions ranged from 17 mol% to 21 mol% as listed in Table 6.1. In general, the LVE compositions were lower for those poly(LVE-*co*-Et) obtained under higher Et pressure because a higher Et pressure corresponds to a larger feed ratio of Et to LVEs.

But the differences of LVE compositions between runs with varying pressure (800 to 1100 psi) were quite small.

Table 6.1. LVE feed volume, ethylene pressure, LVE compositions, M_n, M_w, and PDI of poly(LVE-*co*-Et).

LVEs	Vol. (mL)	Et (psi)	LVE (mol%)	M_n (g/mol)	M_w (g/mol)	PDI (M_w/M_n)
VB	10	1100	15	18266	107310	5.7
VH	10	1100	13	18162	95506	5.3
VB	5	1100	18	17547	89164	5.2
VH	5	1100	15	17411	67905	3.9
VB	10	1000	13	17320	85723	5.0
VH	10	1000	12	17584	83799	4.8
VB	5	1000	16	14961	76189	5.0
VH	5	1000	14	13345	49451	3.7
VD	5	1000	17	17820	76213	4.3
VB	5	900	15	14547	68834	4.7
VH	5	900	13	12080	44683	3.7
VD	5	900	19	17343	71205	4.1
VB	5	800	14	14029	58059	4.1
VH	5	800	12	11592	35852	3.1
VD	5	800	21	17081	68892	4.0

The resulting of MWs and MWDs are listed in Table 6.1. It was observed that the MWs and PDI decreased for poly(LVE-*co*-Et) with the declining of ethylene pressures when the LVE feed volumes were the same as shown in Figure 6.3 (a) and (b). This was because the ethylene pressure was the dominating parameter in controlling by feed ratio of ethylene to LVE. The lower the ethylene pressure, the smaller the ethylene feed ratio. The LVE compositions and MWs of poly(VD-*co*-Et) are a little higher than those of poly(VB-*co*-Et) and poly(VH-*co*-Et), which indicates that the reactivity ratio of VD/Et is probably higher than those of VB/Et and VH/Et.

Also, the MWs decreased with declining LVEs feed volume when the ethylene pressure was the same, as shown in Figure 6.4. This was also attributed to the different feed ratios of LVE to ethylene. It was not possible to determine the reactivity ratios because the ethylene concentration in the liquid phase could not be measured.

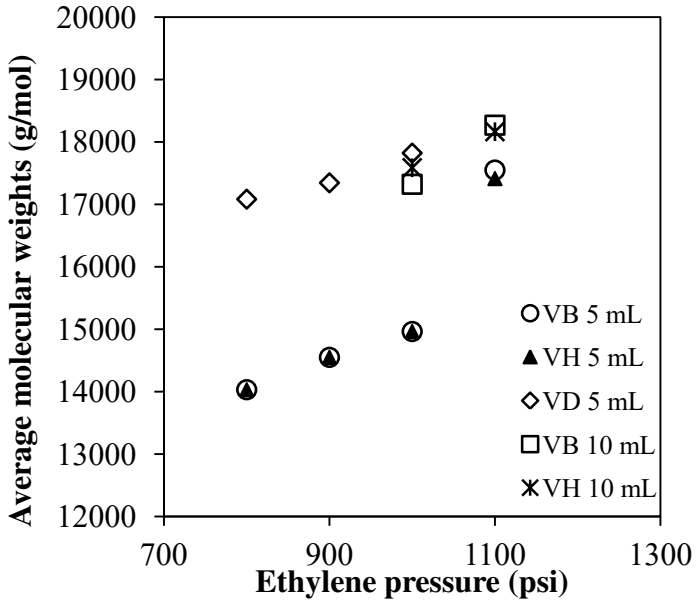

Figure 6.3 (a). The relationship between MWs of poly(LVE-*co*-Et) and ethylene pressure with 5 mL and 10 mL feed volume of LVEs.

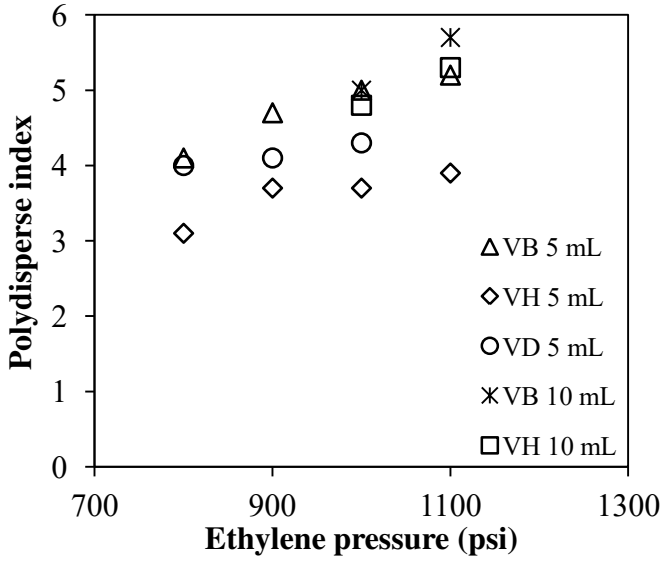

Figure 6.3 (b). The relationship between PDI of poly(LVE-*co*-Et) and ethylene pressure with 5 mL and 10 mL feed volume of LVEs.

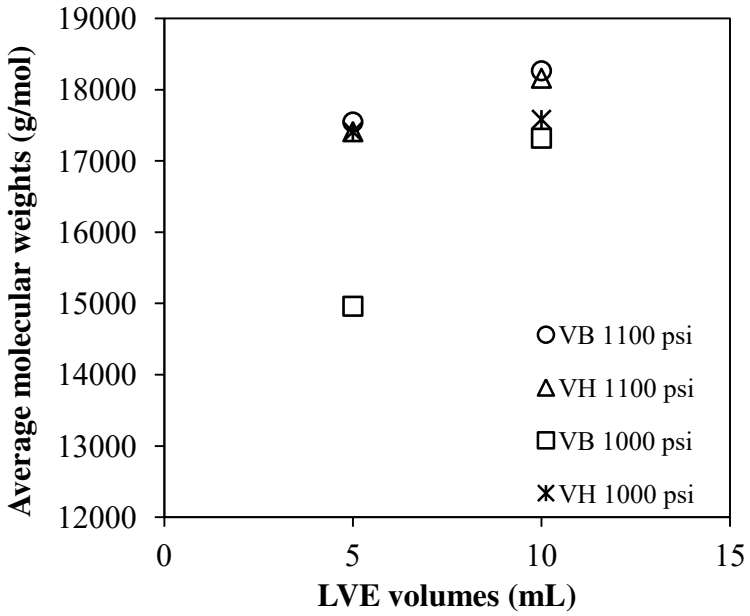

Figure 6.4. The relationship between MWs of poly(LVE-*co*-Et) and LVE volume under ethylene pressure of 1100 psi and 1000 psi.

Poly(LVE-*co*-Et) synthesized in this work were viscous liquid. It indicated that LVE with higher MW were more effective at reducing crystallinity. EVA containing 40 wt % vinyl acetate has 4 wt% (Gladkihi et al., 2010), however, poly(VH-*co*-Et) containing 40 wt % (12 mol%) VH is viscous liquid.

Chapter Conclusions

A series of poly(LVE-*co*-Et) were prepared using solution copolymerizations. The LVE compositions did not change significantly when the ethylene pressure decreased from 1100 psi to 800 psi. The MWs of poly(LVE-*co*-Et) decreased when ethylene pressure decreased. The PDI also declined with the decrease of ethylene pressure.

CONCLUSIONS

This work focused on the synthesis and characterization of thermoplastics, which had similar structures (in some case even identical) as existing commercial polymer products, using different linear vinyl esters (LVEs) that could be produced from biobased sources. The influences of LVE content and LVE molecular weights on the thermomechanical and rheological properties of the resultant copolymers were determined. In addition, the kinetic parameters, including reactivity ratios, were wherever possible, determined.

A series of poly(LVE-*co*-St) samples were prepared. The reactivity ratios of the various LVEs with St were determined. Measurement of these thermoplastics showed that the T_gs of the copolymers were reduced from 87 °C to 53 °C by the incorporation of LVEs ranging from 1 mol% to 19 mol%. The M_n of the copolymers became smaller with greater incorporation of LVE due to the difference in reactivity ratios between St and LVEs. DMA analysis determined that the relative molecular weights, the content of LVEs, and the length of side chains all affected the storage and loss modulus of the copolymers.

Secondly, a series of poly(LVE-*co*-MMA) copolymers were synthesized. The resultant copolymers had different LVE compositions from 3 mol% to 41 mol%. The storage moduli and T_gs of the resultant copolymers decreased with increasing LVE composition. Copolymers with VD exhibited larger reductions in storage moduli and shifts in peak tan δ. The rheological analysis of the resultant copolymers showed that the shear and loss moduli of poly(LVE-*co*-MMA) were primarily dominated by the polymer MW. But the Arrhenius activation energy of flow declined with increasing

LVE length. The flexibility of PMMA was improved by introduction of LVEs.

Thirdly, amphiphilic poly(LVE-*co*-AA) were synthesized using solution copolymerization. The MWs of the resultant copolymers decreased with increasing LVE compositions because of the differences in r_{AA} and r_{LVE}. The thermomechanical property analysis indicated that the T_gs and storage moduli of copolymers were impacted by the LVE length and compositions. Rheological property analysis showed that the shear flow behaviors were mainly affected by the MWs of resultant copolymers. But the lengths of side chains also had an impact on shear flow when the MWs of the copolymers were low.

Finally, a series of poly(LVE-*co*-Et) were prepared using solution copolymerizations. The LVE compositions did not change significantly when the ethylene pressure was increased from 800 psi to 1100 psi. As expected, the MWs of the poly(LVE-*co*-Et) decreased when the ethylene pressure was decreased. The PDIs also declined with decreasing ethylene pressure.

In general, different LVEs were preferred depending on the specific objective. First, VH was the preferred comonomer when the goal was to have copolymers with the highest bio-content based on weight content and with minimal impact on the thermomechanical properties. The VH copolymers had higher bio-content than VP and VD copolymers when molecular weights of copolymers were the same. The incorporation of VH in the copolymers led to some reduction in the storage moduli and glass transition temperatures compared to VP. However, VH did not have nearly the impact on the thermomechanical properties as VD did. Therefore, VH copolymers met the requirement of high bio-content, and relatively high glass transition temperature and strength. If the objective was to produce copolymers with high storage moduli and glass transition temperature, while still incorporating relatively

high bio-content then VP was the ideal LVE. VP did not change the copolymer strength as much as VH and VD but still had higher LVE content then VD copolymers. Therefore, VP copolymers meet the requirements of high bio-content and high rigidness. Finally, VD was the most suitable LVE for copolymers with low bio-content, low glass transition temperature, and high flexibility. VD copolymers exhibited the lowest storage moduli and glass transition temperatures with comparatively low concentration of LVE. The thermomechanical properties of copolymers were changed significantly by introducing small amounts of VD.

FUTURE WORK

Firstly, copolymers of linear vinyl esters and ethylene with higher ethylene content will be prepared. The thermomechanical and rheological properties will be studied in order to make a comparison with commercial poly(vinyl acetate-*co*-ethylene) and linear low density polyethylene products. Secondly, LVEs produced from cracked crop oils rather than petroleum-based monomers will be employed in synthesizing copolymers using the same method in the future work. The obtained copolymers will be characterized in aspects including compositions, MWs, T_gs, storage modulus, and shear storage and loss moduli. In addition, the mechanical properties of the copolymers, including tensile strength and impact strength, will be measured in order to obtain more information for determining the applications of the biobased LVE copolymers.

REFERENCES

Abdelaal, M. Y.; Makki, M. S. I.; Sobahi, T. R. A. "Modification and characterization of polyacrylic acid for metal ion recovery", *Am. J. Polym. Sci.* **2012**, *2*, 73-78.

Ahmad, H.; Hasan, M.K.; Miah, M. A. J.; Ali, A. M. I.; Tauer, K. "Solvent Effect on the Emulsion Copolymerization of MMA and LMA in Aqueous Media", *Polymer*, **2011**, *52*, 3925-3932.

Ahmad, S. Ashraf, S. M.; Sharmin, E.; Zafar, F.; Hasnat, A. "Studies on ambient cured polyurethane modified epoxy coatings synthesized from a sustainable resource", *Prog. Crys. Growth. Charact.* **2002**, *45*, 83-88.

Albrecht, A.; Brüll, R.; Macko, T.; Malz, F.; Pasch, H. "Comparison of high-temperature HPLC, CRYSTAF and TREF for the analysis of the chemical composition distribution of ethylene-vinyl acetate copolymers", *Macromol. Chem. Phys.* **2009**, *210*, 1319-1330.

Anton, G.; Tibor, M.; Volker, D.; Robert, B. "High-temperature two-dimensional liquid chromatography of ethylene-vinylacetate copolymers", *J. Chromatogr. A*, **2010**, *1217*, 6867-6874.

Araujo, O.; Giudici, R.; Saldívar, E.; Ray, W. H. "Modeling and experimental studies of emulsion copolymerization systems. I. Experimental results", J. Appl. Polym. Sci. **2001**, 79, 2360-2379.

Aydin, S.; Akçay, H.; Özkan, E.; Güner, F. S.; Erciyes, A. T. "The effects of anhydride type and amount on viscosity and film properties of alkyd resin", *Prog. Org. Coat.* **2004**, *51*, 273-279.

Braegelmann, M. P.; Azure, A. D.; Stahl, D.; Kubátová, A.; Seames, W. S.; Tande, B. M. *Separ. Sci. Technol.* **2011**, *46*, 2167-2173.

Bugada, D. C.; Rudin, A. "Molecular structure and melting behaviour of ethylene-vinyl acetate copolymers", *Polym. J.* **1992**, 28, 219-227.

Calafate, B. A. L.; Garcia, M. E. F.; Mano, E. B. "The electrocopolymerization of styrene with vinyl acetate in an organic solvent", *J. Polym. Sci. A1*. **1989**, *27*, 847-854.

Caneba, G. T.; Xu, Z. Y.; Dar, Y. L. "Free-radical retrograde-precipitation copolymerization of vinyl acetate and acrylic acid", *J. Appl. Polym. Sci.* **2009**, *113*, 3872-3882.

Can, H. K.; Doğan, A. L.; Rzaev, Z. M. O.; Uner, A. H.; Güner, A. "Synthesis, characterization, and antitumor activity of poly(maleic anhydride-co-vinyl acetate-co-acrylic acid)", *J. Appl. Polym. Sci.* **2006**, *100*, 3425-3432.

Chien, I. L.; Kan, T. W.; Chen, B. S.; "Dynamic simulation and operation of a high pressure ethylene-vinyl acetate (EVA) copolymerization autoclave reactor", *Comput. Chem. Eng.* **2007**, *31*, 233-245.

Chinal, S. N.; Campbell, R. H. "Determination of copolymer composition by Infrared analysis. poly(vinyl acetate)-poly(methyl acrylate)", *Anal. Chem.* **1961**, *33*, 577-579.

Costas Kiparissides, Apostolos Baltsas, and Stratos Papadopoulos, "Mathematical modeling of free radical ethylene copolymerization in high pressure tubular reactor", *Ind. Eng. Chem. Res.* **2005**, *44*, 2592-2605

Chisholm, M.; Hudson, N.; Kirtley, N.; Vilela, F.; Sherrington, D. C. "Application of the "strathclyde route" to branched vinyl polymers in suspension polymerization: architectural, thermal, and rheological characterization of the derived branched products", *Macromolecules*. **2009**, *42*, 7745-7752.

Daniel, N.; Srivastava, A. K. "Free radical copolymerization of styrene with vinyl acetate using *p*-acetylbenzylidene triphenylarsonium ylide as an initiator", *Adv. Polym. Tech*. **2002**, *21*, 108-115.

Daniel, S.; Jordan, J. E. F. "Vinyl laurate and other vinyl esters", *Org. Synth.* **1963**, *4*, 977-981.

De, P.; Sathyanarayana, D. N. "Reactivity ratios for the terpolymerization of methyl methacrylate, vinyl acetate, and molecular oxygen", *J. Polym. Sci. A: Polym. Chem.* **2002**, *40*, 564-572.

de Souza, C. M. G.; Tavares, M. I. B. "NMR study of commercial poly(ethylene-co-vinyl acetate)", *Polym. Test.* **1998**, *17*, 533-541.

Donescu, D.; Fusulan, L.; Petcu, C. "Polymerization of vinyl acetate in homogeneous systems obtained in presence of acrylic acid", *Colloid. Polym. Sci.* **1999**, *277*, 203-209.

Dossi, M.; Liang, K.; Hutchinson, R. A.; Moscatelli, D. "Investigation of free-radical copolymerization propagation kinetics of vinyl acetate and methyl methacrylate", *J. Phys. Chem. B*, **2010**, *114*, 4213-4222.

Dubé, M. A.; Penlidis, A. "A systematic approach to the study of multicomponent polymerization kinetics — the butyl acrylate/methy methacrylate/vinyl acetate example: 1. Bulk copolymerization", *Polymer*. **1995**, *36*, 587-598.

Dubé, M. A.; Penlidis, A. "Emulsion terpolymerization of butyl acrylate/methyl methacrylate/vinyl acetate: experimental results", *J. Polym. Sci. A: Polym.*

Chem. **1997**, *35*, 1659-1672.

Eren, T.; Kusefoğlu, S. H. "Synthesis and polymerization of the bromoacrylated plant oil triglycerides to rigid, flame ‐ retardant polymers", *J. Appl. Polym. Sci.* **2004A**, *91*, 2700-2710.

Eren, T.; Kusefoğlu, S. H. "One step hydroxybromination of fatty acid derivatives", *Eur. J. Lipid. Sci. Tech.* **2004B**, *106*, 27-34.

Erkal, F. S.; Erciyes, A. T.; Yagci, Y. "A new method for the styrenation of triglyceride oils for surface coatings", *J. Coat. Technol.* **1993**, *65*, 37-43.

Erhan, S. Z.; Bagby, M. O.; Nelsen, T. C. "Drying Properties of Metathesized Soybean Oil" *J. Am. Oil. Chem. Soc.* **1997**, *74*, 703-706.

Filley, J.; McKinnon, J. T.; Wu, D. T. "Theoretical study of ethylene−vinyl acetate free-radical copolymerization: reactivity ratios, penultimate effects, and relative rates of chain transfer to polymer", *Macromolecules* **2002**, *35*, 3731-3738.

Gandhi, S.; Kadrmas, J.; Šťávová, J.; Kubátová, A.; Muggli, D.; Seames, W. S.; Sadrameli, M.; Tande, B. M. *Separ. Sci. Technol.* **2012**, *47*, 66-72.

Garofalo, E.; Incarnato, L.; Malo, D. L. "Effect of short-chain branching on melt fracture behavior of metallocene and conventional poly(ethylene/α-olefin) copolymers", *Polym,. Eng. Sci.* **2012**, *52*, 1968-1977.

German, A. L.; Heikens, D. "Highly precise quantitative gas-chromatographic method and its application to the determination of copolymerization kinetics", *Anal. Chem.* **1971**, *43*, 1940-1944.

Gladkikh, Y. Y., Shcherbina, A. A. Chalykh, A. E. "Adhesive properties of ethylene and vinyl acetate copolymer. Deformation strength characteristics: Contribution of plastic deformation work", *Polym. Sci. Ser. D. Glues and Sealing Materials.* **2010**, *3*, 32-37.

Gospodinova, N.; Zlatkov, T.; Terlemezyan, L. "Relationship between microstructure and phaseand relaxation transitions in ethylene-(vinyl acetate) copolymers prepared by emulsion copolymerization", *Polyme*r **1998**, *39*, 2583-2588.

Granel, C.; Jérôme, R.; Teyssié, P.; Jasieczek, C. B.; Shooter, A. J.; Haddleton, D. M.; Hastings, J. J.; Gigmes, D.; Grimaldi, S.; Tordo, P.; Greszta, D.; Matyjaszewski, K. "Investigation of methyl methacrylate and vinyl acetate polymerization promoted by $Al(^{i}Bu)_3$/2,2'-Bipyridine and $Al(^{i}Bu)_3$/2.2'-Bipyridine TEMPO complexes", *Macromolecules*, **1998**, 31, 7133-7141.

Gultekin, M.; Beker, U.; Guner, F. S.; Erciyes, A. T.; Yagci, Y. "Styrenation of castor oil and linseed oil by macromer method", *Macromol. Mater. Eng.* **2000**, *283*, 15-20.

Güner, F. S.; Gumüsel, A.; Calica, S.; Erciyes, A. T. "Study of film properties of some urethane oils", *J. Coat. Technol.* **2002**, *74*, 55-59.

Güner, F.S.; Baranak, M.; Soytas, S.; Erciyes, A. T. "Flow behavior of oil-modified polymer solutions", *Prog. Org. Coat.* **2004**, *50*, 172-178.

Güner, F. S.; Yağcı, Y.; Erciyes, A. T. "Polymers from triglyceride oils", *Prog. Polym. Sci.* **2006**, *31*, 633-670.

Han, Y. F.; Wang, J. H.; Kumar, D.; Yan, Z.; Goodman, D. "A kinetic study of vinyl acetate synthesis over Pd-based catalysts: kinetics of vinyl acetate synthesis over Pd-Au/SiO_2 and Pd/SiO_2 catalysts", W. *J. Catal.* **2005**, *232*, 467-475.

Hirai, T. "Determination of composition in vinyl acetate-vinyl propionate copolymers", *Die. Angew. makromol.* Chem. **1975**, *43*, 93-103.

Huang, X. Y.; Lu Z. J.; Huang, J. L. "Preparation of diblock copolymer of methyl methacrylate and vinyl acetate by successive radical mechanism and selective hydrolysis of the poly(vinyl acetate) block", *Polymer*. **1998**, *39*, 1369-1374.

Huang, X. Y.; Huang, Z. H.; Huang, J. L. "Copolymerization of styrene and vinyl acetate by successive photoinduced charge-transfer polymerization", *J. Polym. Sci. A1*. **2000**, *38*, 914-920.

Islam, M. S.; Yeum, J. H.; Das, A. K. "Synthesis of poly(vinyl acetate-methyl methacrylate) copolymer microspheres using suspension polymerization", *J. Colloid. Interf. Sci*. **2012**, *368*, 400-405.

Kaneyoshi, H.; Matyjaszewski, K. "Synthesis of poly(vinyl acetate)-graft-polystyrene by a combination of cobalt-mediated radical polymerization and atom transfer radical polymerization", *J. Polym. Sci. A1*. **2007**, *45*, 447-459.

Khot, S. N.; Lascala, J. J.; Can, E.; Morye, S. S.; Williams, G. I.; Palmese, G. R. "Development and application of triglyceride-based polymers and composites", *J. Appl. Polym. Sci.* **2001**, *82*, 703-723.

Kim, D. S.; Park, H. B.; Rhim, J. W.; Lee, M. Y. "Proton conductivity and methanol transport behavior of cross-linked PVA/PAA/silica hybrid membranes", *Solid State Ionics.* **2005**, *176*, 117-126.

Kubo, K.; Fukuda, T. "Propagation and termination processes in the free-radical copolymerization of methyl methacrylate and vinyl acetate", *Macromolecules*, **1993**, *26*, 6766-6770.

Li, F.; Perrenoud, A.; Larock, R. C. "Spectroscopic Characterization of linseed oil based polymers", *Polymer*. **2001**, 42, 1567-1579.

Li, F.; Larock, R. C. "Synthesis, structure and properties of new tung

oil-styrene-divinylbenzene copolymers prepared by thermal polymerization", Biomacromolecules, **2003**, *4*, 1018-1125.

Li, H.; Zhang, Y. M.; Liu, G. Y. "Atom transfer radical polymerization of methyl methacrylate initiated with a macroinitiator of poly(vinyl acetate)", *J. Appl. Polym. Sci.* **2006**, *101*, 1089-1094.

Li, Y. G.; Zhang, Y. Q.; Yang, D.; Feng, C.; Zhai, S. J.; Hu, J. H.; Lu, G. L.; Huang, X. Y. "Well-defined amphiphilic graft copolymer consisting of hydrophilic poly(acrylic acid) backbone and hydrophobic poly(vinyl acetate) side chains", *J. Polym. Sci. Part A: Polym. Chem.* **2009**, *47*, 6032-6043.

Mallégol, J.; Lemaire, J.; Gardette J. L. "Drier influence on the curing of linseed oil", *Prog. Org. Coat*., **2000**, *39*, 107-113.

Mark, H. F.; Bikales, N.; Overberger, C. G.; Menges, G.; Kroschwitz, J. I. Encyclopedia of Polymer Science and Engineering; 2nd Ed.; Wiley: New York, **1989A**; Vol 17, p 420.

Mark, H. F.; Bikales, N.; Overberger, C. G.; Menges, G.; Kroschwitz, J. I. Encyclopedia of Polymer Science and Engineering; 2nd Ed.; Wiley: New York, **1989B**; Vol 17, p 440.

Mark, H. F.; Bikales, N.; Overberger, C. G.; Menges, G.; Kroschwitz, J. I. Encyclopedia of Polymer Science and Engineering; 2nd Ed.; Wiley: New York, **1989C**; Vol 17, p 439.

Mark, H. F.; Bikales, N.; Overberger, C. G.; Menges, G.; Kroschwitz, J. I. Encyclopedia of Polymer Science and Engineering; 2nd Ed.; Wiley: New York, **1989D**; Vol 17, p 393.

Mark, H. F.; Bikales, N.; Overberger, C. G.; Menges, G.; Kroschwitz, J. I. Encyclopedia of Polymer Science and Engineering; 2nd Ed.; Wiley: New York, **1989E**; Vol 16, p 6.

Mark, H. F.; Bikales, N.; Overberger, C. G.; Menges, G.; Kroschwitz, J. I. Encyclopedia of Polymer Science and Engineering; 2nd Ed.; Wiley: New York, **1989F**; Vol 1, p 286.

Mark, H. F.; Bikales, N.; Overberger, C. G.; Menges, G.; Kroschwitz, J. I. Encyclopedia of Polymer Science and Engineering; 2nd Ed.; Wiley: New York, **1989G**; Vol 17, p 411.

Mark, H. F.; Bikales, N.; Overberger, C. G.; Menges, G.; Kroschwitz, J. I. Encyclopedia of Polymer Science and Engineering; 2nd Ed.; Wiley: New York, **1989H**; Vol 17, p 422.

Mark, H. F.; Bikales, N.; Overberger, C. G.; Menges, G.; Kroschwitz, J. I. Encyclopedia of Polymer Science and Engineering; 2nd Ed.; Wiley: New York, **1989J**; Vol 6, p 435.

Mark, H. F.; Bikales, N.; Overberger, C. G.; Menges, G.; Kroschwitz, J. I. Encyclopedia of Polymer Science and Engineering; 2nd Ed.; Wiley: New York, **1989K**; Vol 6, p 452.

Mark, H. F.; Bikales, N.; Overberger, C. G.; Menges, G.; Kroschwitz, J. I. Encyclopedia of Polymer Science and Engineering; 2nd Eds.; Wiley: New York, **1989L**; Vol. 17, pp 224-230.

Mark, H. F.; Bikales, N.; Overberger, C. G.; Menges, G.; Kroschwitz, J. I. Encyclopedia of Polymer Science and Engineering; 2nd Eds.; Wiley: New York, **1989M**; Vol. 17, p 286.

Mark, H. F.; Bikales, N.; Overberger, C. G.; Menges, G.; Kroschwitz, J. I. Encyclopedia of Polymer Science and Engineering; 2nd Ed.; Wiley: New York, **1989N**; Vol 17, p 437.

Mishra, M. K.; Yagci, Y. Handbook of Vinyl Polymers Radical Polymerization, process, and Technology; 2nd Ed.; CRC press Taylor & Francis Group: Boca Raton, **2009A**, pp 566-567.

Mishra, M. K.; Yagci, Y. Handbook of Vinyl Polymers Radical Polymerization, process, and Technology; 2nd Ed.; CRC press Taylor & Francis Group: Boca Raton, **2009B**, pp 399-402.

Mishra, M. K.; Yagci, Y. Handbook of Vinyl Polymers Radical Polymerization, process, and Technology; 2nd Ed.; CRC press Taylor & Francis Group: Boca Raton, **2009C**, pp 725.

Nayak, P. L. "Natural oil-based polymers: opportunities and challenges", *J. Macromol. Sci. Rev. Macromol. Chem. Phys.* **2000**, *40*, 1–21.

Odian, G. Principles of Polymerization; 3rd Ed.; Wiley: New York, **1993**, p 243.

Ohnaga, T.; Sato, T. "Synthesis of poly(vinyl acetate) macromonomers and preparation of poly(vinyl acetate) grafted copolymers and poly(vinyl alcohol) grafted copolymers", *Polymer* **1996** ,*3*, 3729-3734.

Oldring, P. K. T.; Turk, N. Polyamides Resins for Surface Coatings; Wiley: New York, **2000**; Vol. III. pp 131-197.

Ozkaynak, M. U, Atalay-Oral, C.; Tantekin-Ersolmaz, S. B.; Güner, F. S. "Polyurethane films for wound dressing applications", *Macromol. Symp.* **2005**, *228*, 177-184.

Paik, H. J.; Teodorescu, M.; Xia, J. H.; Matyjaszewski, K. "Block copolymerizations of vinyl acetate by combination of conventional and atom transfer radical polymerization", *Macromolecules*. **1999**, *32*, 7023-7031.

Ramelow, U. S.; Qiu, Q. H. “Monomer reactivity ratios in UV-initiated free-radical copolymerization reactions”, *J. Appl. Polym. Sci.* **1995**, *57*, 911-920.

Ranjha, N. M.; Mudassir, J. “Swelling and aspirin release study: cross-linked pH-sensitive vinyl acetate-co-acrylic acid (VAC-co-AA) hydrogels”, *Drug. Dev. Ind. Pharm.* **2008**, *34*, 512–521.

Rezaeian, I.; Jafari, S. H.; Zahedi, P.; Ghaffari, M.; Afradian, S. “Improvements of physical and mechanical properties of electron beam irradiation—crosslinked EVA foams”, *Polym. Adv. Technol.* **2009**, *20*, 487-492.

Santos, A. M.; Févotte, G.; Othman, N.; Othman, S.; Mckenna, T. F. “On-line monitoring of methyl methacrylate–vinyl acetate emulsion copolymerization”, *J. Appl. Polym. Sci.* **2000**, *75*, 1667-1683.

Scorah, M. J.; Hua, H.; Dubé, M. A. “Bulk and solution copolymerization of methyl methacrylate and vinyl acetate”, *J. Appl. Polym. Sci.*, **2001**, *82*, 1238-1255.

Scott, P. J.; Penlidis, A.; Rempel, G. L.; Lawrence, A. D. “Ethylene-vinyl acetate semi-batch emulsion copolymerization: Use of factorial experiments for process optimization”, *J. Polym. Sci: Part A: Polym. Chem.* **1994**, *32*, 539-555.

Sharma, V.; Kundu, P. P. “Addition polymers from natural oils—A review”, *Prog. Polym. Sci.* **2006**, *31*, 983-1008.

Silva, F. M.; Lima, E. L.; Pinto, J. C. “Acrylic acid/vinyl acetate suspension copolymerizations. I. partition coefficients for acrylic acid”, *J. Appl. Polym. Sci.* **2004**, *93*, 1077-1088.

Silva, F. M.; Lima, E. L.; Pinto, J. C. “Dynamic Optimization of Semibatch Vinyl Acetate/Acrylic Acid Suspension Copolymerizations”, *Polym. Eng. Sci.* **2010**, *50*, 697-708.

Sperling, L. H.; Devia, N.; Manson, J. A.; Conde, A. “Simultaneous interpenetrating networks based on castor oil elastomers and polystyrene—a review of an international program”, *ACS. Symp. Ser.* **1980**, 407-421.

Stadler, F. J.; Gabriel, C.; Münstedt, H. “Influence of short chain branching of polyethylenes on the temperature dependence of rheological properties in shear”, *Macromol. Chem. Phys.* **2007**, *208*, 2449-2454.

Steinmacher, F. R.; Bernardy, N.; Moretto, J. B.; Barcelos, E. I.; Araújo, P. H. H.; Sayer, C. “Kinetics of MMA and VAc Miniemulsion Polymerizations Using Miglyol and Castor Oil as Hydrophobe and Liquid Core”, *Chem. Eng. Technol*. **2010**, *33*, 1877-1887.

Stevens, M. P. Polymer chemistry: An introduction; 3rd Ed.; Oxford University Press: USA, **1998**, p 70.

Tang, L. G.; Weng, Z. X.; Pan, Z. R. “Kinetic studies on emulsion copolymerization of vinyl acetate and acrylics in the batch process”, *Eur. Polym. J.* **1996**, *32*, 1139-1143.

Tian, Q.; Larock, R. C. “Novel Biobased Plastics, Rubbers, Composites, Coatings and Adhesives from Agricultural Oils and By-Products”, *J. Am. Oil. Chem. Soc.* **2002**, *79*, 479-88.

Tuman, S. J.; Chamberlain, D.; Scholsky, K. M.; Soucek, M. D. “Differential scanning calorimetry study of linseed oil cured with metal catalysts”, Prog. Org. Coat. **1996**, *28*, 251-258.

Uyama, H.; Kuwabara, M. “Enzymatic synthesis and curing of biodegradable epoxide containing polyesters from renewable resources”, *Biomacromolecules*, **2003**, *4*, 211–215.

Van Krevelen, D. W.; Nijenhuis, K. T. Properties of polymers: their correlation with chemical structures; their numerical estimation and prediction from additive group contributions; 4th Ed.; Elsevier: Amsterdam, **2009**. p 275.

Vasanthy, B. K.; Palanichamy M.; Krishnasamy, V. “Side-Chain Alkylation of Toluene with Isopropanol and Methanol over Alkali Exchanged Zeolites”, *Appl. Catal. A-Gen*. **1996**, *148*, 51-61.

Vilela, C.; Rua R.; Silvestre, J. D. A.; Gandini, A. “Polymers and copolymers from fatty acid-based monomers”, *Ind. Crop. Prod.* **2010**, *32*, 97-104.

Vinogradov, G. V.; Malkins, A. Y. Rheology of Polymers-viscoelasticity and Flow of polymers; Springer-Verlag: Berlin, Heidelberg, New York, **1980A**. pp 239-242.

Vinogradov, G. V.; Malkins, A. Y. Rheology of Polymers-viscoelasticity and Flow of polymers; Springer-Verlag: Berlin, Heidelberg, New York, **1980B**. pp 198-201.

Warwel, S.; Brüse, F.; Demes, C.; Kunz, M.; gen Klaas, M. R. “Polymers and surfactants on the basis of renewable resources”, *Chemosphere,* **2001**, *43*, 39-48.

Warwel, S.; Brüse, F.; Demes, C.; Kunz, M. “Polymers and. Polymer Building Blocks from Meadowfoam Oil”, *Ind. Crops. Prod*. **2004**, *20*, 301-309.

Wei, X.; Collier, J. R.; Petrovan, S. “Shear and elongational rheology of polyethylene with different molecular characteristics. I. Shear rheology”, *J. Appl. Polym. Sci.* **2007**, *105*, 309-316.

Xia, J. H.; Paik, H. J.; Matyjaszewski, K. “Polymerization of vinyl acetate promoted by iron complexes”, *Macromolecules*. **1999**, *32*, 8310-8314.

Xue, X. Q.; Zhu, J.; Zhang, Z. B.; Cheng, Z. P.; Tu, Y. F.; Zhu. X. L. “Synthesis and characterization of azobenzene-functionalized poly(styrene)-b-poly(vinyl acetate) via the combination of RAFT and "click" chemistry”, *Polymer*. **2010**, *51*, 3083-3090.

Xu, W. Z.; Charpentier, P. A. “FTIR study measuring the monomer reactivity ratios for ethylene-vinyl acetate polymerization in supercritical CO_2”, *Ind. Eng. Chem. Res.* **2009**, *48*, 1384-1390.

Yang, D. J.; Fu, X. K.; Gong, Y. F. “Study on the preparation and performances of P(VAc-MMA) polymer electrolytes for lithium ion battery”, *Chinese. J. Polym. Sci.* **2008**, *26*, 375-380.

Yenwo, G. M.; Manson, J. A.; Puido, J.; Sperling, L. H. “Castor-oil-based interpenetrating polymer networks: Synthesis and characterization”, *J. Appl. Polym. Sci.* **1977A**, *21*, 1531-1541.

Yenwo, G. M.; Sperling, L. H.; Puido, J.; Manson, J. A.; Conde, A. “Castor oil based interpenetrating polymer networks, IV. Mechanical behavior”, *Polym. Eng. Sci.* **1977B**, *17*, 251-256.

Zaldívar, C.; del Sol, O.; Iglesias, G. D. “On the preparation of acrylic acid vinyl acetate copolymers with constant composition — 1. Copolymerization reactivity ratios ”, *Polymer*, **1998A**, *39*, 245-246.

Zaldívar, C.; Iglesias, G.D.; del Sol, O.; Pinto, J. C. “On the preparation of acrylic acid vinyl acetate copolymers with constant composition—2. Refractive indexes for in-line evaluation of monomer conversion and copolymer composition”, *Polymer*, **1998B**, *39*, 247-251.

Zaldívar, C.; del Sol, O.; Iglesias, G. D.; Pinto, J. C. “On the preparation of acrylic acid vinyl acetate copolymers with constant composition—4. Modelling batch and continuous free-radical AA /VA copolymerization”, *Polymer* **1997**, *38*, 5823-5833.

Zhu, L. H.; Ji, Y., Chen, M. F.; Ding, M. T. “Copolymerization of MMA with VAc by starch/manganic pyrophosphate initiation”, *Polym. Plast. Technol. Eng.* **2007A**, *46*, 61-62.

Zhu, L. H.; Tang, Y. J.; Ji, Y.; Chen, M. F.; Ding, M. T. “Copolymerization of MMA with VAc by starch catalysis”, *J. Elastom. Plast.* **2007B**, *39*, 23-32.

Zou, Y. S.; Lin, J.; Zhuang, R. C.; Ye, J. L.; Dai L. Z.; Zheng, L. S. “Synthesis of block copolymer from dissimilar vinyl monomer by stable free radical polymerization”, *Macromolecules* **2000**, *33*, 4745-4749.